CELL-TARGETED RIBOSOME-INACTIVATING PROTEINS DERIVED FROM PROTEIN COMBINATORIAL LIBRARIES

By

Subodini Perampalam

A thesis submitted in conformity with the requirements for the degree of Doctor of Philosophy

Graduate Department of Medical Biophysics in the University of Toronto

Your file Votre référence
ISBN: 978-0-494-57909-1
Our file Notre référence
ISBN: 978-0-494-57909-1

ABSTRACT

CELL-TARGETED RIBOSOME-INACTIVATING PROTEINS DERIVED FROM PROTEIN COMBINATORIAL LIBRARIES

Degree of Doctor of Philosophy, 2008

Subodini Perampalam

Graduate Department of Medical Biophysics in the University of Toronto

Combinatorial protein libraries based on a protein template offer a vast potential for deriving protein variants harboring new receptor specificity while retaining other template functions to serve as library search-engines, cell-routing sequences and therapeutic domains. This concept was tested with the design and synthesis of protein libraries where short random peptide motifs were embedded directly within the catalytic A subunit of the bacterial ribosome-inactivating protein (RIP) known as Shiga-like toxin 1 (SLT-1). More precisely, a seven amino acid peptide epitope (PDTRPAP) was inserted between residues 245-246 of its A subunit (SLT-1A^{PDTRPAP}) and shown to preserve catalytic function while exposing the epitope. SLT-1 A chain libraries harboring tripeptide and heptapeptide random elements were subsequently constructed, screened and shown to express more than 90% of expected cytotoxic A chain variants. Finally, more than 9,000 purified SLT-1 A chain variants were screened using their ribosome-inactivating function in a cell-based assay to identify mutants that are able to kill human melanoma 518-A2 cells. This search led to the striking discovery of a single chain RIP that displays selectivity for a panel of human melanoma cell lines as well as minimal immunogenicity when injected repeatedly into mice. This directed evolution of a RIP template provides a broad platform for identifying cell type specific cytotoxic agents.

DEDICATION

This thesis is dedicated to my father for instilling in me a sense of confidence by trusting me and supporting me every step of the way from childhood to adulthood.

ACKNOWLEDGEMENTS

Research work embodied in this document is the result of guidance and support provided by many individuals. I am grateful for my supervisor, Dr. Jean Gariepy, who provided me an opportunity to work in a field that has the potential to directly impact the lives of many. Dr. Gariepy was instrumental in helping me identify innovative avenues to contribute, yet work independently to assess the viabilities of these avenues. My committee members, Dr. Rama Khokha and Dr. Armen Manoukian, have played an equally important role by providing insight and guidance throughout my graduate life. Their ability to provide both formal and informal guidance in steering my research is much appreciated. I would also like to thank Dr. David Rose for his guidance.

My research work required interaction with researchers and students spread across several departments at University of Toronto. Dr. Xin Wei and MTI Corporation's staff members (Leigh, Reza, Erin and Alison) are thanked for all their technical support related to research work outlined in Chapter 4 of this thesis. Dr. Mark Bray is thanked for mentoring me before and throughout my doctoral student life. My laboratory members are thanked for making my student life a lively one. Particularly, Nora, Paul, Kim, Reza and Qhing Hong are thanked for being my 'extended family' at the university. Finally, this research work would have been impossible if it was not for the relentless support of my husband, Thas, and rest of my family, especially my parents-in-law. My kids have been a source of inspiration and motivation.

Abbreviations

ABTS	2,2'-azino-bis(3-ethylbenzthiozoline-6-sulphonic acid)
ADCC	Antibody dependent Cell cytotoxicity
CDC	Complement dependent cytotoxicity
CEA	Carcinoembryonic antigen
CT	Cholera toxin
D	Dalton
DNA	Deoxyribonucleic acid
DT	Diphtheria toxin
DTIC	Dacarbazine
DTT	Dithiothreitol
EF-1	Elognation factor 1
ELISA	Enzyme linked immuno assay
ER	Endoplasmic reticulum
ERAD	Endoplasmic reticulum associated degradation
Fab	Fragment antigen binding
Fc	Fragment crystallizable region
FITC	Fluorescein isothiocyanate
Gb3	Galactose 1-4galactoseb1-4glucosylceramide
HD	Hydrophobic domain
HRP	Horse raddish peroxidase
HUS	Hemolytic Uremic Syndrome
ITs	Immunotoxins
kDa	kilo Dalton

mRNA	messenger ribonucleic acid
mAb	monoclonal antibody
NMR	nuclear magnetic resonance
PCR	polymerase chain reaction
PBS	phosphate-buffered saline
PE	Pseudomonas exotoxin
PEG	Polyethylene glycol
PT	Pertussis toxin
SDS-PAGE	Sodium dodecyl sulfate-polyacrylamide gel electrophoresis
RNA	ribonucleic acid
RIP	ribosome inactivating protein
SLT-1 A	Shiga like toxin 1 A chain
SRB	Sulforhodamine B
SLT-1APDTRPAP	Shiga like toxin-1 with a PDTRPAP insertion between residues 245 and 246 of its A chain
SLT-1APDXXXAP	Shiga like toxin-1 library with a PDXXXAP insertion between residues 245 and 246 of its A chain and where XXX represents a random tripeptide element
SLT-1AIYSNKLM	Shiga like toxin-1 with a IYSNKLM insertion between residues 245 and 246 of its A chain.
TK	Tyrosine kinase
VLS	Vascular leak syndrome

TABLE OF CONTENTS

LIST OF TABLES

LIST OF FIGURES

CHAPTER 1: INTRODUCTION

1.1 Rationale for designing targeted Therapeutics

Chemotherapy has become the prevelant form of treatment for most cancers. However, conventional chemotherapeutic agents exhibit poor specificity in reaching tumor tissue and are often constrained by dose-limiting toxicity. This has prompted the exploration of targeted therapeutics.

Targeted therapeutics refers to drugs that target a specific cellular pathway in the growth and development of tumor. The targets consist of various molecules that are believed to play a role in cancer formation. However, most tumors are linked to alterations in more than one cellular pathway. Hence, multi-targeting approaches are necessary to eliminate tumor cells as well as prevent drug resistance from developing. Defining new cancer specific targets may thus yield the next generation of cancer therapies to be used with conventional treatments with improved clinical benefits. For example, the relevance of cancer cell surface receptors as therapeutic targets is shown by the successful use of monoclonal antibodies such as Herceptin, Zevalin, Rituxan, and Mylotarg (Table 1.1) [1-4]. These monoclonal antibodies have served as excellent prototypes for the design of protein-based therapeutics in cancer.

Our laboratory started working on protein combinatorial libraries as a way to develop new classes of targeted therapeutics in the field of cancer [5]. The term combinatorial library refers to a collection of protein molecules built on a common structural template. Specifically, our group has been using Shiga like toxin 1 (SLT-1), a ribosome inactivating protein, as a structural template. A major advantage of mining such toxin libraries is that families of toxins may address issues such as tumor antigen heterogeneities. Further, the use of a protein toxin as a structural template provides an opportunity to generate binding reagents that have a toxic property. My thesis project was to design and analyze first generation toxin libraries based on the catalytic A chain of SLT-1. I first demonstrated that such SLT-1A libraries yielded stable A chain variants that were catalytically active. Secondly, these libraries were screened to derive toxin variants with specificity for proteins and cells.

1.2 Targeted therapeutics and cancer

1.2.1 Targeting

The concept of targeted tumor killing has been around since the early 20th century [6]. In 1906, Paul Ehrlich introduced his "magic bullet" concept which stated:

> "The antibodies are therefore magic bullets which find the targets themselves….we must therefore concentrate all our powers and abilities on making the aim as accurate as we can contrive, so as to strike the parasites as hard and the body cells as lightly as possible."

The term “magic bullet” refers to a reagent capable of selectively detecting and destroying tumor cells. The possibility to implement this concept was observed after the discovery of the methods for producing monoclonal antibodies [7]. A major expectation for targeted therapeutics is that they show high efficacy and low toxicity. Traditional cancer therapeutics block the metabolism of dividing cells and do not discriminate between cancer cells and healthy cells that divide frequently such as hair follicles, and cells in the gastrointestinal tract and bone marrow. The lack of specificity exhibited by anti-cancer agents can lead to adverse side effects which limit their clinical success. At present two main classes of targeted therapeutic agents are used in the clinic: monoclonal antibodies and small molecules (Table 1.1).

Table 1.1: FDA-approved targeted agents and the spectrum of targeted cancers*

Agent (mAb)	Target	Type of Cancer	References
Cetuximab (Erbitux) 2004	EGFR (chimeric)	CRC, HNSCC	[8]
Trastuzumab (Herceptin)-1998	Her2/neu (Humanized)	Breast cancer	[1]
Bevacizumab (Avastin)-2004	VEGF (Humanized)	Colorectal cancer	[9]
Rituximab (Rituxan) 1997	CD20 (Chimeric)	Non-Hodgkins lymphoma	[3, 4]
Ibritumomab tiuxetan (Zevalin)-2002	CD20 (murine)	Non-Hodgkins lymphoma	[2]
Tositumomab-I-131 (Bexxar)-2003	CD20 (murine I-131)	Non-Hodgkins lymphoma	[10]
Alemtuzumab (Campath)-2001	CD52 (Humanized)	B-cell Chronic lymphocytic leukemia	[11]
Small molecules			
Imatinib (Gleevec) – 2002	TKs (BCR-ABL, KIT, PDGFR)	GIST	[12, 13]
Gefitinib (Iressa)-2003	TK (EGFR)	NSCLC	[14]
Erlotinib (Tarceva) -2004	TK (EGFR)	NSCLC, Pancreatic cancer	[15]
Sunitinib (Sutent) -2006	TKs (VEGFR, PDGFR, KIT, FLT3)	GIST, Renal cancer	[16]
Sorafenib (Nexavar) – 2005	Kinases (B-Raf, VEGFR2, EGFR)	Renal cancer	[17]
Zolinza (Vorinostat)-2006	Histone deacetylase	Percutaneous T-cell lymphoma	[18]
Bortezomib (Velcade) 2003	28S protease	B-cell lymphoma	[19, 20]

*Adapted from Ref. [21, 22]

1.2.2 Cancer specific markers

Eukaryotic cells exhibit a collection of surface molecules which can serve as targets for ligands in the development of targeted therapeutics. Developing strategies to identify novel cancer cell surface markers is fundamental to drug discovery. A variety of solid tumor markers have been identified that are up-regulated on cancer cells such as the HER-2/neu, epidermal growth factor receptor (EGFR), carcinoembryonic antigen, the Lewis Y-related carbohydrate antigen and the epithelial cell adhesion molecule (Ep-CAM) [23-25]. Ligands binding to cell surface receptors preferentially expressed on cancer cells may be useful for directing therapeutics to sites of disease with increased therapeutic windows [26, 27]. For instance, it has been shown that tissue homing peptides coupled to drugs are more effective and less toxic than the drugs alone [26, 28]. Many molecules selected for their homing potentials to tumors have been used as carriers to deliver cytotoxic drugs [27], cytotoxic peptides and pro-apoptotic [29, 30], metalloprotease inhibitors [31], cytokines [32], and imaging agents in mouse models of human tumors [33]. Many of the FDA approved monoclonal antibodies such as Cetuximab (EGFR) and Trastuzumab (HER-2/neu) and small molecules such as Gefitinib (EGFR) and Erlotinib (EGFR) were developed against cancer cell specific markers.

1.2.3 Current combinatorial therapeutics

A combinatorial approach offers the opportunity to explore a large number of potential drug candidates and this technology can be classified into two groups. The first one is comprised of low molecular weight compounds (less than 500 Da) based on small organic scaffolds or natural products and prepared by synthetic methods [34-36]. Members of these libraries are generated by solid or solution phase methods. The

diversity of these libraries is usually less than 10,000 elements and they involve iterative searches to identify improved lead compounds. Small molecule drugs are less expensive, less immunogenic, less specific, may gain access to intracellular targets and are more convenient to administer (oral bioavailability) as compared to large molecule drugs such as antibodies, nucleic acids and peptides [37]. The second class of combinatorial libraries include all biological polymers such as nucleic acids, peptides and proteins [38]. There is considerable amount of research that focuses on this class of combinatorial libraries since in oncology, proteins (monoclonal antibodies) entering clinical studies have higher success rates (18-24%) compared to small molecules (5%) [39, 40]. Examples of both antibody and small molecule therapeutics now approved for human uses are listed in Table 1.1. Monoclonal antibodies as a major form of approved cancer therapeutics and as a prototype for protein-based therapeutics are discussed next.

1.3 Monoclonal antibodies as cancer therapeutics

Kohler and Milstein developed the monoclonal antibody technology in the 1970s [7]. This technology has allowed researchers to contemplate the design of monoclonal antibody (mAb) for cancer therapy, as it has many desired features such as high specificity combined with high affinity, a long serum half life as well their organization into distinct structural and functional domains [41, 42]. There are eight anti-cancer mAbs approved by FDA and many more are under clinical development (Table 1.1). IgG, the predominant class of serum antibody, has been used almost exclusively in therapeutic applications. Functionally, an IgG molecule is divided into two antigen binding fragments (Fabs) and an Fc region which is responsible for mediating effector functions.

1.3.1 Mechanisms of action of monoclonal antibodies

Antibodies possess three different types of therapeutic activities to mediate cytotoxicity to tumor cells. The first one is unmodified monoclonal antibodies causing antibody dependent cellular cytotoxicity (ADCC) and complement dependent cytotoxicity (CDC). These effector functions have been important in the case of Rituxan, alemtuzumab and Herceptin [43, 44]. However, there have been reports of resistance to ADCC and CDC among cancer cells [45-47]. Furthermore, these effector functions require the presence of certain level of antigen expression on the target cells and the effector response in the case of ADCC is affected by the Fc-receptor polymorphism [48].

The second mechanism of action is by diminishing signaling through receptors whose over-expression promotes tumor growth. One example for this class is the mAb Cetuximab which works by physically blocking the binding of the ligand to its receptor [49]. Monoclonal antibodies can also induce apoptosis directly as in the case of Rituximab (anti-CD20 antibody) [50].

The third category works by delivering a cytotoxic payload such as monoclonal antibodies conjugated to toxins [51], chemotherapeutics (eg. Calicheamycin conjugated to Mylotarg) [52], radioisotopes, (^{131}I, ^{90}Y) or enzymes (bacterial carboxyl peptidase) [53]. The tumor targeting in all these categories is mediated by the antigen binding fragment (Fab) of the mAb. For the last category, the antibody simply behaves as a homing device to direct the payload to the target site. For majority of mAbs, regardless of the mechanism of action, a necessary first step is penetration of antibody into tumor tissue to mediate target binding.

1.3.2 Challenges of mAbs

Although, IgG molecules provide bivalency, human origin, and a long serum half life, they are very large molecules with multi-subunit architecture containing disulfide bonds and glycosylation. These properties make antibodies difficult and expensive to manufacture. Even though solid tumors represent over 85% of human cancers, only 3 (trastuzumab, cetuximab, and bevacizumab) out of the 8 approved mAbs as cancer therapeutics target solid tumors [54]. One of the three mAbs (bevacizumab) targets a soluble ligand and not a surface protein within solid tumors. This inequality in efficiency might be due to poor tumor penetration of intact antibodies (150 kDa) into the interior of large tumor masses which have inadequate blood supply [55, 56]. Another issue is the non-specific binding of the antibody molecules by the reticuloendothelial system such as the liver, spleen and bone marrow.

1.3.3 The use of antibody fragments

Due to the discussed limitations of intact antibody molecules, antibody fragments in the form of single chain Fv, Fab and multivalent fragments which can be obtained from combinatorial libraries have become important alternatives. Many of these molecules are in clinical and preclinical trials and a list is provided in Table 1.2. Any molecule smaller than intact immunoglobulin molecules (150 kDa) can provide improved tumor penetration and faster blood clearance. It has become evident that a major determinant of diffusion speed through tumors is size [57, 58]. ScFv molecules diffuse through tumors at least 6 times faster than intact IgG molecules due to their sizes and other properties and they also show improved tissue penetration [59].

Table 1.2. Antibody fragments in clinical and preclinical development*

Name	Target antigen	Fragment/format	Indication	Stage (ref)
CEA-scan (arcitumomab)	CEA	Fab/mouse	Colorectal cancer imaging	FDA approved (http:www.immunomedics.com)
CDP791	VEGF	Fab/PEGylated humanized	Cancer	Phase 1 (http://www/nektar.com
MDX-H210	Her2/Neu & CD64	Fab/bispecific humanized	Breast cancer	Phase 2 (http://www.medarex.com)
SGN-17	P97 antigen	ScFv fused to β-lactamase	Melanoma	Preclinical (http://www.seagen.com)
F5 scFv-PEG Immunoliposome	Her2	ScFv fused to PEG human	Breast cancer as drug targeting	Preclinical [60]
C6.5K-A	Her2/Neu	Diabody	Ovarian & breast cancer	Preclinical [61]
T84.66	CEA	ScFv dimer Fc	Colorectal cancer	Preclinical [62]
r28M	CD28 & MAP	Bispecific ScFv	Melanoma	Preclinical [63]
BiTE MT103	CD19 &CD3	Bispecific ScFv	B-cell tumors	Phase 1 (http://www.micromet.de)
BiTE	Ep-CAM & CD3	Bispecific ScFv	Colorectal cancer	Preclinical (http://www.micromet.de)
Tandab	CD19 & CD3	Bispecific tandem diabody	B-cell tumors	Preclinical (www. affimed.de)

*adapted and modified from [64].

1.3.4 Challenges of antibody fragments

Smaller antibody fragments can be produced in *E.coli*, yet their stability still relies on intra-domain disulfide bonds. Antibody fragments provide better tissue penetration, but offer very low avidity due to single valence affinity [65]. Furthermore, some antibody fragments tend to aggregate when fused to other domains to achieve therapeutic efficacy. The addition of single cysteine residue that is convenient during conjugation of FITC or PEG molecule is not handled well in antibody fragments. Hence, for several applications, antibody fragments may not be ideal and other protein combinatorial strategies are preferred.

1.4 Protein combinatorial libraries

Combinatorial protein libraries represent a powerful strategy that can be used to accelerate the evolution of protein scaffolds. The application of combinatorial libraries requires the creation of a vast collection of molecules and the development of an effective screen to select members with the desired trait. The basis for combinatorial peptide libraries was used by arachnids 400 million years ago for the evolution of neurotoxins, as well as the complex evolution of vertebrate immune system [66]. A combinatorial library involving the mutations of as little as 7 amino acids within a given protein scaffold would consist of a billion molecules (20^7) that share an underlying structural fold while displaying distinct elements from one another. Because of this vast diversity, it is possible to isolate library members that bind specifically to any target [67]. The affinity and specificity of molecules isolated from libraries are linked to the library size. Hence

a library must be of sufficient size to offer the possibility of containing members with desired properties. A library with a diversity of 10^{10} clones resulted in the selection of antibodies with nanomolar range affinities and a diversity of 3×10^{7} clones yielded only antibodies with micromolar affinities [68, 69]. However, the library size must be within reasonable limits to be screened practically even if robotic approaches are employed for all screening steps.

1.4.1 Display strategies

Display strategies refer to combinatorial library searches. They have been developed in the past two decades to select and evolve random polypeptide sequences into peptides and proteins with novel functions. Display libraries can either be screened using cell-based (display on the surface of phage, other viruses, bacteria, yeast or mammalian cells) or cell-free (ribosome display or mRNA display) systems [70-72].

1.4.2 Phage display

The most common method for creating biomolecular combinatorial libraries is via the display of peptides and proteins on phages. In 1985, Smith et al established a method for displaying polypeptides on the surface of filamentous phage by fusing a random peptide element on viral coat proteins [70]. In phage display, a DNA library is fused to a gene encoding one of the M13 phage coat proteins. The fusion proteins are then expressed on the surface of the phage and the mutants can be screened for binding to a target. The bound phages can then be recovered and the nucleic acids can be sequenced. This method allowed for the rapid mapping of epitope binding sites recognized by antibodies [73, 74]. The methodology was further popularized by Winter and Wells who demonstrated the display of functional folded proteins on the phage surface [75, 76].

Antibodies, especially the Fab and scFv fragments were among the first protein libraries developed. Many high affinity antibodies have been selected using this approach [68, 77, 78].

A great advantage of phage display which also accounts for its popularity is the convenience with which libraries can be screened on targets for specific binders through biopanning. Biopanning is a process where phages carrying peptides or antibodies are incubated with a target and phage binders are eluted and enriched by amplification in the appropriate host cell (described in Figure 1.1). Biopanning provides peptides or antibodies with affinity constants typically in the micromolar (peptides) to nanomolar (antibodies) range. Cell-based display strategies such as phage display are limited by the efficiency of transformation ($>10^9$-10^{10}) in the host system and by the nature of the protein template used to create libraries [68].

1.4.3 Ribosome Display and mRNA display

Ribosome display is an *in vitro* selection and evolution technology for proteins which can be used to create proteins that can bind to a desired ligand [79]. The process leads to ribosomes and mRNA in a complex with the newly formed protein which can bind to an immobilized target or ligand [80] (strategy described in Figure 1.2). Then the mRNA of the complexes is reverse transcribed to produce the DNA encoding the molecule responsible for binding to the immobilized target. Alternatively, mRNA display relies on a direct covalent link between the mRNA and the protein it encodes [81]. However, this procedure is limited by chemical synthesis and purification of puromycin-attached oligonucleotides. These *in vitro* strategies allow screening of very large initial libraries

(>10^{12} members) and it has been shown that increasing the size of the library leads to a significant improvement in the average affinity of peptides selected against protein targets [80]. Another advantage of these *in vitro* selection techniques is the built-in evolution process where one can obtain increased target affinities or stability of a member by low fidelity polymerases [82, 83]. However, ribosome display strategies require low temperature in order to preserve the integrity of the protein-ribosome-mRNA ternary complex and the recovered mRNA after the first round of panning is very minimal reflecting the large reduction in the initial library diversity [84]. Moreover, ribosome display can only be performed on immobilized targets and not on intact cells since the system is extremely sensitive to RNAse activity present on cell surfaces.

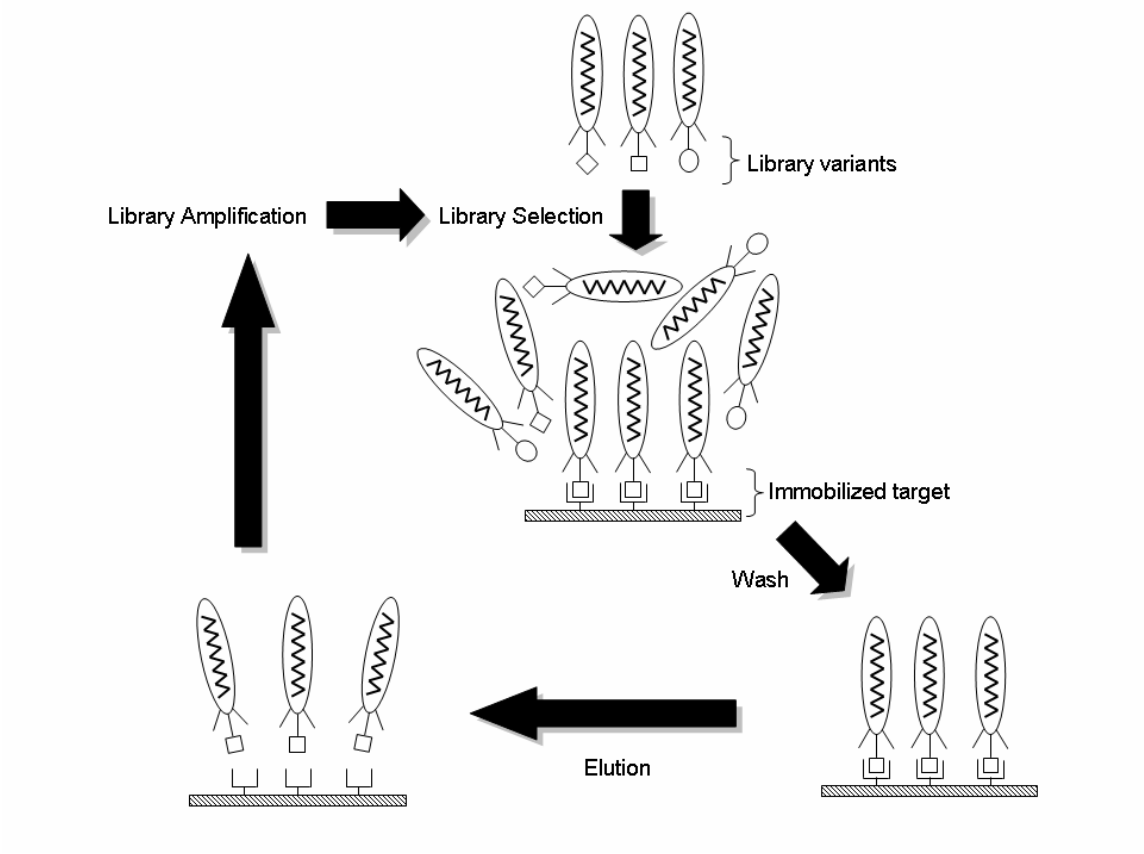

Figure 1.1: The *in vitro* panning of immobilized targets by phage display.

In phage display technologies, a DNA random library element coding for peptides or proteins is fused to a gene coding for one of the M13 phage coat proteins. The library is incubated with an immobilized target to select for binders and the unbound phages are removed by washing. Bound phages are then eluted and amplified in *E.coli*. The amplified and pooled phages are subjected to further rounds of selection to enrich for binders and eventually the sequences of individual binders can be identified by sequencing the encapsulated DNA. (Diagram adapted and modified from [85]).

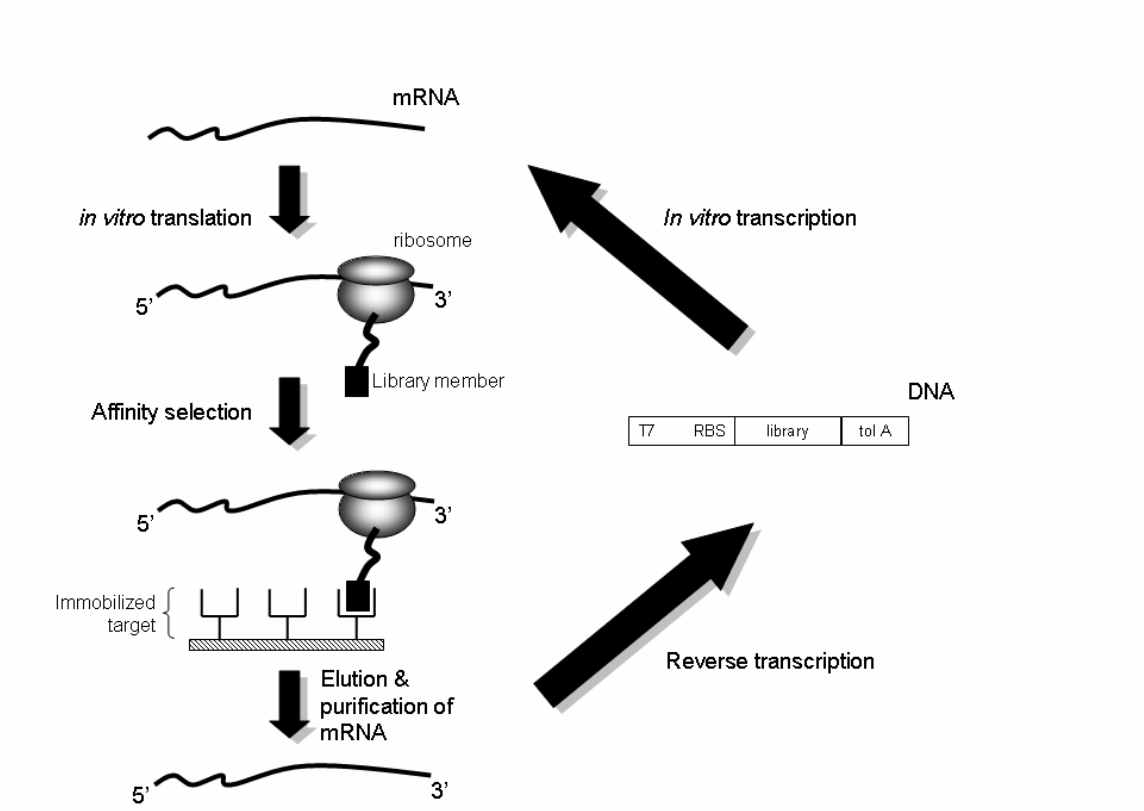

Figure 1.2: The *in vitro* panning of immobilized targets by ribosome display.

In ribosome display, the construct is obtained by PCR amplification of a library insert and the flanking regions present in the vector. *In vitro* transcription of this PCR product yields mRNA that is used for translation. The ribosome stalls at the end to the message because of the absence of stop codons, which generates a library of proteins attached to their messages via the ribosomes. The mRNA-ribosome-protein ternary complexes are then used for affinity selection on an immobilized target. The message can be recovered from binders after washing, which then can be reverse transcribed and amplified. The binders can be used in further rounds of selection or they can be analyzed further by cloning into expression vectors.

1.4.4 Possible applications of protein combinatorial libraries

Peptide libraries can be used to map cell surface receptor proteomes. Peptides targeting specific receptors on cell surface involved in disease can be used for directing imaging agents (radiolabels, fluorochromes), reporter enzymes, drugs, or gene delivery vectors. Peptide libraries have been a rich source of ligands for many targets, in particular those that recognize a continuous stretch of amino acid residues (eg. proteases and SH3 domains). Peptide libraries have also been used to identify motifs mimicking epitopes of antibodies. However, most molecular recognition events are mediated by folded proteins [86, 87]. This technology can provide human antibody fragments which are less immunogenic, do not bind to the reticulo-endothelial system in a non-specific manner and are rapidly excreted by the kidneys [88]. This approach also allows the generation of polypeptides other than antibodies (linear peptides, constrained peptides, or small globular proteins) as binding reagents.

1.4.5 Examples of application

Furthermore, *in vivo* panning has been used to identify peptides binding to targets involved in angiogenesis and metastasis [89]. Linear peptide libraries have been successfully used to select high affinity binders [74, 90, 91]. Phage display also provides a tool to identify peptides with similar pharmacological properties to antibodies but with smaller molecular mass. Peptides binding to one of the vascular endothelial growth factor receptors (VEGFRs), flt-1, was identified by screening a 12-mer peptide library [92]. These peptides inhibited angiogenesis and the growth of human gastric cancer nodules *in vivo*. Peptides were also isolated that bound to Her2/neu receptor and shown to possess anti-proliferative effects against breast cancer cells expressing the receptor

[93]. Simple structural constraints such as disulfide bond have been shown to provide marginal improvements in affinity during the selection of new binders [94, 95]. In the case of developing antibodies, phage display provides a way to identify and develop specific binding reagents very fast with less cost. Several companies have developed phage display libraries that contain a large repertoire of human immunoglobulin sequences which have been used to screen on various ligands (eg, Cambridge Antibody Technology and MorphoSys AG).

Alternatively, display strategies have also accelerated the translation of antibodies into targeted therapeutics. For example, the human anti-TNF IgG1 (Adalimumab known as HUMIRA) is an FDA approved antibody to treat rheumatoid arthritis and was developed using phage display [96]. There are many other phage display derived antibodies that are in clinical trials including CAT-2888 (anti-CD22) against leukemias, CAT-354 (anti-IL-13) against asthma, CG-1008 (anti-TGF) against idiopathic pulmonary fibrosis, MYO-029 (anti-GDF-8) against muscular dystrophy, ABT-874 (anti-IL12) against T cell derived autoimmune diseases, as well as HGS-ETR1 (anti-TRAIL-R1) and anti-TRAIL-R2 against various cancers. Phage display derived tumor binding peptides and antibody fragments that have been conjugated with radionuclides and toxin molecules have yielded several potential anti-cancer therapeutic agents [97-99]. Hence, phage display and other display strategies offer the potential for production of therapeutic proteins. The use of antibody domains highlight that protein scaffolds may be needed to devise better classes of targeted ligands.

1.4.6 Alternate protein scaffolds

A library is designed by choosing a suitable protein as a scaffold with a known three dimensional structure so that insertion or substitution sites can be selected easily. A scaffold chosen for the derivation of a protein library should ideally possess all of the following properties: a large and diverse target binding surface, high thermodynamic stability under all conditions, efficient folding and expression properties and low immunogenicity. Antibodies, by virtue of their use in adaptive immune responses, have served a prominent role in designing high affinity, protein based binding reagents. The target binding surface of antibody molecules is largely formed by the complementary determining region loops [100]. However, due to the limitations of antibodies and their fragments discussed in Sections 1.3.2 and 1.3.4, researchers have been exploring alternate binding scaffolds to increase the reservoir of agents. There are over 30 scaffolds used for library construction and most of the scaffolds used are involved in binding interactions with other ligands under natural conditions. Examples of some alternate scaffolds are presented in Table 1.3. These scaffolds present distinct advantages over antibodies. Many of these scaffolds form stable structures without disulfide bonds which may simplify their production in bacteria [101, 102]. Moreover, most of these scaffold molecules are single domain proteins that do not require post-translational modifications. Many of these scaffolds also display high thermal stability and robustness in terms of their purification [101-103].

Scaffold proteins can be classified into those consisting of: 1) alpha-helical framework (eg Z-domain of affibodies, and ankyrin repeat proteins) [101, 102], 2) few secondary structures or irregular architecture of alpha-helices and beta-sheets (eg. Kunitz, and PDZ

domain proteins) [104, 105], and 3) beta-sheets (knottins, and fibronectin type-III domains) [106, 107]. Libraries based on these scaffolds have been screened by most of the *in vitro* display technologies. There are only a few examples of functional proteins that have been used as scaffolds for protein display. The beta-barrel green fluorescent protein served as a scaffold and peptides exhibiting anti-proliferative effects were isolated [108].

1.4.7 Limitations of existing library scaffolds

Alternate binding proteins and antibody fragments are limited to therapeutic applications in which the mere event of binding is responsible for the activity of the drug. Intact immunoglobulins possess effector functions such as ADCC and complement activation. Hence, in some cases, additional effector functions are needed to obtain therapeutic potential. Novel effector functions could be provided by conjugating mAbs, their fragments or alternate binding proteins with diverse classes of molecules such as toxin, cytotoxic drug, cytokine, enzyme, and radioisotopes. In our study, we explored the option to use a single chain toxin protein with an inherent functional domain (enzyme function which causes cell death) as a library scaffold.

Table 1.3: Examples of alternative protein display scaffolds

Name	Scaffold (size)	Randomized elements	Target proteins	Selection method (ref)
Affibodies	Z-domain of protein A (58 aa)	13 aa on flat surfaces	Insulin, CD28, HER-2/neu, factor VIII	Phage display [101]
Repeat motif proteins	Ankyrin repeat (166 aa)	7aa, on β-turn & first α–helix of every loop	MBP, p38, JNK2, APH	Ribosome display [109]
Avimer	(LDLR-A-module) (43 aa)			Phage display [110]
^{10}Fn3/Trinectin	Fibronectin III (94 aa)	2-3 loops	VEGF-R2 & TNF- α	Yeast display [106, 111]
Kunitz domains	BPTI/APPI (58 aa)	5 aa in loops	Human neutrophil elastase/TF-FVIIa, plasma Kallikrein	Phage display [104, 112]
PDZ domains	Ras-binding protein AF-6	Entire domain	Peptides with free C terminus	Yeast two-hybrid, phage display [113, 114]
Scorpion toxins	Charybdotoxin	Loop Grafting or 4aa	Acetylcholine receptor, gp120, mAbs	Rational design and phage display [115]
Anticalins	Lipocalins (160-180 aa)	16 aa in 4 loops	VEGF, CTLA-4, Streptavidin	Phage display & ribosome display [116, 117]
Knottins	Cellulose binding domain	11 aa on loops/7 aa on flat surface	Alkaline phosphatase, α-amylase	Phage display [118]
Knottins	Tendamistat	1-2 loops (6-8aa)	mAb, integrins	Phage display [119]

Table adapted and modified from [120].

1.5 Toxins

Protein toxins have historically been regarded as pathogenic agents. Advances in molecular techniques have provided us with tools to use the unique properties of toxins to fight diseases. Toxins are proteins produced by plants, bacteria, animals and insects to act as either virulence factors (bacteria) or protect plant seeds from predators. Bacterial toxins have been extensively studied due to their involvement in the progression and pathogenesis of human diseases and for their ability to exploit host cellular mechanisms. Specifically, they have been invaluable in terms of understanding endocytic processes and mechanisms of intracellular transport as well as in the construction of immunotoxins [121-123].

1.5.1 Immunotoxins and targeting

In order to increase the response of antibody therapy, scientists have engineered antibodies to carry payloads such as toxins [51], enzymes [52], chemotherapeutics [53] or radionuclides. The creation of various antibody formats through protein engineering such as single chain antibody fragments (scFv), and Fabs led to molecules possessing enhanced tumor penetration and optimal serum half life as well as the possibility of fusing toxic payloads. Immunotoxins (ITs) are protein toxins linked to a cell binding ligand of immunologic proteins such as monoclonal antibodies, cytokines or growth factors. Toxins can be chemically conjugated to the targeting moiety by either using disulfide or thioether bonds, or they can be linked to these molecules at the genetic level. A single IT can kill a tumor cell, whereas at least 10^5 molecules of chemotherapeutic drugs are needed to obtain the same effect, which reduces the likelihood of an adverse reaction [124]. Immunotoxins bind to target cells through the binding domain and

undergo endocytosis. The ITs are cleaved in the cytoxol to release the toxin which causes the inhibition of protein synthesis leading to cell death. Since most toxins exert their effect in the cytosol by disrupting protein synthesis, a pre-requisite for IT therapy is the selection of an internalizing antigen. Receptor mediated endocytosis is essential for the toxins to exert their effect on their targets. Toxins naturally contain a cell binding domain which is removed during the generation of IT to ensure that toxin targeting is mediated only through the desired cell binding domain such as antibody or cytokines. The toxins that are commonly used in the generation of IT that are also being tested in clinical trials are ricin, diphtheria toxin and Pseudomonas exotoxin. Some examples of ITs that are undergoing clinical trials are shown in Table 1.4 [125]. Only one IT, denileukin diftitox (diphtheria toxin fragments fused to interleukin-2), is approved by FDA for refractory cutaneous T-cell lymphoma.

There are many issues that face the development of ITs as therapeutic agents for solid tumors such as immunogenicity and vascular leak syndrome (VLS) which is characterized by edema, hypo-albuminemia and weight gain [126, 127] . Even though the etiology of VLS is not clear, there is experimental evidence to support that toxin activation of the arachidonic acid metabolism pathway may induce vascular leak. Structural motifs have been identified in toxins that target endothelial cells leading to loss of vascular integrity. In order to increase the potency of ITs, recent research has focused on the optimal design of the antibody fragment and linker designs. Furthermore, the safety profiles of these ITs can be improved through the discovery of new and more selective tumor targets. These improvements may increase the clinical use of antibody/toxin

based immuno-therapeutics. Even though phage display and other strategies can accelerate the finding of specific tumor targets, the issue remains to optimize the pharmacokinetics and immunogenicity of the targeting and toxic moieties in combination.

Table 1.4: Summary of immunotoxin clinical trials*

Name	Clinical Stage	Indication	Administration	Side Effects	Reference
Denileukin diftitox	Phase III	CD25+CTCL	Intravenous	Acute hypersensitivity reactions, VLS, constitutional symptoms.	[128]
LMB-1	Phase I	Lewis Y cancers, primarily colorectal	Intravenous	VLS, severity and prevalence increased with dose.	[129]
BL-22	Phase I	CD22+B-cell malignancies	Intravenous	Dose limiting cytokine release syndrome; transient hypoalbunemia	[130]
Tf-CRM-107	Phase II	Glioblastoma multiforme	Intratumoral	Generally well tolerated; symptomatic progressive cerebral edema	[131]
Proxinium	Phase I	SCCHN	Intratumoral	Well tolerated with mild drug-related effects	[132]

*Table adapted from [125]

1.6 Bacterial toxins as combinatorial protein library scaffolds

The surface of a cell can be probed for the presence of internalized markers with ribosome-inactivating proteins (RIPs) that kill eukaryotic cells. A distinct advantage of proteins over small molecules in designing combinatorial libraries is that proteins often incorporate multiple functional domains. Large protein templates such as cell-surface determinants, immunoglobulins, adapter proteins and enzymes display a modular architecture in which protein domains exist either as distinct subunits or as defined motifs embedded into a single peptide chain [100, 133-138]. Another advantage of proteins as scaffolds is that they offer constrained and exposed domains on their surface which permits the integration of new functional domains. RIPs represent one such class of protein templates optimized to kill cells and they contain multiple domains coding for their cell binding, cell routing, processing and selective inhibition of protein synthesis. These optimized templates rank as some of the most toxic molecules engineered by nature. It has been shown that a single molecule of SLT-1 is enough to kill a cell [139].

1.6.1 Ribosome inactivating proteins

RIPs are a family of potent protein toxins that inhibit protein synthesis by directly interacting with and inactivating ribosomes or by modification of factors involved in translation. Many RIPs are produced by plants and examples include abrin, ricin, gelonin, momordin, and mistletoe lectin. Type I RIPs have only a single toxin subunit, while type II RIPs contain an enzymatic A subunit and a lectin-like binding subunit. The toxicity of the A chains of RIPs are due to their N-glycosidase activity which depurinates adenine at position 4324 in the 28 S rRNA as shown in Figure 1.3. This

single irreversible event prevents the formation of a critical stem-loop configuration which is necessary for the translocation step in translation. As a result, there is a complete halt of cellular translation. The B chains of type II RIPs mediate cell binding and internalization through specific sugar residues of glycoproteins or glycolipids. There are many bacterial and fungal type II RIPs including diphtheria toxin (DT), pseudomonas exotoxin (PE), Shiga toxin (ShT), alpha-sarcin and restrictocin. Most of these toxins differ in their mode of action except Shiga toxin which is identical to the plant RIPs. DT and PE are known to ADP-ribosylate the EF-2 and lead to its inactivation [140-144].

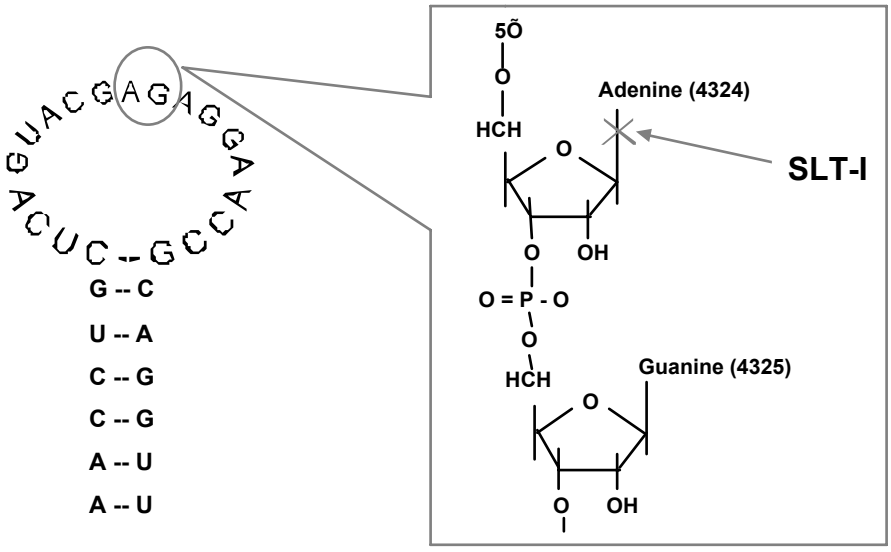

Figure 1.3: N-glycosidase activity of the SLT-1 A chain.

The A chain of SLT-1 inactivates ribosomes by cleaving the adenine residue at position 4324 of 28s rRNA in the 60 S ribosomal subunit. The stem loop structure is referred to as the sarcin-ricin domain and its conserved from bacteria to humans [145]. This event leaving the ribose-phosphate backbone intact is enough to inhibit protein synthesis.

1.6.2 SLT-1 and catalytic activity

SLT-1 is a bacterial protein toxin produced by a pathogenic strain of *E. coli* and it acquired its name because of its similarity to shiga toxin which is produced by *Shigella dysenteriae*. The most famous SLT-1 producing *E. coli* strain is serotype 0157/H7 which has been involved in many outbreaks of hemorrhagic colitis and hemolytic uremic syndrome [146, 147]. The three dimensional structure as well as detailed structure-function information derived from mutational analysis are available for ricin and SLT-1 [148, 149]. SLT-1 is similar to ShT in terms of sequence and is immunologically cross-reactive with ShT whereas SLT-II and its variants have 60% homology at the amino acid level. SLT-1 assembles into a characteristic AB_5 arrangement where a single A subunit is associated with a pentamer of identical B subunits responsible for binding to receptors on target cells. Ricin, DT, and PE contain a single receptor binding B subunit [150-152]. Shiga toxins, *E. coli* heat labile enterotoxin, cholera toxin (CT) and pertussis toxin (PT) possess pentameric B subunits [149, 153-155]. The B subunits generally act as lectins since they bind to glycolipids or glycoproteins on target cells with the exception of DT which binds to a protein receptor.

The A subunit of shiga like toxins and other toxins such as ricin and abrin possess N-glycosidase activity that depurinates a single adenosine residue at position 4324 in the 28S rRNA in the 60S ribosomal subunit leaving the ribose-phosphate backbone of the molecule intact [156, 157] (Figure 1.3). This event is irreversible and prevents the association of elongation factor 1 (EF1)-dependent amino-acyl tRNA to the ribosomes and halts protein synthesis [158]. The SLT-1 A chain binds to a conserved stem-loop in the 28S rRNA known as the sarcin-ricin domain [159]. Expression of SLT-1 A chain

mutants in yeast have identified residues tyrosine 77, glutamic acid 167, arginine 170 and tryptophan 203 as critical residues in its catalytic activity [160-162]. There is high sequence homology between all members of this class of RIPs in regions involved in forming the catalytic cleft.

1.6.3 Structure of SLT-1

SLT-1 is composed of a 32 kDa A subunit which inserts via its C-terminal domain into the central pore created by the pentameric arrangement of five identical B subunits (7.7 kDa) (Figure 1.4). The A subunit consists of an enzymatic A_1 chain (27 kDa) and a C-terminus A_2 chain that associates with the B subunit pentamer. SLT-1 B subunits act as lectins and recognize glycolipids that contain the terminal disaccharide Galα1-4Galβ in order to enter into target cells [163]. SLT-1 specifically binds to the carbohydrate moiety on the glycolipid called globotriaosylceramide (Galα1-4Galβ1-4glucosylceramide, CD77, Gb3) [163-165]. CD77 is present on a number of cell types including platelets, gut epithelial cells, endothelial and epithelial cells in renal glomerulus and on germinal center tonsillar B lymphocytes [165-168]. NMR and crystallographic studies have identified one site per each B subunit monomer as the functional binding site for Gb3 [169, 170].

Receptor binding is the first step in the process of intoxication of cells by SLT-1. Once bound to cells, the receptor-toxin complex is internalized by a clathrin-dependent mechanism and is routed in a retrograde manner through the Golgi apparatus and to the ER and the enzymatic A subunit is retrotranslocated to the cytosol [171]. Ricin, PE, pertussis toxin, CT and the *E. coli* heat labile enterotoxin share the same characteristic

routing pattern (Figure 1.5). Cells that are normally sensitive to SLT-1, ricin, PE, PT, CT and the *E. coli* heat labile enterotoxin are protected by a drug called Brefeldin A which disrupts Golgi apparatus [172-177]. Even though these cells can internalize the toxins, their insensitivity illustrates the relevance of routing through the Golgi apparatus [177]. Toxins that are routed to the ER (SLT-1, ricin, cholera, LT, PE, and PT) have lysine deficiency, predominantly in their catalytic domain. The catalytic domains of these toxins are believed to act as mis-folded proteins and use the ER-associated degradation pathway (ERAD) for escaping the ER and it has been proposed that they escape degradation in the cytosol due to their lysine deficiency [178, 179]. It is believed that the separation of the SLT-1 A_1 fragment from the holotoxin in the ER results in the exposure of a hydrophobic domain which can interact with membranes. The hydrophobic C-terminal peptide of SLT-1 A_1 chain has been shown to have membrane insertional properties in experiments with cell free membranes [180].

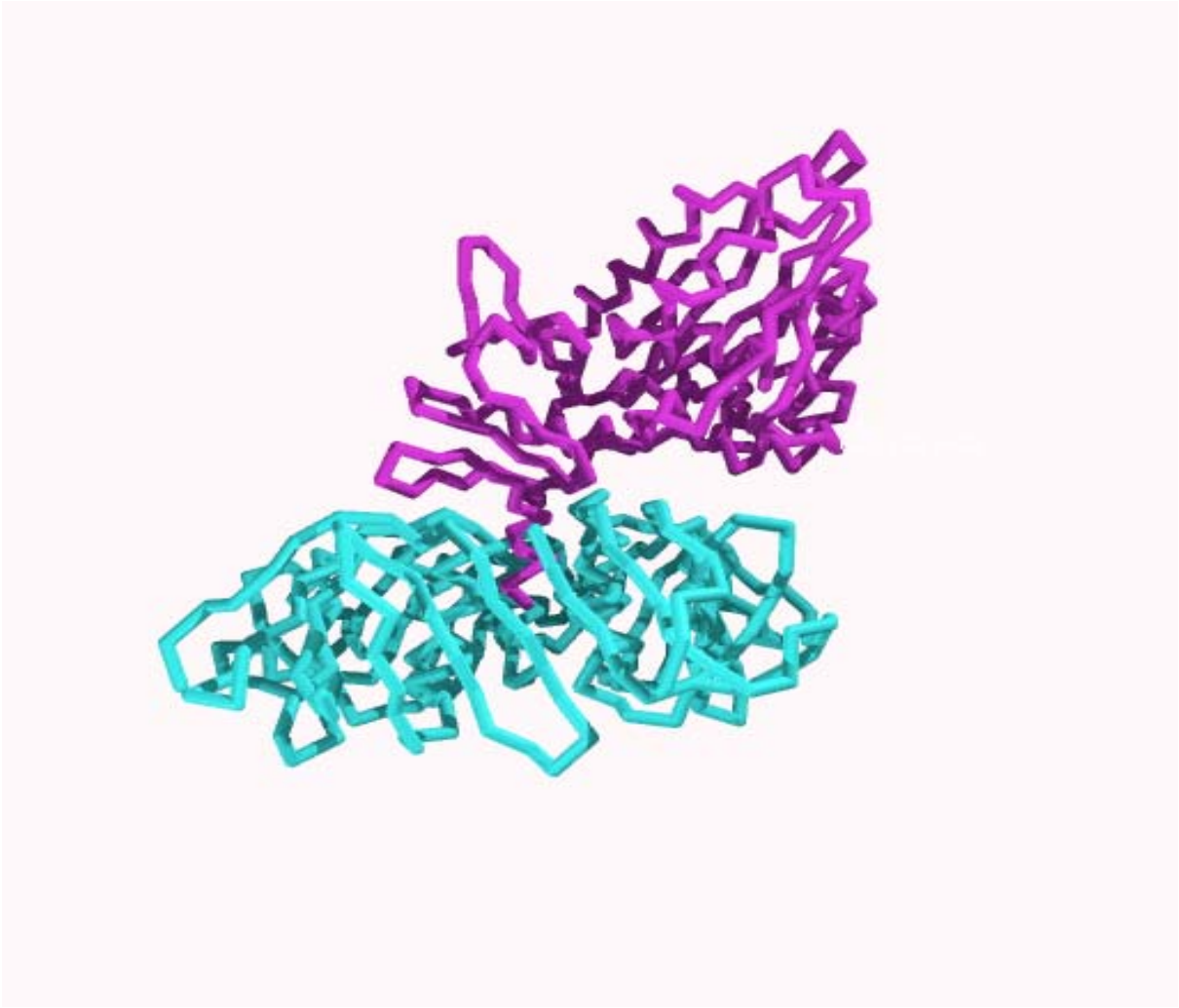

Figure 1.4: An α–carbon backbone representation of SLT-1.

The A subunit consists of two domains, namely the catalytic A_1 domain and A_2 domain (both shown in purple). The A_2 domain inserts itself into the central hole formed by a pentamer of B subunits (shown in cyan). The A subunit is responsible for the ribosome inactivating function while the B subunit pentamer mediates binding and internalization of the toxin.

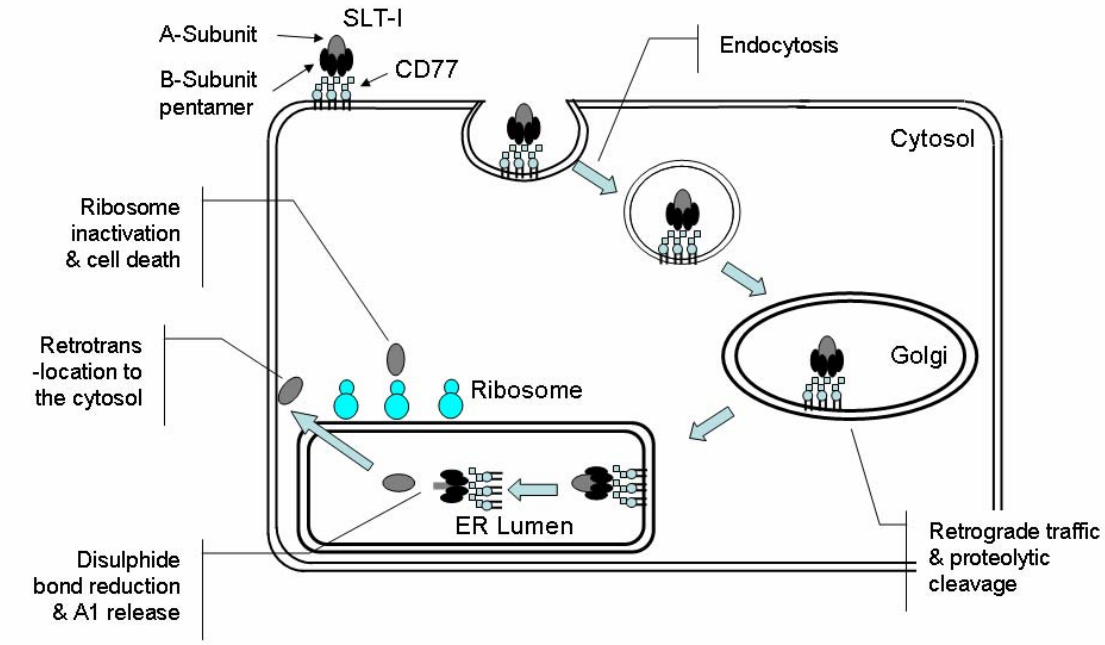

Figure 1.5: Routing of SLT-1 into mammalian cells expressing CD77 receptor.

The receptor bound holotoxin is internalized via clathrin-mediated endocytosis. The complex then undergoes retrograde transport through the Golgi apparatus (protease sensitive loop is cleaved by furin) to the endoplasmic reticulum (ER). In the ER lumen, the disulfide bond is reduced and the A_1 subunit of the toxin dissociates from the rest of the complex and enters the cytosol where it inactivates ribosomes.

1.7 Summary of previous work

Our laboratory has been working on the properties of SLT-1 and its uses in cancer therapy. The goal of our initial study was to establish the potential of SLT-1 in purging B cell lymphomas from bone marrow [181-183]. We had shown that SLT-1 can be successfully used to purge a human Burkitt's lymphoma cell line from a murine bone marrow graft *ex vivo* before transplantation into SCID mice while sparing bone marrow progenitor cells [182]. We then reported the expression of SLT-1 receptors on clinical tumor specimens and cell lines of cancers including breast cancer, multiple myeloma and lymphoma [181]. We also showed that the $CD34^+$ stem cells are resistant to the toxin which suggests the potential use of SLT-1 as an *ex vivo* purging agent in removing tumor cells from autologous stem cell grafts. There are many theoretical advantages to using SLT-1 as opposed to chemotherapeutic drugs. SLT-1 can in theory kill a cell at a low dose of 1 molecule per cell [139]. However the actual number of molecules will be higher due to the efficiency of routing and translocation events in cells [184]. SLT-1 can be cytotoxic throughout the cell cycle and is soluble in most aqueous media. Finally, it possesses a novel mechanism of action when compared to conventional drugs suggesting that known mechanisms of drug resistance will not counter the action of SLT-1. However, the use of SLT-1 is limited to *ex vivo* application because its toxicity includes endothelial cell damage and hemolytic uremic syndrome.

1.7.1 Combinatorial libraries based on SLT-1

We later developed the concept of modifying the SLT-1 template to target any cancer cell. Combinatorial SLT-1 libraries were created by randomly mutating two discontinuous loop regions of the B subunit that were previously identified as essential for its wild-type receptor binding function [5]. More specifically toxin libraries were constructed with residues randomly mutated at 9 positions, namely residues 15–19 (loop 1) and residues 30–33 (loop 2) (Figure 1.6). Since all toxin variants retain their cytotoxicity, this property was used as a search engine to identify mutants from these libraries that were able to kill target cells expressing internalizable receptors. Minimal searches from screening bacterial colonies randomly picked from this library have identified toxin mutants able to kill prostate and breast cancer cell lines resistant to the wild-type toxin.

A B

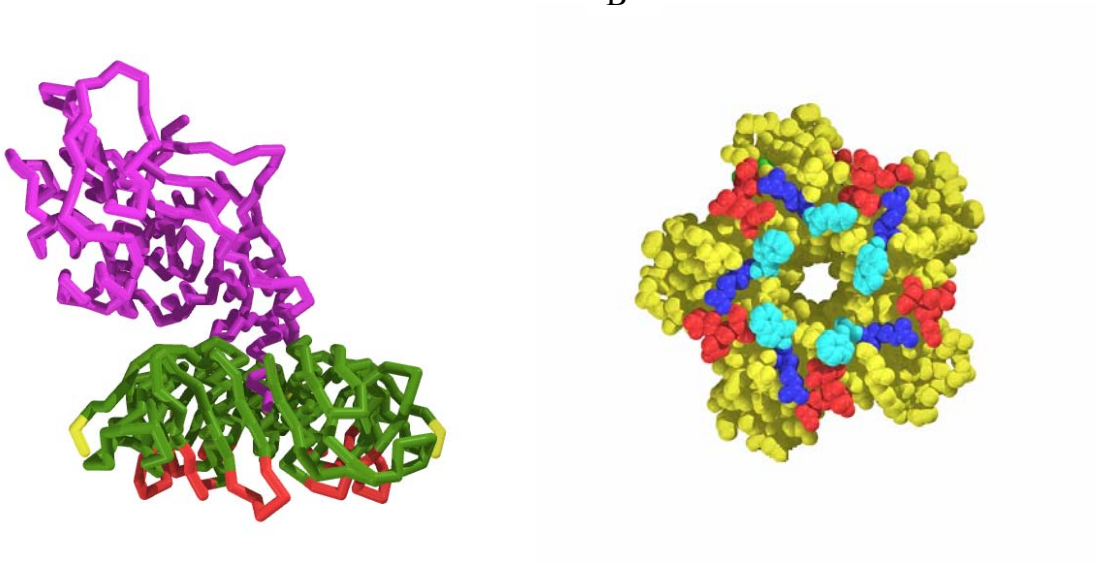

Figure 1.6: An α-carbon backbone representation of SLT-1 and space filling model of the B subunit pentamer.

A) The catalytic A subunit is shown in purple and the receptor binding B subunit is shown in green. Residues in two loop regions of the B subunit (residues 15–19 in loop 1 and residues 30–33 in loop 2) responsible for receptor specificity of SLT-1 (in red) were selected as sites for randomization. B) The B subunit pentamer showing the 3 sites that play a role in binding CD77. Site 1 is shown in red and includes residues Asp17, Thr21, Glu28, and Gly60. Site 2 is shown in blue and includes residues Asp16, Asn32, Arg33, Asn55, and Phe63. Site 3 is shown in cyan and includes residues Asp18, Trp34 and Asn35.

1.7.2 Advantages of SLT-1 libraries

Toxin libraries provide a strategy to delineate the spectrum of receptors on eukaryotic cells. The development and screening of such libraries offer practical outcomes such as the rapid discovery of specific toxins able to destroy cancer cells. This approach does not suffer from the present limitations associated with immunotoxins or other constructs where such constructs must be re-engineered to be properly routed and processed by cells. More importantly, there are no *apriori* assumptions made about the nature of the receptors to be targeted on tumor cells. Another feature that was of an advantage was the multi-valency (pentamer) of the B subunit which may provide binding with higher avidity. Even though these libraries demonstrated the proof-of-concept for a library based on a protein toxin, some challenges existed in screening such libraries.

1.7.3 Challenges of SLT-1 libraries

It was experimentally observed that the stability and oligomerization properties of the binding subunit (B pentamer) are sensitive to the introduction of multiple mutations within the B subunit sequence. This finding is not surprising considering the compact packing and highly ordered structure of the B subunit pentamer as evident from its crystal structure [149]. A major consequence of perturbing the B subunit was the lack of expression or the rapid degradation of most SLT-1 mutants within such libraries. A peptide domain has recently been introduced at the C-terminus of the B subunit of SLT-1 [185], a site previously shown to tolerate the insertion of short peptide antigens [186]. It may thus be possible to insert a peptide library element at the C-terminus of the B subunit. Unfortunately, such B subunits could not be reconstituted with their A chain. The second challenge in developing such libraries relates to the size and complexity of

the SLT-1 AB_5 template itself, features that reduce the penetration potential of such targeted agents into solid tumors and potentially increase their immunogenicity. Although these molecules are considerably smaller than mAbs, their sizes were still of the order of 70 kDa. Tissue penetration is directly related to the size of the targeting agent: the smaller the targeting agent, the better the penetration [57, 58].

1.8 SLT-1 A chain libraries

In this thesis, we propose to engineer a receptor binding site in the A chain by inserting or embedding short combinatorial peptide libraries within its scaffold. A careful analysis of the A chain structure revealed several sites that could accommodate local structural perturbations outside the immediate environment of its catalytic domain. However, the site to be used has to be assessed carefully for being ideal for inserting a ligand peptide without compromising other desired properties of the template.

Residues 1-239 were defined as representing the minimum catalytic domain needed for toxicity of the A_1 fragment when tested in a rabbit-reticulocyte lysate assay [187]. Secondly, residues 240 to 245 are necessary to facilitate the escape of SLT-1 A_1 from the ER lumen [187]. The toxin A subunit contains two cysteines (Cys242 and 261) which form a disulphide bond. The loop region flanked by the two cysteines is referred to as the protease sensitive loop and contains the motif R-V-A-R, which is a substrate for cleavage by furin following the A chain routing into susceptible cells or by trypsin *in vitro*. This cleavage separates the N-glycosidase containing 27.5 kDa A_1 from the 4.5

kDa A_2 fragment (Figure 1.7). Like many other bacterial toxins, the toxicity of the A subunit of SLT-1 is enhanced by proteolytic cleavage [188]. The two fragments are covalently linked by the disulphide bond and remain associated with the B subunit pentamer until after the reduction of the disulphide bond which occurs in the ER lumen [189]. In the crystal structure, the disulphide bond is seen but not residues including 243-257. There are two possible explanations for the absence of structure associated with residues 243-257 in the crystal structure: the loop is intrinsically disordered or the loop was cleaved during purification [149].

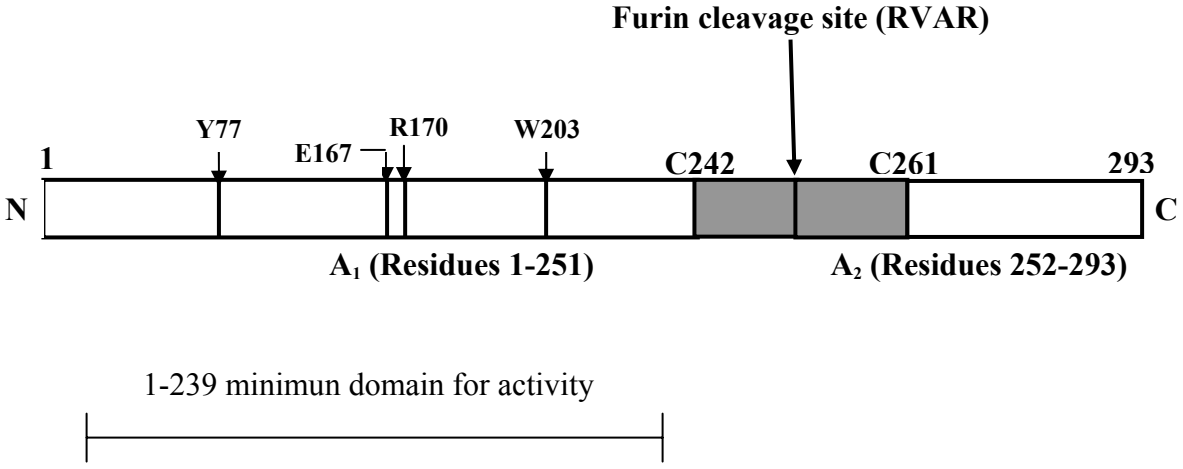

Figure 1.7: A schematic diagram showing the A_1 and A_2 chains of SLT-1.

The A chain is composed of 293 amino acids and is cleaved by furin at the C-terminus of residue 251(Arg). The protease sensitive loop (shaded) is flanked by two cysteine residues (242 & 261) and the furin cleavage site is indicated by a long arrow. Furin cleavage of the toxin leads to the generation of an A_1 catalytic fragment (first 251 aa) and an A_2 (42 aa) fragment. The 4 residues crucial for catalytic activity are shown by small arrows.

1.9 Thesis Objectives

Considering all the challenges of the holotoxin as a template for combinatorial library, one could simply focus on creating libraries using the catalytic A chain alone. Interestingly, most of the functional properties of SLT-1 reside within the cytotoxic A subunit (A_1 fragment) covering residues 1 to 251 of the A subunit. I thus propose to engineer a receptor binding site in the A chain by inserting short combinatorial peptide libraries within its scaffold. The protease sensitive loop region of the A chain was selected as a ligand site since it is naturally constrained by a disulfide bond (Cys-242 and Cys-261), is situated outside the minimal catalytic domain of the A chain (residues 1-239; [187], and is accessible to large protein entities such as proteases. Furthermore, the A chain does not have any known receptor binding function.

The concept of combinatorial libraries based on a toxin is novel and interesting for a number of reasons. Toxins are very potent cytotoxic agents and one molecule of the SLT-1 A chain in the cytosol can kill the cell [139]. Their potency is due to the fact that they are enzymes with a high turnover rate. Another reason for their potency is the fact that they are foreign to mammalian cells which makes their activities not regulated by established cellular pathways. The third reason for their potency is due to the fact that they are very stable in hosts; the enzymatic domains are especially very stable and resist proteolytic degradation. More importantly toxins target common and conserved components of mammalian cells. The ribosome is the target of RIP, so the toxins have to be internalized to exert their effect on cells. A surface of a cell can be easily probed for markers that can be internalized with such a toxin library leading to the identification of

toxin variants that can target as well as kill a cell of interest. Hence, this strategy can also serve a role in identifying novel receptors on cancer cells.

The objective of my thesis was to overcome some of the limitations that were associated with the original SLT-1 library approach by re-designing libraries around the simpler A chain itself. Our study explores the concept of compressing all functional features present in the SLT-1 AB_5 complex (> 70 kDa) into its catalytic A_1 domain (30 kDa) with a view to creating cell-targeted single chain ribosome-inactivating proteins.

Specifically, my first objective was to select a site in the A chain of SLT-1 that can withstand insertion of a peptide without affecting the expression and the function(s) of the protein. I demonstrated that a 7-residue long peptide element can be inserted within residues 245 and 246 of an exposed loop region (protease sensitive loop; residues 242-261) of the SLT-1 A chain; that this insertion does not affect the expression of stable and functional protein. My second objective was to construct an SLT-1 A chain tripeptide library and verify whether the majority of constituent variants were *de facto* expressed in bacteria, and whether the library could be mined for ligands recognizing a known target. The library was constructed by introducing a random tripeptide element within the known mucin MUC-1 epitope PDTRPAP. It was screened by picking individual colonies and purifying proteins and testing them by ELISA. Our third objective was to construct a heptapeptide library in the A chain of SLT-1 protease sensitive loop and screen on cell lines that were resistant to the wild type toxin. The final objective of my thesis was to explore if existing ligands (available through other approaches) to known

receptors on cells can be inserted within the protease sensitive loop or anywhere on the A chain in order to target and eliminate those cells.

1.10 Thesis Organization

In chapter 1, the promise of targeted protein-based therapeutics is discussed. Also, combinatorial library strategies are discussed. This chapter lists limitations of mono-clonal antibodies and introduces other protein scaffolds. Specifically, the use of SLT-1 as a protein scaffold is presented.

In chapter 2, I have identified a region in the protease sensitive loop of SLT-1 A chain to insert a peptide as a targeting moiety. A seven amino acid peptide, PDTRPAP, from the MUC-1 tandem repeat which binds a mAb was inserted and shown to bind to the mAb while maintaining toxicity.

In chapter 3, I have described the successful construction of a simple tripeptide library within the seven amino acid epitope described above. The library variants were screened exhaustively using an ELISA-based assay to reconstitute the known epitope. I explored the entire diversity of the library and identified the expected number of TRP peptides (3), proving that the constructed library expressed most of the expected mutants of the SLT-1A chain.

In chapter 4, the seven amino acid library was inserted in the protease sensitive loop of SLT-1 with a view to finding new toxin variants able to kill cancer cells. This chapter

highlights the potential for using a cytotoxic function of a protein template as a screening tool.

Finally, a summary and future directions are provided in Chapter 5.

CHAPTER 2: VALIDATING A SITE FOR INSERTING PEPTIDE EPITOPE IN SLT-1A$_1$

2.1 Abstract

The directed evolution of a multifunctional protein template offers the potential of creating combinatorial protein libraries with one or more embedded search engines. This concept was established by our group with the construction of a Shiga-like toxin 1 (SLT-1) library harboring random mutations in its receptor-binding B subunit [5]. The conserved cytotoxic A chain was then used to identify new variants from this library able to kill cancer cells resistant to the wild type toxin [5]. Despite its advantages as a protein scaffold, the quaternary structure of SLT-1 could not be maintained in most variants when many residues were randomized simultaneously within its B subunit. Furthermore, SLT-1 is composed of 6 subunits (1A and 5 B subunits) and a smaller protein scaffold would be preferred in terms of increased tumor penetration [57, 58, 190] and reduced immunogenicity [127]. Hence, we explored the possibility of using the catalytic A_1 subunit as a scaffold for inserting a random peptide element. A seven amino acid peptide epitope (PDTRPAP) recognized by the anti-mucin mAb, *Onc*-M27, was first inserted within residues 245 and 246 of the SLT-1 A subunit (SLT-1A^{PDTRPAP})

protease sensitive loop without loss of catalytic activity. The epitope was detected by Western blot analysis and by ELISA in the context of the toxin variant, indicating that the site of the library insert was readily accessible to large proteins such as IgGs. The peptide insertion at this site did not prevent furin from cleaving the protein at the expected site which readily leads to the generation of a single chain protein with the inserted peptide ligand.

2.2 Introduction

Large protein templates such as cell-surface determinants, immunoglobulins, adapter proteins and enzymes display a modular architecture in which protein domains exist either as distinct subunits or as definable motifs embedded into a single peptide chain [100, 133-138]. Conceptually, these constant functional domains could be employed as embedded search engines to mine such protein libraries with the aim of identifying variants with altered functional features.

Combinatorial toxin libraries based on the SLT-1 template have been constructed and screened to identify toxin variants able to recognize and bind specifically to new receptors on cancer cells [5]. In this earlier study, random mutations were introduced into two discontinuous loop regions of the B subunit previously identified as essential for its wild-type receptor-binding (CD77) function. This library of SLT-1 toxins with altered receptor specificities was subsequently mined using the cytotoxic A subunit function as a search engine to identify mutants able to kill target cells expressing internalized receptors [5]. However, the quaternary structure of the AB_5 scaffold introduces folding constraints, which are often not met if several residues within each B subunit are simultaneously mutated. The frequently observed consequences of such mutations are the loss of pentamer formation and the rapid degradation of toxin variants.

Interestingly, most of the functional properties of SLT-1 reside within a catalytic fragment of its cytotoxic A subunit (A_1 fragment) covering residues 1 to 251 of the A subunit. One solution to the structural constraints associated with the AB_5 scaffold may

thus be to redesign the library template solely around the simpler A_1 fragment itself. The objective of the present study was to demonstrate that the structural complexity associated with the AB_5 template of SLT-1 (70 kDa) can be simplified by introducing a receptor-binding domain within its catalytic A_1 fragment (residues 1-251 of SLT-1 A, 30 kDa) thus removing the need for its remaining A_2-B_5 protein complex. The 7 amino acid peptide representing a well known tumor-associated epitope, namely the MUC-1 tandem repeat (PDTRPAP), was inserted in a selected site within the protease sensitive loop of SLT-1 A chain to verify if the site is suitable for embedding a library to be screened using binding as well as functional assays.

2.3 Materials and Methods

2.3.1 Cell lines, antibodies, and bacterial strains

The VERO cell line (African green monkey kidney cells) were purchased from ATCC (Manassas, VA) and cultured at 37°C in Minimum Essential Medium (MEM) supplemented with 10% fetal calf serum (FCS). Hybridomas generating monoclonal antibodies reactive against mucin glycoproteins were a gift from Peter Linsley [191]. The mAb *Onc*-M27 used in this study was purified by protein A affinity chromatography. The anti-SLT-1 A chain polyclonal antibody was generated by immunizing rabbits with a detoxified form of the A chain (reduced catalytic activity). DNA sequencing and cloning steps were performed using the *E. coli* strain DH5α (Invitrogen, Carlsbad, CA) while the strain JM101 (Promega, Madison, WI) was employed for the recombinant production of wild-type SLT-1 and all its variants.

2.3.2 Construction of SLT-1 expression vectors and embedded libraries

The 7-amino acid long human mucin MUC-1 peptide PDTRPAP was inserted into the SLT-1-A chain between residues 245 and 246 (Figure 2.1) using a PCR-based approach (described in Figure 2.2). The reason for choosing this approach for cloning versus any other method of cloning was due to the lack of unique restriction enzyme sites in this region of the gene. Briefly, two flanking primers A and B containing the restriction sites Hind III and Pst I were annealed to the 5' and 3' end of the SLT-1 operon and two mutagenic (overlapping) primers containing the inserted nucleotide sequence were used to build the construct. The 5'-end of the A subunit was amplified with primers A and C, and the 3'-end with primers B and D. The resulting overlapping fragments were annealed at an equimolar ratio followed by amplification of the full cassette with primers A and B. The final PCR product was digested with the restriction enzymes Pst I and Hind III (Invitrogen) and cloned into an SLT-1 constitutive expression vector (pECHE 9A) (Molecular Templates Inc., Toronto) (Figure 2.3). The construction was confirmed by diagnostic restriction analysis with Nsi I (Nsi I was a unique restriction site in the wt-SLT-1 which is lost when the peptide was inserted between residues 245 and 246) and subsequent sequence analysis of the entire cassette region. A diagram of the pECHE vector map is given in Figure 2.3. Other constructs used in this study were generated using a similar strategy with the primers listed under Figure 2.2.

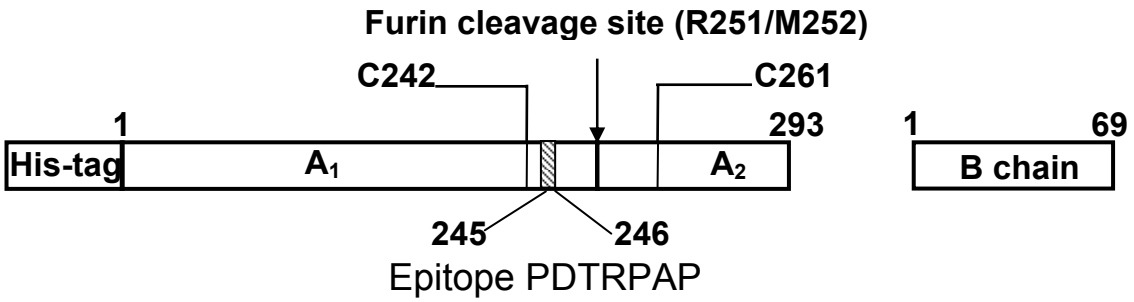

Figure 2.1: A schematic illustration of SLT-1 construct comprising its A and B subunits.

A histidine tag was inserted at the N-terminus of the A chain for affinity purification. Furin cleavage occurs between residues 251 and 252 of the A subunit (arrow) within its protease-sensitive loop (residues 242-261), releasing a cytotoxic A_1 fragment (residues 1-251) and an A_2 fragment (residues 252-293) non-covalently linked to the B subunit pentamer. The peptide epitope PDTRPAP was inserted between residues 245 and 246 of the A_1 domain.

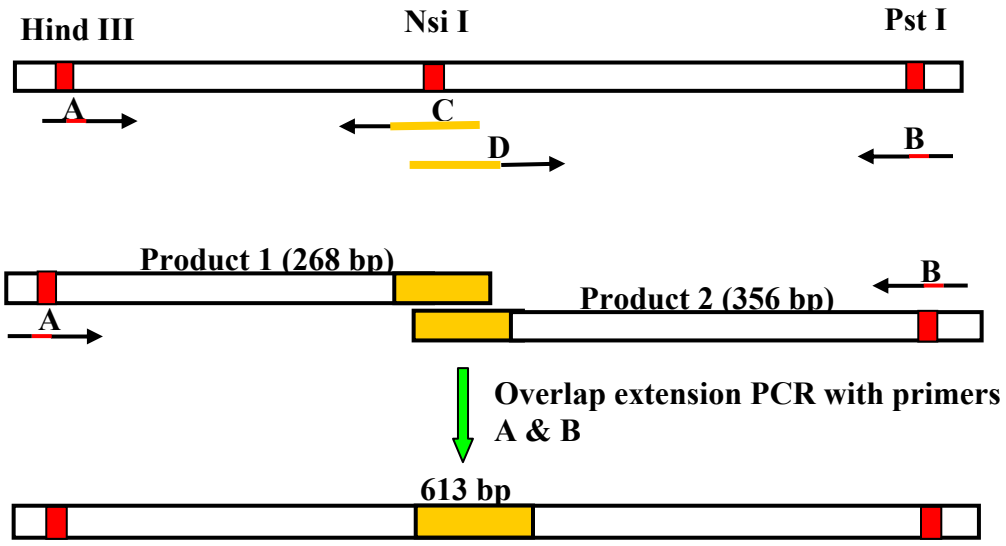

Figure 2.2: Insertion of a 7 amino acid peptide into the A chain of SLT-1 using a PCR based approach.

The wt-SLT-1 plasmid was used as the initial template for PCR. The first PCR was done using the flanking primer A (containing a restriction enzyme site, Hind III) and the mutagenic primer C (which had part of the new peptide sequence). The second PCR was done using the flanking primer B (containing a restriction enzyme site, Pst I) and mutagenic primer D (it had part of the PDTRPAP). The two products were allowed to anneal and then amplified using the two flanking primers, A and B. The two RE sites shown in red were used for cloning the PCR products into pECHE9A. The restriction sites on the primers and the gene are shown in red. The primers used for this construct are listed below.

Primer A: GTT ACT GTG ACA GCT GAA GCT TTA CGT TTT CG

Primer B: GAG AAG AAG AGA CTG CAG ATT CCA TCT GTT G

Primer C: GCT GGT CGC GTG TCT GGA TGA TGA TGA CAA TTC AGT AT

Primer D: GAC ACG CGA CCA GCT CCA GCA TCG CGA GTT GCC AGA ATG

Other primers used in this chapter:

Muc P-A: CGA TGC TGG AGC TGC TCG CGT GTC TGG

MUC T-S: GGA GCT GGT CGC GAG TCT GGA TGA TGA TGA CAA TTC AG

Muc R-K: GCT GGA GCT GGT TTC GTG TCT GGA TG

10xFSEQ: GGT GAC AGT AGC TAT ACC ACG (Primer used in sequencing constructs)

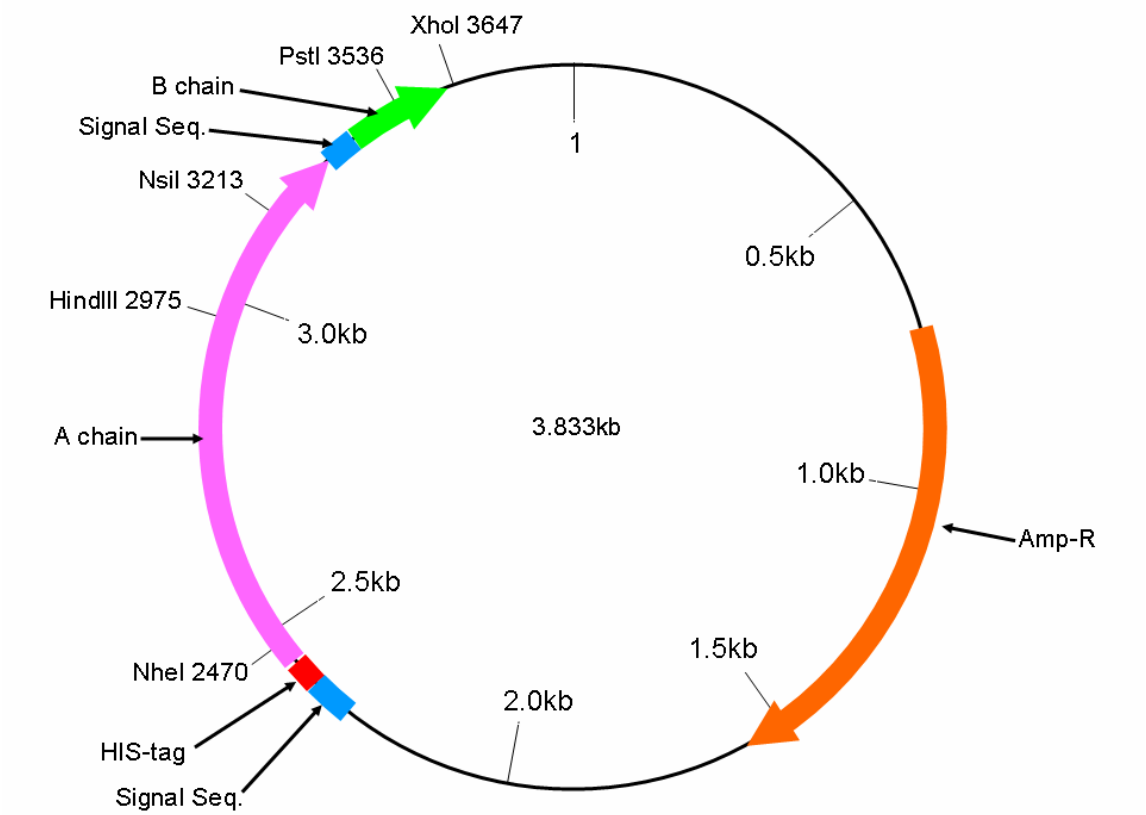

Figure 2.3: Vector map of pECHE 9A.

The signal sequences for the A and B chains are shown in blue. The His-tag at the N-terminus of A chain is shown in red. The A chain is shown in magenta and the B chain is shown in green. The critical restriction enzyme sites used during the construction of SLT-1A^{PDTRPAP} are marked (Hind III, Nsi I and Pst I). The SLT-1 gene was placed under the control of the natural promoter of SLT-1. The plasmid also contains the amphicillin resistance gene.

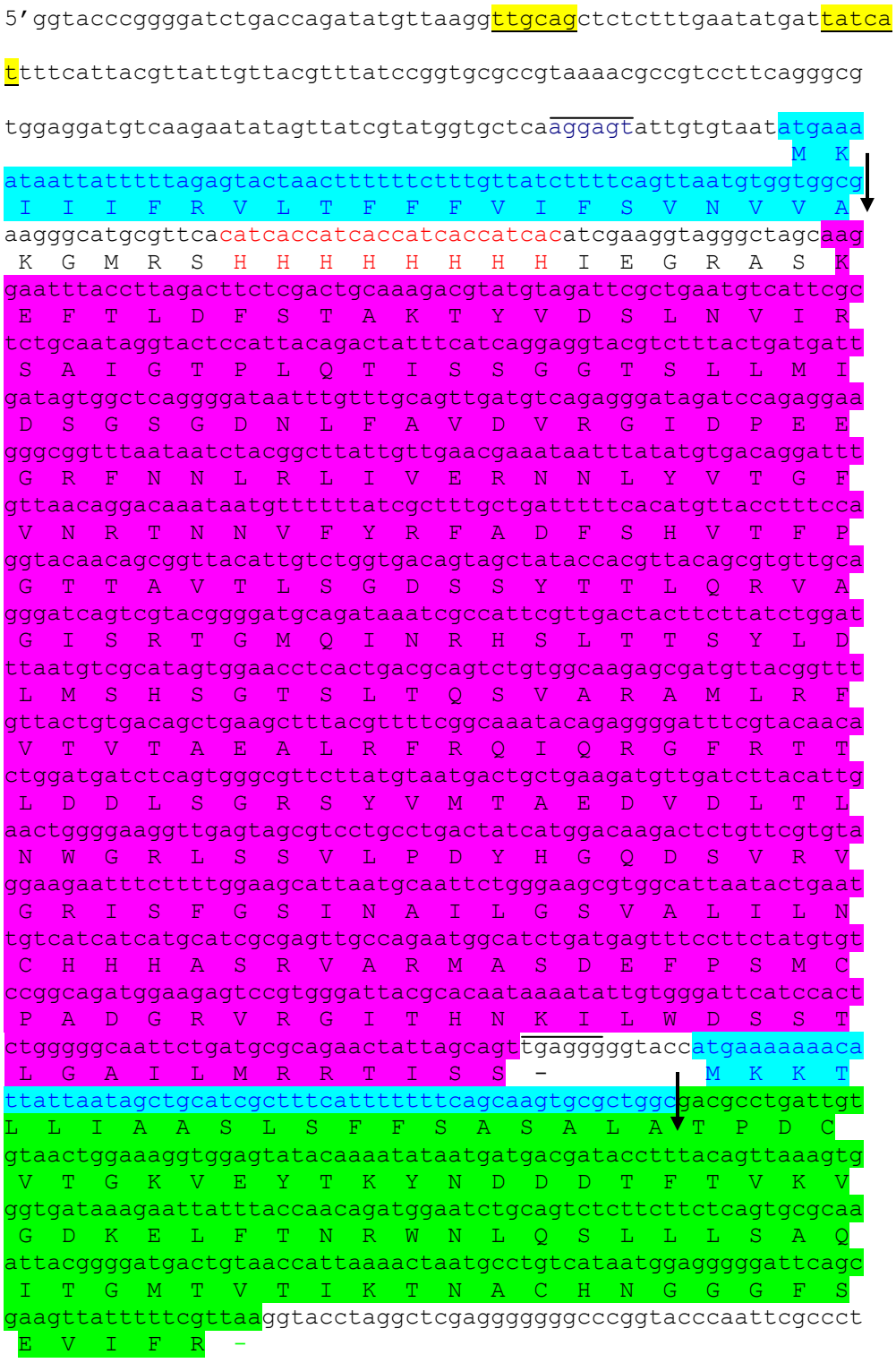

Figure 2.4: The sequence of the SLT-1 gene and the translated protein sequence in a pECHE vector.

The A subunit is highlighted in purple and the B subunit in green. The signal sequences are shown in blue and the arrows indicate the signal peptide cleavage sites. The ribosome binding sites (RBS) at the 5’ end of A and B subunits have lines above the

sequence while the two promoter elements at the 5' end of the A chain are underlined and shown in yellow.

2.3.3 Expression and purification of SLT-1A

Wild-type SLT-1 and SLT-1A^{PDTRPAP} contain histidine tags at the N termini of their A chain (Figure 2.1). These toxins were extracted from 6-liter bacterial culture pellets and purified by metal affinity chromatography on a Ni-NTA HIS-SELECT column (Sigma-Aldrich). The A-subunits were selectively recovered by treating the column with 50 mM phosphate buffer, 300 mM NaCl, and 10 mM imidazole, pH8.0 containing 6 M guanidinium-HCl, a denaturing condition which removes the B subunit pentamer that is non-covalently associated with its A chain. The A subunit bound on the column was re-folded by subjecting the protein to decreasing amounts of guanidinium-HCl in a step-wise manner (ie. 80 %, 60%, 40%, and 20% guanidinium-HCl). The columns were then washed with washing buffer (50 mM phosphate buffer, 300 mM NaCl, and 10mM imidazole) prior to elution of the toxins with a buffer containing 150mM imidazole (50 mM phosphate buffer, 300 mM NaCl and 150 mM imidazole). Proteolytic cleavage under reducing conditions to release the cognate A_1 fragments from their respective A chain was achieved by incubating the purified A subunits with recombinant furin (New England Biolabs, MA) in 100 mM MES buffer (pH 6.0), 5 mM $CaCl_2$ and 1mM β-mercaptoethanol. Typically, 1 mg of SLT-1-A chain was cleaved with 10 units of furin for 48 hours at 30° C and then subjected to washing with PBS containing 100 mM DTT and subsequent buffer exchange into PBS using an Amicon ultra-filtration unit (Milli-pore; 10 kDa cut off). The resulting A_1 fragments were isolated by a second round of

affinity purification on Ni-NTA Superflow resin. The toxin was assessed for catalytic activity (Section 2.3.5) after each stage of purification.

2.3.4 Mapping the mucin MUC-1 peptide epitope recognized by the mAb *Onc*-M27

The monoclonal antibody *Onc*-M27 recognizes a peptide determinant within the mucin MUC-1 tandem repeat [191]. The 20-residue tandem repeat has the following sequence: GVTSAPDTRPAPGSTAPPAH. The precise epitope for *Onc*-M27 within this sequence was mapped by synthesizing a series of 20 overlapping octapeptides spanning the entire sequence of the tandem repeat. The peptides were assembled by Fmoc chemistry on aminomethylated grafted plastic lanterns (Mimotopes, Raleigh NC) following previously described methods [192, 193]. Six copies of each peptide were synthesized and the resulting MUC-1 octapeptides, covalently attached to a lantern support, were incubated in blocking buffer (1% [w/v] bovine serum albumin, 1% [w/v] ovalbumin, 0.1% [v/v] Tween 20 in 10 mM phosphate-buffered saline [PBS, pH 7.4]) for 1 hour and subsequently incubated overnight at 4˚ C in wells containing the mAb *Onc*-M27 (1 µg) prepared in blocking buffer. After 4 washes in PBS containing 0.05% (v/v) Tween 20, the lanterns were incubated for 1 hour in wells containing anti-mouse Ig-HRP conjugate (1:1,000 dilution). All lanterns were finally washed with PBS and the binding of mAb *Onc*-M27 was detected by first incubating the lanterns in 96-deep well plates containing ABTS (0.05% (w/v) 2,2'-azino-bis(3-ethylbenzthiazoline 6-sulfonate) dissolved in 0.1 M sodium phosphate-0.08 M citric acid (pH 5.0) and 0.003% (v/v) hydrogen peroxide per well and by finally transferring the colored solutions into microtitre plates after a 20-minute incubation period. Absorbance readings at 450 nm were recorded with a microtitre plate reader.

2.3.5 Cell viability assays

The sensitivity of VERO cells to wt-SLT-1 and SLT-1 variants was determined by seeding 2,000 cells/well into 96-well flat-bottom microtiter plates (NUNC Inc., Naperville, IL) and culturing overnight at 37° C to a semi-confluent monolayer. The cells were then treated with purified toxins diluted in phosphate buffered saline (PBS) for 1 hour at 37° C, followed by removal of excess toxin. Once fresh medium was added to the wells, the plates were returned to 37° C for 48 hours. The plates were then fixed with 10% w/v ice-cold trichloroacetic acid for 30 min at 4° C, washed extensively with water, and stained with a 0.4% w/v solution of sulforhodamine B in 1% v/v acetic acid to assay total cellular protein [194]. After extensive washing with 1% v/v acetic acid, the residual dye was released with 10 mM Tris-HCl (pH 10.0) and the absorbance at 570 nm was recorded using a microtitre plate reader.

2.3.6 *In vitro* coupled transcription and translation assay

The ribosome-inactivating property of SLT-1 and variants was measured using an *in vitro* coupled transcription/translation reticulocyte lysate assay (TNT assay; Promega Corp, Wisconsin). Briefly, serially diluted, purified toxin variants were added to an assay mixture comprising rabbit reticulocyte lysate, SP6 RNA polymerase, amino acid mixtures, ribonuclease inhibitor and a plasmid containing the luciferase gene. The reactions were incubated at 30° C for 30 minutes. Luciferase expression (RLU/mg protein) was correlated to the level of protein synthesis in each sample. Usually 5 µl of the reaction mixture was added to 100 µl of Luciferase Assay Reagent (substrate) and mixed well. The light emitted when luciferase is mixed with the luciferin substrate is measured using a luminometer.

2.3.7 ELISA assay

Wells of 96-well ELISA plates (Nalgene Nunc, Rochester, NY) were coated overnight with 1 μg of wild type SLT-1, SLT-1A^{PDTRPAP}, SLT-1A^{PDSRPAP}, SLT-1A^{PDTKPAP}, SLT-1A^{PDTRAAP}. The variants were prepared in a 10 mM sodium carbonate buffer (pH9.0) for the coating stage. The wells were blocked for 1 hour with 0.5% w/v bovine serum albumin (BSA) and 0.5% v/v Tween 20 in PBS (blocking buffer). After washing the wells 3 times with PBS, they were treated for 1 hour at 37° C with 0.01 μg of mono-clonal antibody *Onc*-M27 prepared in blocking buffer. The mAb *Onc*-M27 (IgG1) recognizes the tripeptide epitope TRP in the context of the mucin MUC-1 tandem repeat sequence PDTRPAP [191]. The wells were washed with PBS and incubated for 1 hour with a 1:1,000 dilution of a goat anti-mouse IgG-peroxidase conjugate (Sigma, St. Louis, MO). TMB (3,3',5,5'–tetramethylbenzidine, Boehringer Mannheim, Mannheim) was used as a substrate to visualize the binding of *Onc*-M27 to toxins displaying the expected mucin MUC-1 epitope. A stock solution of the chromogen TMB (6 mg/ml in DMSO) was diluted to 100 μg TMB/ml in 0.1 M sodium acetate buffer (pH 5.5) containing 1.3 mM H_2O_2 [195]. The substrate reaction was developed in the dark and stopped by the addition of 1M H_2SO_4 after 30 minutes. Absorbance values were read at 450 nm using a microtitre plate reader. The ELISA was followed similarly for checking expression of toxin with an anti-SLT-1 A chain polyclonal antibody. A rabbit IgG-HRP conjugate was used as a second antibody for this ELISA.

2.4 Results and discussion

The protease sensitive loop was chosen as a site to embed a library. How could one verify whether such a site can tolerate changes without losing its ability to adopt a

defined tertiary structure or without becoming much less stably folded? Past studies have indicated that the conformation and sequence of an exposed loop may be rather crucial for the folding and the stability of the protein, even though the packing of secondary structural elements predominantly determine the three dimensional structure of the protein [196, 197]. Hence, we had to verify whether the structure of SLT-1 A chain is conformationally stable enough to support a variety of library sequences and to impose geometrical constraints to define their three dimensional structure. Therefore, we embedded a known peptide sequence in the protease loop (between residues 245 and 246) and looked at whether this insertion affected the expression and function of the resultant protein.

2.4.1 Expression in bacteria

Theoretically, the ease of production of a bacterial product such as SLT-1 A variants should be high when compared to that of other classes of protein-based therapeutic agents such as monoclonal antibodies and growth factors. However, our initial attempts to use commercially available expression vectors such as pET (Novagen) to express the A_1 chain in *E. coli* resulted in very low yields of toxin (Perampalam and Gariepy). We were able to express the attenuated version of the A_1 chain implying toxicity of this molecule towards the bacterial ribosomes. This is in accord with the literature suggesting that the Shiga toxin attacks bacterial ribosomes at higher concentrations [198]. This was further supported by the knowledge that ricin A chain does not attack bacterial ribosomes and it can be expressed in very high yields (40-50 mg/L culture) in bacterial expression systems [198-200]. We also experimentally observed that the bacterial

expression of A subunit variants of SLT-1 in the absence of its B subunit led to very low levels of protein expression (Bray, Perampalam, and Gariepy; unpublished results).

For these reasons, we have used the pECHE expression vectors developed by Molecular Templates Inc (MTI, Toronto). These vectors were designed in house to incorporate properties of the pUC expression vectors (amphicillin resistance) and the natural promoter of SLT-1 in *E.coli* which aids in the constitutive expression of the toxin in higher amounts (Figure 2.3). The nucleotide sequence of the A and B cistrons of SLT-1 were cloned from bacteriophage H-19B and both cistrons were preceded by the Shine-Delgarno sequences [201, 202]. The expression of A chain variants in the context of AB_5 holotoxins generated stable A chain variants with yields comparable to that of the wild-type toxin (2-10 mg/liter). A diagram of the SLT-1 construct used for expression is presented in Figure 2.1. The wild type B subunit thus appears to act as a chaperone for the A chain during protein expression and folding. In view of this advantage, all A chain variants were initially expressed as AB_5 holotoxins. In addition, an N-terminal octa-histidine tag was introduced at the N-terminus of all mutated A chains in order to subsequently isolate their respective A chains by metal affinity chromatography under denaturing condition. The A_1 fragment was generated by treating the A chain with furin followed by reduction and capturing on a metal affinity column [203].

2.4.2 Selection of a site within the sequence of the SLT-1 A_1 fragment for inserting a peptide ligand

Our first objective was to identify a site within the A_1 template that could tolerate the insertion of a peptide ligand domain without perturbing other functions associated with

this fragment. The selection of a site was based on three criteria. Firstly, the inserted peptide element had to be displayed on the surface of the A chain such that any peptide ligand from libraries designed using this altered AB_5 template would be exposed to the solvent and thus be able to potentially interact with cell surface receptors. Secondly, the insertion of the peptide library must occur at a site that would not cause a loss of catalytic activity since this activity is to be preserved and later used as a screening tool. It has been established that residues 1-239 of SLT-1 A are required for full catalytic activity while residues 240-245 are needed for retrotranslocation from the ER lumen to the cytosol [187]. So the insertion should take place outside of the 1-245 residues. Finally, the SLT-1 A subunit contains a protease-sensitive loop delimited by a disulfide bond linking Cysteine 242 to Cysteine 261. This loop region harbors a furin cleavage site (between residues 251 and 252 and requiring the sequence RAVR starting at residue 248) needed to create single A_1 chain toxins (Figure 2.1). This protease-sensitive loop indicates that this region of the loop is accessible to molecules such as proteases. The protease sensitive loop in SLT-1 A chain is naturally constrained due to the presence of a disulfide bond bridging Cys242 to Cys261. These three conditions led us to insert a peptide between residues 245 and 246 (Figure 2.1).

2.4.3 Accessibility of a heptapeptide ligand inserted between residues 245 and 246 of the SLT-1 A_1

To validate if the selected site was exposed, the heptapeptide epitope PDTRPAP was inserted within the A_1 fragment of SLT-1. This epitope represents part of the sequence of the mucin MUC-1 tandem repeat, a well-known tumour-associated antigen present on the surface of epithelial cancer cells [204]. The reason for selecting this specific peptide

for insertion is because there are a number of mAbs that recognize this linear epitope. The accessibility of the selected site (inserted peptide) to large molecules was evaluated using the monoclonal antibody *Onc*-M27 directed at this epitope [191]. A detailed peptide mapping of the epitope recognized by this antibody indicates that mAb *Onc*-M27 specifically binds to the tripeptide sequence TRP within this epitope (Figure 2.5). Mutating residues within this tripeptide region is sufficient to abolish binding to the mAb.

Table 2.1: ELISA results from engineered TRP variants

Clone	***DNA Sequence***	***Protein Sequence***	***Absorbance values (ELISA) (450nm)***
Engineered SLT1A^{PDTRPAP}	ACG CGA CCA	TRP	1.1±0.22
Engineered SLT1A^{PDSRPAP}	TCG CGA CCA	SRP	0.1±0.04
Engineered SLT1A^{PDTRAAP}	ACG CGA GCA	TRA	0.1±0.02
Engineered SLT1A^{PDTKPAP}	ACG AAA CCA	TKP	1.4±0.26

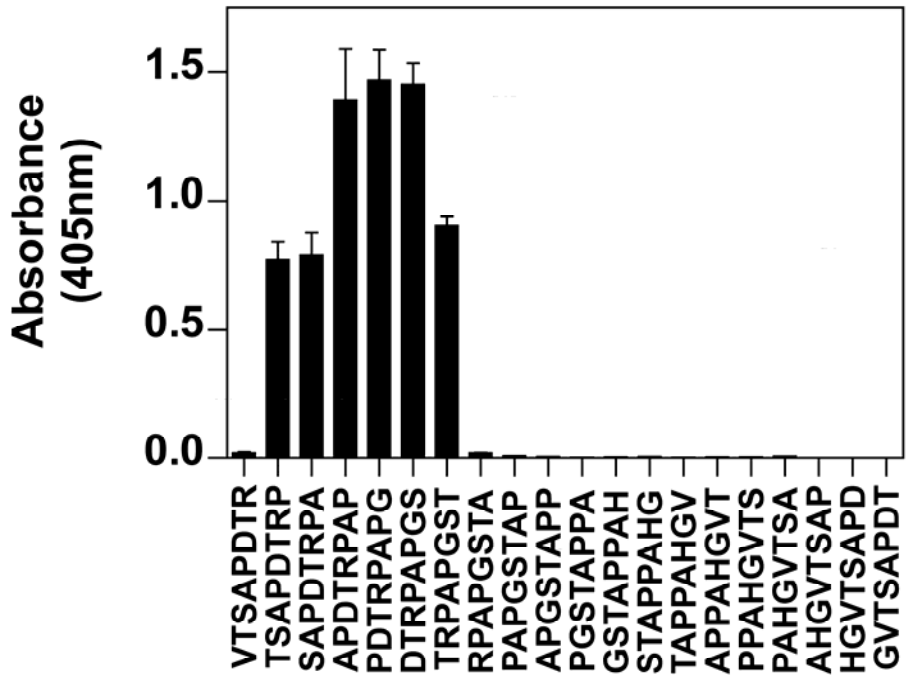

Figure 2.5: Mapping the mucin MUC-1 peptide epitope recognized by the mAb *Onc*-M27.

The precise epitope recognized by the mAb *Onc*-M27 within the MUC-1 tandem repeat was mapped by synthesizing a series of 20 overlapping octapeptides spanning the entire sequence of the tandem repeat. Each bar represents the average absorbance readings calculated for assays performed on six copies of each overlapping MUC-1 octapeptides. The tripeptide TRP was identified as containing the key residues defining the recognized epitope.

This toxin variant containing the PDTRPAP heptapeptide was termed SLT-1A^{PDTRPAP} and modeled α-carbon representations depicting its AB_5 and A_1 structures respectively are presented in Figure 2.6. The toxin variant was expressed in *E. coli* and purified to homogeneity by metal-affinity chromatography using the octa-Histidine tag at the N-terminus of its A chain. Purified wild-type SLT-1 and SLT-1A^{PDTRPAP} were character-

ized by SDS-PAGE and by Western Blot analyses using antibodies raised against SLT-1 A (rabbit anti-serum) or PDTRPAP (mAb *Onc*-M27). Similar levels of expression were observed for the A and B chains of both toxins (Figure 2.7). As expected, the band corresponding to the A chain of SLT-1A^{PDTRPAP} migrated more slowly than the wild-type SLT-1 A chain protein band, indicating the insertion of 7 additional amino acids. More importantly, subsequent ELISA assays confirmed that the epitope was accessible to the mAb *Onc*-M27 (Figure 2.7). An ELISA signal of around 1.0 was observed for the variant toxin as opposed to about 0.1 for wt-SLT-1. As a positive control for the ELISA assay, the 20 amino acid MUC-1 peptide (GVTSAPDTRPAPGSTAPPAH) was used. Toxin variants were also engineered, expressed and purified with conserved substitutions at each position within the key tripeptide region (Table 2.1). ELISA results demonstrated that conservative substitutions at the threonine (SLT-1A^{PDSRPAP}) and proline (SLT-1A^{PDTRAAP}) positions in the TRP sequence within the context of the full heptapeptide epitope essentially led to a loss of antibody binding and ELISA signal (Table 2.1). The conservative substitution of arginine to lysine (SLT-1A^{PDTKPAP}) yielded a stronger binding response indicating that the epitope could tolerate or favor such a change.

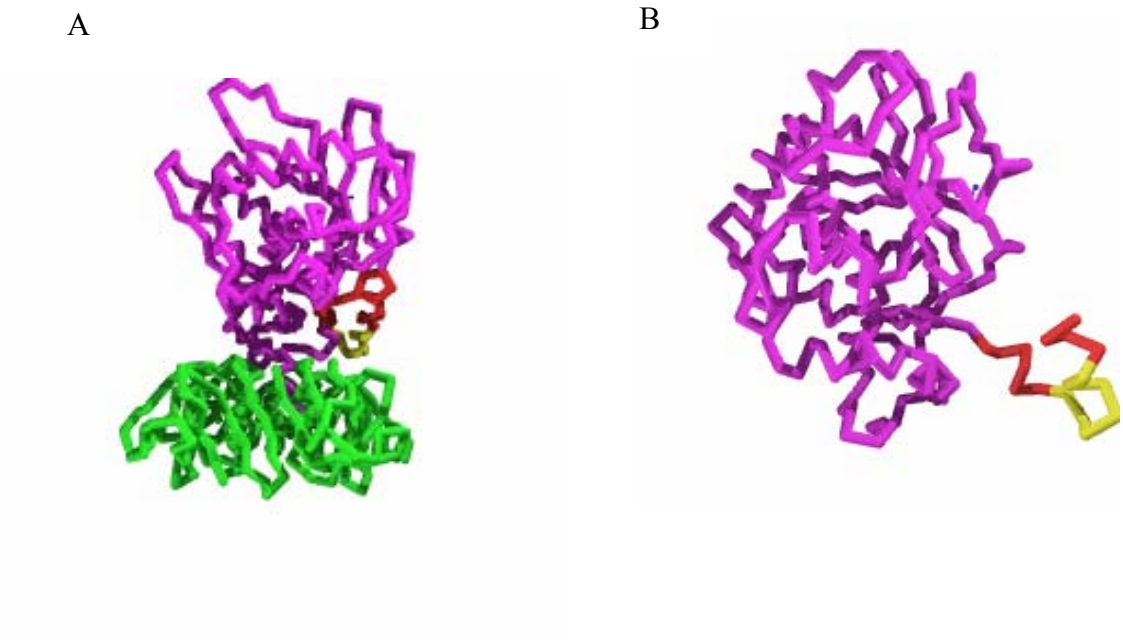

Figure 2.6: SLT-1 serves as a robust molecular template for the design and construction of combinatorial SLT-1 libraries

A) α-carbon chain representation of wt-SLT-1 derived from the crystal coordinates of Shiga toxin ([149] with the heptapeptide epitope (PDTRPAP; in yellow) inserted between residues 245 and 246 within the protease-sensitive loop (in red) of the A subunit (in magenta). The pentamer of B subunits is shown in green. B) Predicted α-carbon chain representation of the A_1 fragment of SLT-1 harboring the peptide epitope insertion (yellow). Coordinates for both models were derived by submitting the crystal structure coordinates and the desired site and inserted sequences (sequence of peptide and site of insertion) to SWISS MODEL [205, 206]**.**

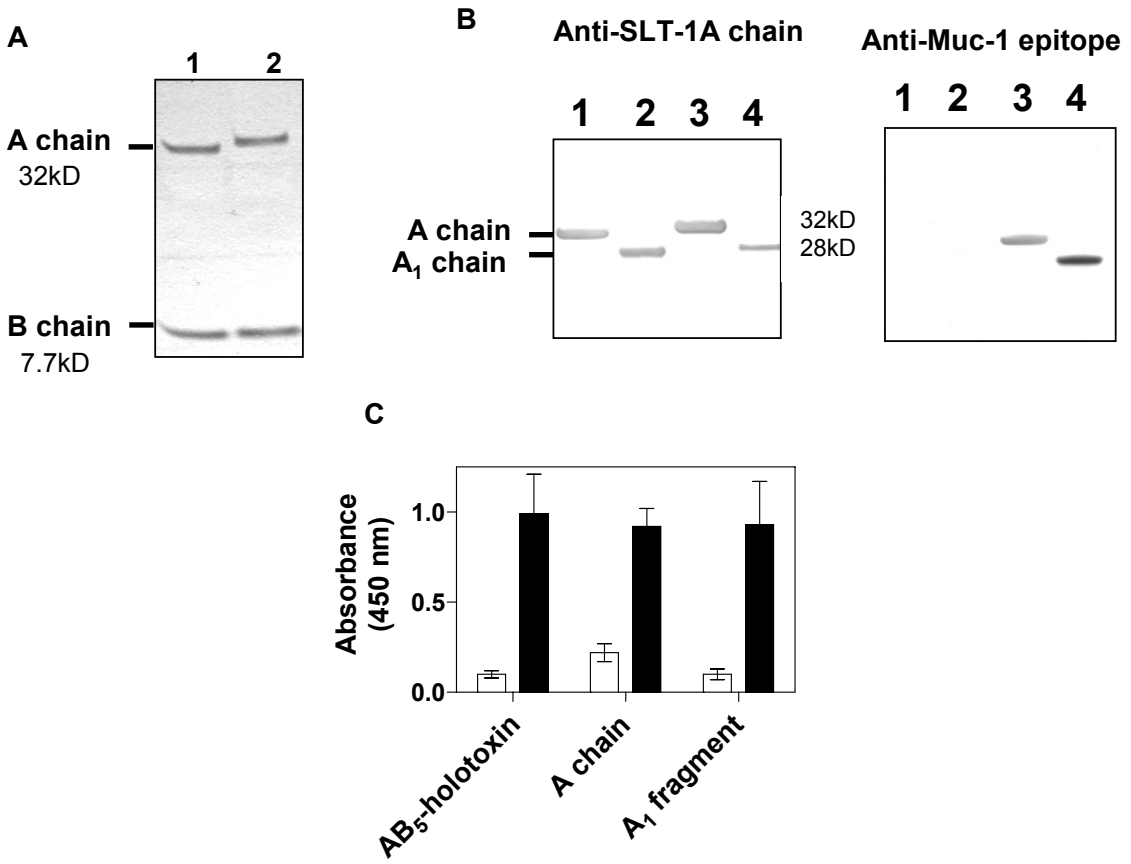

Figure 2.7: Effect of inserting a heptapeptide within the protease sensitive loop of the A chain of SLT-1.

A) SDS-PAGE gel stained with Coomassie blue showing the comparable expression of both chains (A and B) of His-tagged purified wild-type SLT-1 (lane 1) and SLT-1A^{PDTRPAP} (lane 2). B) Western blots of the purified A subunits and A_1 fragments of wt-SLT-1 and SLT-1A^{PDTRPAP} as revealed using a rabbit polyclonal anti-serum recognizing the SLT-1 A subunit (left panel) and the anti-MUC1 mAb, *Onc*-M27 (right panel). Lanes 1, 2, 3, and 4 contain wt-SLT-1, wt-SLT-1A$_1$, SLT-1A^{PDTRPAP}, and A_1 of SLT-1A^{PDTRPAP} respectively. C) ELISA results comparing the immunoreactivity of the A chain towards mAb *Onc*-M27 in the context of the intact wt-SLT-1 (white bar) and SLT-1A^{PDTRPAP} (black bar) holotoxins and their respective purified A subunits and furin-cleaved A_1 fragments. Bars represent the average of two experiments performed in triplicate.

2.4.4 The cleaved A_1 fragment contains the integrated peptide ligand

The octa-histidine-tagged A_1 fragment containing the peptide insert was readily isolated from its A chain following its treatment with furin and the reduction of the disulfide bond linking the A_1 fragment to the A_2-B_5 protein complex. Furin cleavage was monitored by Western blotting with the polyclonal antibody against SLT-1 A (Figure 2.7). The expected mass of the SLT-1 A_1 fragment was calculated to be 29,879 kDa and was confirmed by MALDI mass spectrometry. Similarly, the expected mass of 30,614 kDa for SLT-1A^{PDTRPAP} was experimentally verified by MALDI mass spectrometry. The furin-cleaved and disulfide-reduced A_1 fragment was shown to contain the inserted peptide by Western blotting with the mAb *Onc*-M27 (Figure 2.7). The epitope PDTRPAP was also detected by ELISA on the recovered A_1 fragment of SLT-1A^{PDTRPAP} using the mAb *Onc*-M27, confirming the presence of the integrated peptide ligand within the scaffold of the A_1 fragment (Figure 2.7). This study also confirms that insertion of peptide at this site does not inhibit cleavage of the toxin by furin.

2.4.5 The catalytic activity of SLT-1A^{PDTRPAP} is identical to that of the wt-SLT-1

The catalytic activity of wt-SLT-1 and SLT-1A^{PDTRPAP} A chains were compared using two separate approaches in order to establish that the peptide insertion had not resulted in a loss of enzymatic activity. AB_5 holotoxins corresponding to the wt-SLT-1 and SLT-1A^{PDTRPAP} share the same wild-type B subunit and can thus intoxicate Vero cells. Cytotoxicity curves depicting the concentration-dependent killing of Vero cells by both holotoxins are presented in Figure 2.8. The two toxins yielded super-imposed cytotoxicity curves suggesting that the peptide insertion did not have an impact on either the

folding of the toxin variant into an active AB_5 holotoxin or exhibiting catalytic activity (Figure 2.8). An *in vitro* coupled transcription/translation assay (rabbit reticulocyte lysate) was also used to assess the catalytic activity of the furin cleaved SLT-1A^{PDTRPAP} (A_1) in relation to the wild-type SLT-1 A chain. Both toxins were able to equally abolish the synthesis of luciferase reflecting that the N-glycosidase activities of the A chains are intact and not attenuated by the peptide insertion (absence of luciferin signal reported as relative light units [RLU]; Figure 2.8).

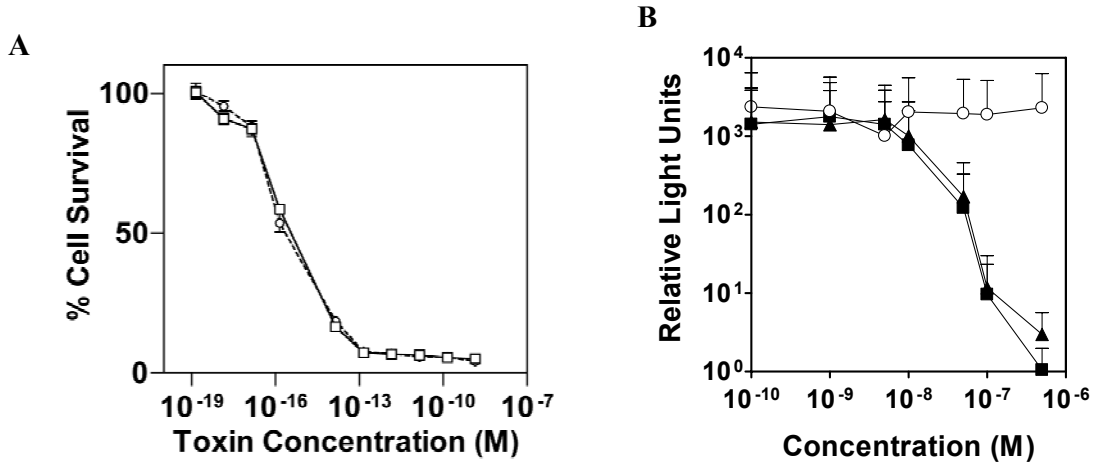

Figure 2.8: The heptapeptide insertion did not abolish the cytotoxicity or the ribosome inactivating property of the resulting SLT-1.

A) The ability of a SLT-1 toxin containing a peptide insertion to kill VERO cells (○) was comparable to that of wt-SLT-1 (□). B) The ribosome-inactivating activity of purified A_1 chain as measured in a rabbit reticulocyte lysate, coupled transcription/translation assay. Luciferase synthesis (measured as relative light units) for the wt SLT-1 A_1 (■) and SLT-1^{PDTRPAP} A_1(▲), and an inactive SLT-1 variant bearing E167A and R170A mutations in the catalytic site (○). Experiments were performed in duplicate.

2.4.6 Inserting known ligands within the A chain

Finding new cancer targeting ligands could improve the diagnosis and treatment of cancer. The purpose of the present study was to demonstrate that one can reduce the structure and functional features of a ~70 kDa AB_5 ribosome-inactivating protein template to a single A chain variant of ~30 kDa. Specifically, we demonstrated that a 7-amino acid long peptide motif can be inserted between residues 245 and 246 of the A chain of SLT-1 without loss of catalytic activity and that the new peptide element was exposed and could readily interact with putative large proteins acting as receptors such as the monoclonal antibody *Onc*-M27. The identification of a site to embed a ligand domain within the catalytic A chain of SLT-1 offers the potential of inserting existing peptide ligands directed at tumor antigens, which are derived from other combinatorial approaches. For example, past searches through synthetic or phage display peptide libraries, have yielded peptides displaying selective binding to tumor antigens on ne-ovasculature [27, 31, 207, 208] and colon carcinomas [209, 210]. Cancer cells are known to up-regulate membrane receptors [211] which in theory represent useful markers in designing tumor homing ligands.

The identification of a site within the A chain where such ligands can be inserted may offer opportunities for incorporating known ligands within this site. Studies in the past have shown that fusion proteins containing the full length A subunit as well as truncated A subunits (of SLT-1) fused to the N-terminus of CD4 retain the N-glycosidase activity and are cytotoxic to cells expressing the HIV-1 gp120/gp41 complex [212, 213]. Similar results were observed when SLT-1A subunit or SLT-$1A_1$ subunit was fused to VEGF or hGM-CSF (granulocyte-macrophage colony-stimulating factor [214]. A fusion protein

containing the A_1 subunit of SLT-1 linked to the carboxyl terminus or amino terminus of anthrax toxin lethal factor (LF1-254) was also toxic to CHO cells [215].

Therefore, we explored the possibility to insert a few such peptides in the protease-sensitive loop and studied their effect on specific target cells. The two peptides that were inserted at this site were: A) LTVSPWY – a peptide that was found to bind specifically to breast cancer cells (SKBR3) [216], B) GRGDSP – a peptide binding to V 4 integrin receptors on cells [27]. The two variant toxins expressed to the same extent as wt-SLT-1 and were detected by anti-SLT-1 A chain polyclonal antibodies. However, the two variants did not have any selective cytotoxic effects on the specific cancer cell lines compared to the wt-SLT-1, indicating that the targeting was not specific (Perampalam and Gariepy, unpublished results). There could be a number of reasons for not observing specific killing by these toxin-peptide variants. For instance, the peptides are presented in a multivalent format when displayed on phages [217], but only a single copy of the peptide is inserted into the protease sensitive loop of the toxin. It has also been suggested that the multivalent presentation of the peptides improves cellular internalization process [218].

2.5 Summary and future prospects

The aim of the present study was to generate a single chain toxin that could tolerate a new targeting site within its structure while retaining all other functions linked to its cellular routing and toxicity. The subsequent approach of introducing existing ligands into the toxin A chain was not successful in terms of targeting the toxins to cells. In the next chapter, I will explore the concept of inserting a combinatorial library within this site of the toxin. The promise for attempting this approach is that the single chain toxin template offers a distinct advantage over other ligand binding templates such as immunoglobulins for designing combinatorial libraries due to the fact that it incorporates a cytotoxic domain capable of identifying internalized cell-surface markers in cell-based assays.

CHAPTER 3: DESIGN AND CHARACTERIZATION OF THE SLT-1A^{PDXXXAP} TRIPEPTIDE LIBRARY

3.1 Abstract

One strategy to redefine the specificity of the A chain for cancer cells may be to create libraries of this cytotoxic domain harboring a random peptide motif and to screen such libraries for novel toxin variants that can target and kill such cells. In this chapter, I will discuss the design of a structurally compressed SLT-1 toxin library where a random peptide element was directly embedded within the C-terminal domain of its cytotoxic A chain in order to reduce both the complexity and mass of the template itself. More precisely, I have previously discussed that (Chapter 2) a seven amino acid peptide epitope (PDTRPAP) recognized by the anti-mucin mAb *Onc*-M27, can be inserted within the protease sensitive loop (residues 245-246) of the SLT-1 A subunit (SLT-1A^{PDTRPAP}) without loss of catalytic activity. A SLT-1 library (SLT-1A^{PDXXXAP}) was then constructed where the critical tripeptide sequence TRP within this epitope was randomized. After assessing the quality of the library in terms of diversity and protein expression, 10,000 clones from this library of (20^3) 8,000 variants were screened by ELISA to identify library members able to bind to mAb *Onc*-M27. The expected number of variants that

coded for the TRP motif was 3 and the library screening also identified 3 toxin variants coding for the expected epitope (TRP) as well as 5 other mutants displaying related and distinct peptide motifs. These results support the creation of compressed single chain toxin libraries harboring both a putative ligand and catalytic activity.

3.2 Introduction

Immunoglobulins exhibit tremendous diversity in terms of the targets they can bind: proteins, peptides, sugars and small molecules. As noted in Section 1.3.2, there are many limitations in using immunoglobulins as targeting scaffolds (size and architecture). These challenges have led investigators to look at alternate protein scaffolds. The term 'scaffold" describes a protein framework which can be used for introducing novel functions. The selection of a scaffold best suited for building a combinatorial library depends on three factors: the library diversity, the properties of the scaffold and the desired applications. Combinatorial libraries with higher diversity offer a greater probability of harboring molecules with a desired function than smaller libraries [68, 219]. The compatibility of a novel binding protein scaffold with a particular selection method should be verified experimentally.

In our case, having established that a peptide ligand could be integrated between residues 245 and 246 of the SLT-1 A chain, our next objective was to demonstrate that a random peptide element could be inserted within this site yielding a combinatorial library of SLT-1 toxins, where each variant may harbor a potentially new receptor-binding domain within its A_1 fragment. The reason for choosing a RIP template such as the A chain of SLT-1 was to utilize the cytotoxic activity of the toxin in the future as a search engine. However, the idea of a single chain toxin as a library scaffold is novel and one has to confirm that the selected site can accommodate all possible combination of sequences within that site without any restrictions or bias. Hence the proof-of-concept of designing such libraries was experimentally validated by mining a simple

tripeptide library in search of A_1 variants able to recognize a receptor mimic, in the present case, the mAb *Onc*-M27. The theoretical diversity of a tripeptide library is 8,000 (20^3) variants and one can potentially screen all variants in the library as opposed to variants from a higher diversity library. The rationale behind choosing a mAb such as *Onc*-M27 was discussed in Chapter 2 (Section 2.4.2). Specifically, the epitope of the mAb selected is a linear heptapeptide of which the middle 3 residues (TRP) are the ones crucial for binding to the mAb. We used ELISA assays to screen the library for variants reconstituting the known epitope.

3.3 Materials and methods

3.3.1 Construction of the SLT-1A^{PDXXXAP} tripeptide library

A combinatorial SLT-1A tripeptide library (SLT-1A^{PDXXXAP}) was generated using PCR by randomly mutating the core tripeptide within the inserted heptapeptide domain of SLT-1A^{PDSRPAP} (strategy described in Figure 3.1). The reason for choosing the PDSRPAP inserted toxin as opposed to the toxin with the PDTRPAP as the parental template in the construction of the library was to minimize false positives from ELISA screening (due to wild type sequence emerging). The library design comprised the replacement of the TRP codons with degenerate NNS codons [220, 221] (N is defined as A, C, G, or T in an equimolar ratio; S is defined as an equimolar mixture of C or G). This randomization scheme prevents 2 (opal and ochre) of the 3 stop codons from occurring within any given nucleotide sequence. Expression of the library clones were carried out in a suppressor strain that inserts glutamine at the amber stop codon TAG,

thus removing a source of premature termination of the protein. PCR using the degenerate primer E (anti-sense strand) in conjunction with primer A produced dsDNA that was subsequently purified and used to prime a second PCR, paired with primer B, generating an amplified library cassette that was then cloned into pECHE9A and transformed directly into the amber-suppressing (*glnV*) *E.coli* expression strain JM101 (Figure 3.1). The diversity of the library was assessed by sequencing 11 randomly selected clones and comparing the DNA sequences.

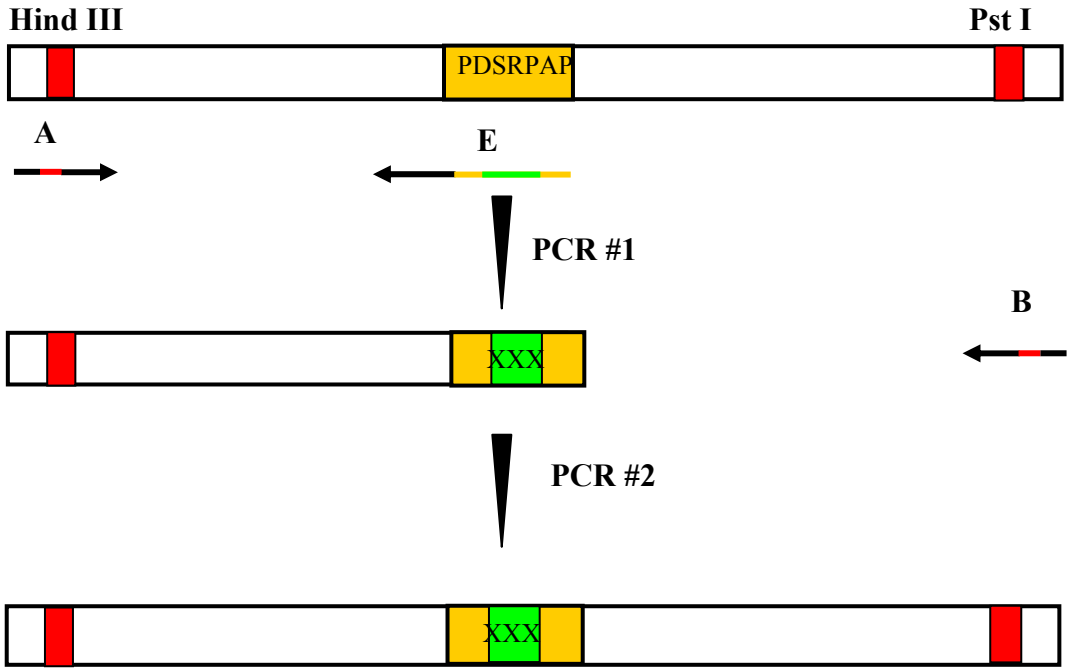

Figure 3.1: The construction of a tripeptide library in the A chain of SLT-1A^{PDSRPAP} using a PCR based approach.

The SLT-1^{PDSRPAP} plasmid was used as the initial template for PCR. The first PCR was performed using the flanking primer A (containing a restriction enzyme site, Hind III) and the library primer E. The PCR product was carefully purified from a gel and it was used along with the flanking primer B (containing a restriction enzyme site, Pst I) in a second PCR. The purified PCR product was digested with the two restriction enzymes (marked in red) and cloned into the pECHE vector. The plasmids were transformed into JM101 strain of *E. coli*. The synthesized primers used in this study had the following sequences**:**

Primer A: GTT ACT GTG ACA GCT GAA GCT TTA CGT TTT CG

Primer B: GAG AAG AAG AGA CTG CAG ATT CCA TCT GTT G

Primer E: CGA TGC TGG AGC SNN SNN SNN GTC TGG ATG ATG ATG ACA ATT CAG TAT TAA TGC

3.3.2 Expression and purification of toxin mutants

Individual library colonies were picked from carbenicillin-selective LB-agar plates and grown overnight at 37° C in 1 mL of LB-broth in 96-well culture blocks. The next day, glycerol stock of each mutant was made by taking 50 µl of culture and dispensing it into wells of a 96 well plate containing 50 µl of 30% glycerol. The bacterial pellets were lysed by one cycle of freeze-thawing and then the toxins were extracted using a Bug-Buster Protein Extraction Reagent (Novagen) supplemented with Benzonase nuclease (EMD Biosciences, San Diego, CA). The cleared lysates were transferred to individual wells of 96-well plates containing 2 µL Ni-NTA magnetic agarose beads (Promega) and incubated for 30 minutes at room temperature. The magnetic beads were washed with phosphate buffer (50 mM phosphate buffer (pH8.0), 300 mM NaCl, and 10 mM imidazole) and the toxin variants were eluted with the same buffer containing 150 mM imidazole (this process is clearly depicted in Figure 3.2).

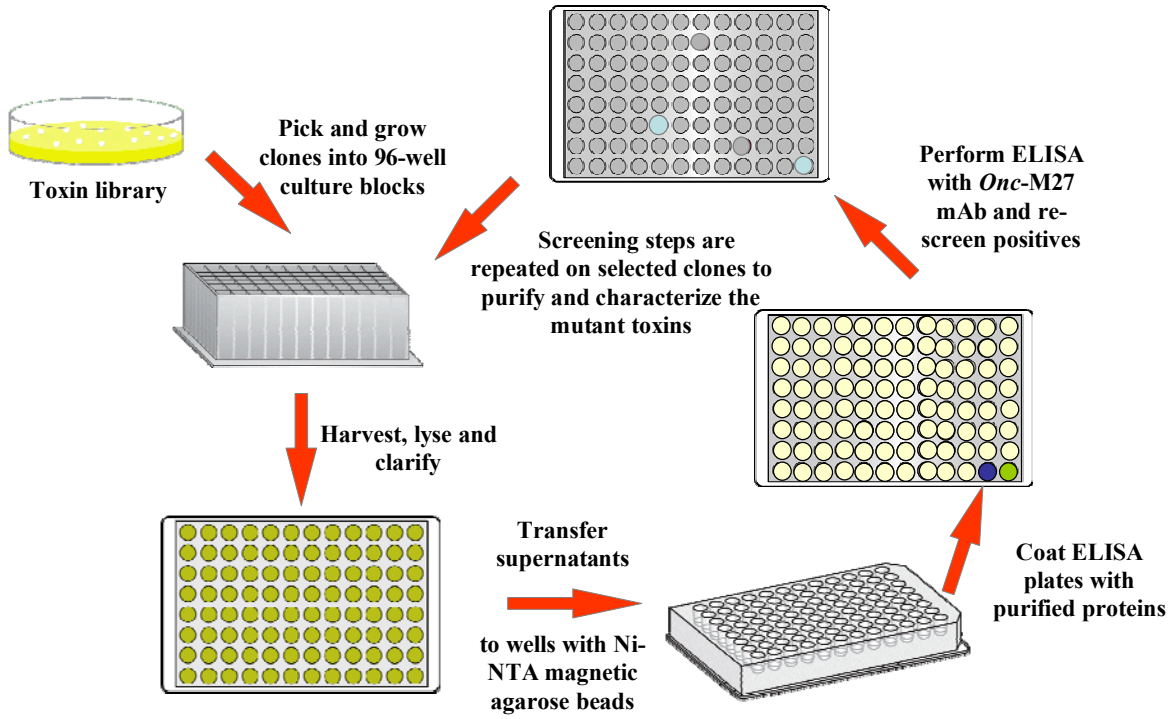

Figure 3.2: A depiction of the tripeptide library screening strategy.

Bacterial colonies were picked from LB plates and grown overnight in deep well plates with 1 mL LB broth. The cultures were spun down, lysed and purified using magnetic Ni-NTA agarose beads. Individual purified proteins were adsorbed onto wells of 96-well plates and ELISA assays were carried out to detect variants that bound to the mAb *Onc*-M27.

3.3.3 ELISA-based screening of toxin variants from the SLT-1A^{PDXXXAP} tripeptide library

Wells of 96-well ELISA plates (Nalgene Nunc, Rochester, NY) were coated overnight with 1 μg of wild type SLT-1, SLT-1A^{PDTRPAP} or individual purified toxin variants (from a 1 mL bacterial culture grown overnight in LB) derived from the SLT-1A^{PDXXXAP} tripeptide library. The variants were prepared in a 10 mM sodium carbonate buffer (pH9.0) (30 μl of eluted protein diluted in 70 μl of 10 mM sodium carbonate buffer) for the coating step. The wells were blocked for 1 hour with 0.5% w/v bovine serum albumin (BSA) and 0.5% v/v Tween 20 in PBS (blocking buffer). The wells were washed 3 times with PBS. The mAb *Onc*-M27 (0.01 μg in 100 μl) was then added to each well for 1 hour at 37° C in blocking buffer. The mAb *Onc*-M27 (IgG1) recognizes the tripeptide epitope TRP in the context of the mucin MUC-1 tandem repeat sequence PDTRPAP [191]. The wells were subsequently washed with PBS (3x) and exposed for 1 hour with a 1:1,000 dilution (50 μl in blocking buffer) of a goat anti-mouse IgG-peroxidase conjugate (Sigma, St. Louis, MO). TMB (3,3',5,5'–tetramethylbenzidine, Boehringer Mannheim, Mannheim) was used as a substrate to visualize the binding of *Onc*-M27 to toxins displaying the expected mucin MUC-1 epitope. A stock solution of the chromogen TMB (6 mg/ml in DMSO) was diluted to 100 μg TMB/ml in 0.1 M sodium acetate buffer (pH 5.5) containing 1.3 mM H_2O_2 [195]. The substrate reaction was allowed to proceed in the dark and was stopped by the addition of 1M H_2SO_4 after 30 minutes. Absorbance values were read at 450 nm using a microtitre plate reader. The same procedure was followed for checking the level of expression of SLT-1 A chain by library mutants. An SLT-1 A chain polyclonal antibody (1:3,000 dilution) was also used

as the primary antibody and an anti-rabbit IgG-HRP conjugate was used as a secondary antibody in order to detect the presence of the A chain scaffold.

3.3.4 Competition ELISA assay

A competition ELISA assay was performed to further analyze the nature of interactions between mAb *Onc*-M27 and variants SLT-1A^{PDMCYAP} and SLT-1A^{PDMCYAP}. The TAP24 (TAPPAHGVTSAPDTRPAPGSTAPP) peptide was used as a competing peptide for this experiment. Wild type SLT-1 (no MUC-1 epitope present) and the variant SLT-1A^{PDTRPAP} protein (where the TAP24 peptide should abolish binding) were used as controls. The ELISA assay was performed as described in Chapter 2 (Section 2.3.7) with the exception that 5 µg of competing peptide, TAP24, was added along with the mAb *Onc*-M27.

3.4 Results and discussion

An SLT-1 A_1 tripeptide library (SLT-1A^{PDTRPAP}) was designed to verify whether the majority of the variants were expressed *de facto,* and whether the library could be mined for ligands recognizing a known target. The theoretical diversity of this library was 8,000 A_1 variants which presents a possibility for screening each of the variants in a chosen assay.

3.4.1 Quality of the SLT-1A^{PDXXXAP} tripeptide library

The tripeptide sequence SRP was randomized within the structural template of the toxin variant SLT-1A^{PDSRPAP}. The resulting library was termed SLT-1A^{PDXXXAP}**.** The library

was constructed using NNS codons (see section 3.3.1) in order to limit the level of codon bias and the number of possible stop codons [222]. Using the NNS scheme allowed us to work with a 32 codon population instead of a 61 codon population which gives a better representation of each of the 20 natural amino acids. The library was characterized in terms of its sequence diversity and protein expression. Specifically, the insert region of eleven randomly selected clones from the library was sequenced and the nucleotide sequences are presented in Table 3.1. All 11 tripeptide DNA sequences observed were distinct from one another. Each of the library mutant sequenced showed that at least 6 out of 9 bases were different (3 clones showed 6/9, 3 clones showed 7/9, 3 clones showed 8/9 and 2 clones with 9/9). Even at the level of amino acids, the tripeptides were distinct from each other. Since all toxin variants in the library harbor an octa-histidine tag at the N-terminus of their A chains, it was possible to examine the spectrum of protein expression associated with individual toxins randomly selected from the library. Holotoxins expressed by 7 distinct bacterial colonies picked from the SLT-1A^{PDXXXAP} library, were recovered by metal affinity chromatography and examined by SDS-PAGE and Western blot analysis (anti SLT-1 A chain polyclonal antibody). The gel shown in Figure 3.3 illustrates that both A and B subunits were similarly expressed in a representative set of 7 library mutants. The Western blot also confirmed that most of the randomly picked clones express A chains (Figure 3.3). In order to generate a more quantitative understanding of the expression profiles of the library clones, proteins from many different sets of 94 different clones were purified and tested by ELISA using the SLT-1 A chain anti-sera (Figure 3.3). The results showed that more than 90% of the library clones expressed protein.

Table 3.1: Nucleotide sequence and amino acid diversity within tripeptide SLT-1 A chain library

SLT1A^{PDSRPAP} CCA GAC **ACG CGA CCA** GCT CCA

Randomly Selected Clones	Library Sequence	# of Mutated Bases
#1	CCA GAC **GGG ATC GGG** GCT CCA	**8/9**
	G I G	
#2	CCA GAC **CTG GAG ATG** GCT CCA	**8/9**
	L Q M	
#3	CCA GAC **GAC GAC TTG** GCT CCA	**9/9**
	D D L	
#4	CCA GAC **GTC CGG TGG** GCT CCA	**7/9**
	V R W	
#5	CCA GAC **CAG CGC TGG** GCT CCA	**6/9**
	Q R W	
#6	CCA GAC **TCC CAG GAG** GCT CCA	**7/9**
	S Q E	
#7	CCA GAC **TCC GAC CCC** GCT CCA	**6/9**
	S D P	
#8	CCA GAC **TAG GGC TAC** GCT CCA	**7/9**
	Q G Y	
#9	CCA GAC **AGC ATG TTC** GCT CCA	**8/9**
	S M F	
#10	CCA GAC **AAC TAC CCG** GCT CCA	**6/9**
	N Y P	
#11	CCA GAC **GTC GCC TGC** GCT CCA	**9/9**
	V A C	

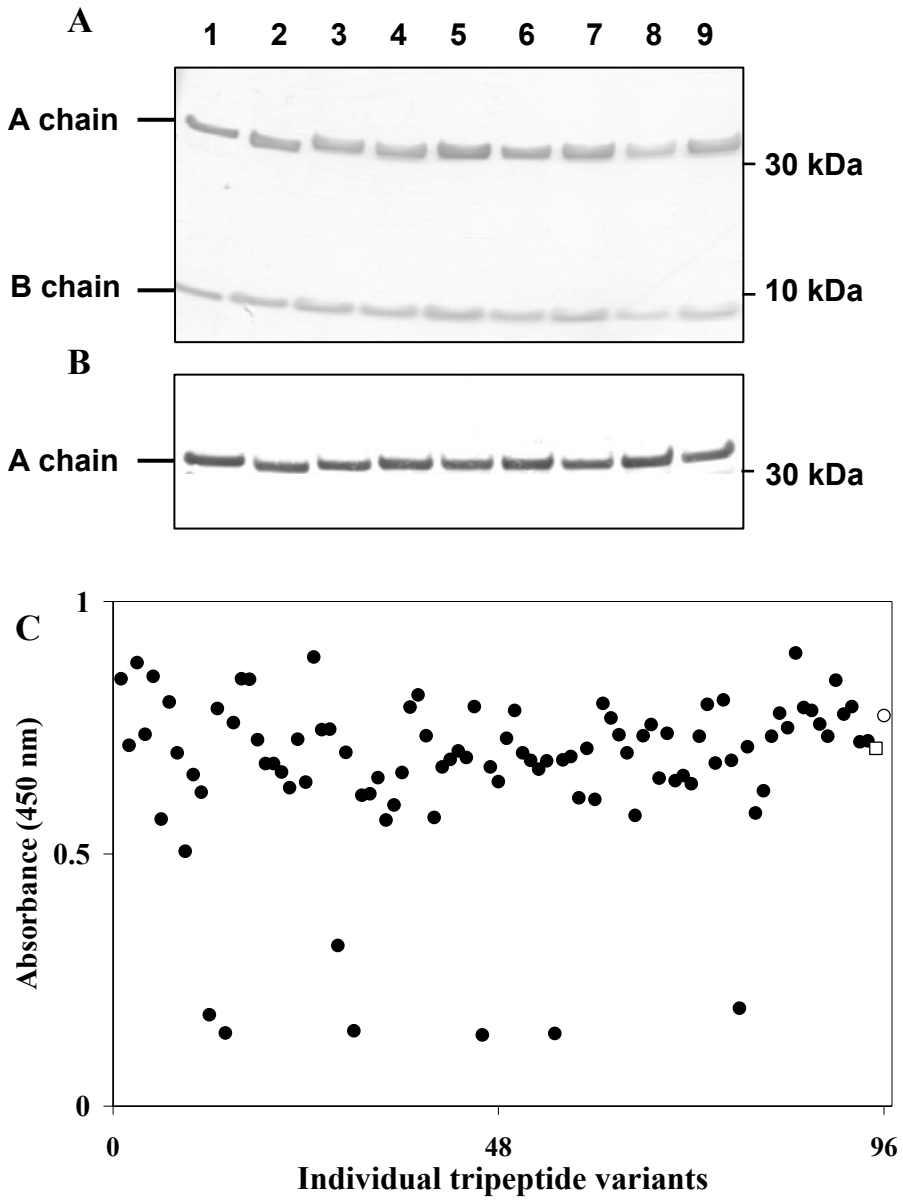

Figure 3.3: Expression validation of the SLT-1A^{PDXXXAP} tripeptide library.

Comparable expression levels from 1 mL overnight bacterial cultures of SLT-1A^{PDTRPAP} (lane 1), wild-type SLT-1 (lane 2), and 7 randomly selected toxin variants from the SLT-1A^{PDXXXAP} library following metal affinity purification (lanes 3 to 9), as revealed on a Coomassie blue - stained SDS-PAGE gel (A), and by Western blotting using a rabbit polyclonal anti-serum raised against the A chain of SLT-1 (B). C) ELISA was performed with an anti-SLT-1 A chain polyclonal antibody on 94 different variants (•). Majority of the library clones expressed protein to similar levels as wt-SLT-1 (□) and SLT-1A^{PDTRPAP} (o). Six out of 94 variants did not express SLT-1 A chain when tested with the SLT-1 A chain polyclonal antibody (absorbance was less than 0.3).

3.4.2 Screening of the SLT-1A^{PDXXXAP} tripeptide library

Assuming a uniformed sampling of all possible tripeptide sequences within the SLT-1A^{PDXXXAP} library, the maximal diversity of the library is of the order of 8,000 (20^3) toxin elements. The diversity of this library was fully explored by picking 10,000 bacterial clones and purifying their individual toxin by metal-affinity chromatography. The screening strategy used is depicted in Figure 3.2. Each well of 96-well plates (except well #95 - wt-SLT-1 and well #96 - SLT-1A^{PDTRPAP}) were coated with a distinct toxin from individual mutants and subsequently probed by ELISA using the mAb *Onc*-M27 for the presence of the TRP determinant. Results from four screening ELISA plates are presented in Figure 3.4. An ELISA signal greater than 3 standard deviations from the averaged baseline signal observed for most toxins tested (0.1 O.D. unit at 450 nm) was considered to be positive and selected for further screening. The DNA coding for toxins that were positive by ELISA after re-screening were sequenced and the results are summarized in Table 3.2. The screening identified 3 toxins displaying ELISA signals comparable to that of SLT-1A^{PDTRPAP} (Table 3.2). The calculated or theoretical outcome of the screen based on a statistical distribution of possible codons within the randomized region is presented in Table 3.3. The analysis predicts that at least 3 toxins (12/32,768 or 1/2,731 mutant) with the expected TRP motif should have been identified in our ELISA-based screen (10,000 mutants tested) and that their nucleotide sequences (codons) should be distinct. These predictions were experimentally confirmed (Table 3.2) and indicate that the repertoire of molecules within the constructed library closely approximates the projected random distribution of peptide elements. In addition, three other sequences containing the essential threonine and proline residues within the TRP

epitope were identified during the screen (TQP, TLP and TEP). Interestingly, the ELISA signals observed for these variants were significantly weaker than for variants integrating the known epitope TRP, suggesting that only a few amino acids can substitute for the central arginine residue. Our screen did not identify any clones with the sequence TKP (there should be at least be one in our 10,000 clones) present in the library. Finally, two mutants displaying the tripeptides CAC and MCY were weakly but consistently recognized by the mAb *Onc*-M27 (Table 3.2). However, the presence of a peptide containing the MUC-1 epitope (TAP24 peptide) did not reduce the ELISA signal observed for these toxins to mAb *Onc*-M27 suggesting that their binding to the monoclonal antibody may occur at a site distinct from the antigen-combining site (Figure 3.5). The TAP24 peptide did compete off the binding of the SLT-1A^{PDTRPAP} toxin to the mAb *Onc*-M27 as expected.

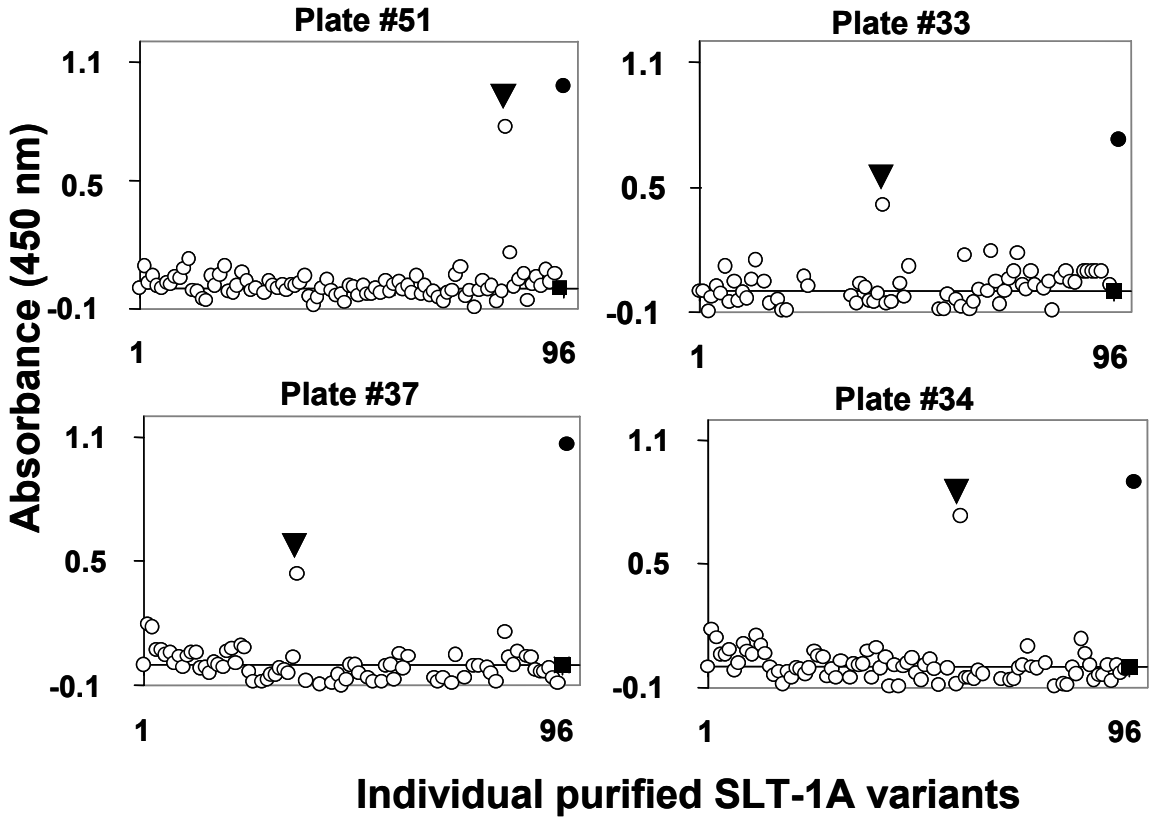

Figure 3.4: Representative ELISA results derived from screening a SLT-1A^{PDXXXAP} library.

The monoclonal antibody *Onc*-M27 specifically recognizes the tripeptide epitope TRP. Scatter-plots of ELISA signals from four 96-well plates coated with 376 randomly selected and purified toxin variants. The majority of SLT-1A variants derived from the SLT-1A^{PDXXXAP} library gave absorbance readings at 450 nm of less than 0.25 while absorbance readings of 1.0 were observed for toxins harboring the TRP tripeptide epitope. Well #95 on each plate was coated with wild-type SLT- 1 (■, negative control) while well #96 corresponded to SLT-1A^{PDTRPAP} (●, positive control). Toxin variants giving rise to an absorbance reading higher than 3 standard deviations from the averaged baseline signal observed for most toxins (▼) were selected for further analyses.

Table 3.2: Summary of tripeptide library screening using the mAb *onc*-M27

Clone	DNA Sequence	Protein Sequence	Absorbance values (ELISA) (450 nm)
Engineered SLT1A^{PDTRPAP}	ACG CGA CCA	TRP	1.1±0.22
3.C5	ACC AGG CCC	TRP	1.1±0.24
34.E9	ACG AGG CCG	TRP	1.1±0.15
51.G11	ACC AGG CCG	TRP	1.0±0.27
37.C11	ACG CAG CCG	TQP	0.4±0.12
11.G5	ACG TTG CCC	TLP	0.3±0.11
22.A10	ACG GAG CCG	TEP	0.3±0.08
12.G1	TGC GCC TGC	CAC	0.4±0.20
33.D6	ATG TGC TAC	MCY	0.3±0.12
1.B8	ACC AAG TTG	TKL	0.1±0.02
10.A4	CTG CAG ATG	LQM	0.1±0.06
1.B19	CAG TCC AGC	QSS	0.1±0.03

Table 3.3: Expected outcome of a tripeptide library screen using a mAb recognizing TRP

Expected epitope	T	R	P	TRP
Total # of NNS codons	32 (4x4x2)	32	32	32768
Possible NNS codons for TRP	ACC ACG	AGG CGC CGG	CCC CCG	
Expected # of TRP codons	2	3	2	12

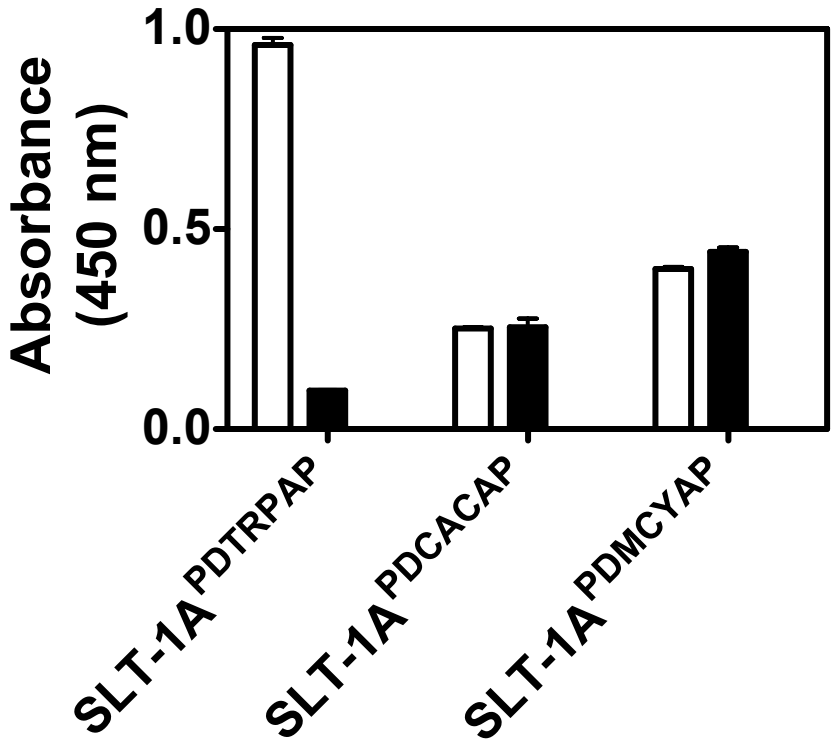

Figure 3.5: A competition ELISA was performed to further analyze the nature of interactions between mAb *Onc*-M27 and variants SLT-1A^{PDMCYAP} and SLT-1A^{PDCACAP}.

The TAP24 (TAPPAHGVTSAPDTRPAPGSTAPP; entire MUC-1 tandem repeat) peptide was used as a competing peptide for this experiment. Wild-type SLT-1 (no MUC-1 epitope present) and variant SLT-1A^{PDTRPAP} (where the TAP24 peptide should abolish binding) were used as negative and positive controls respectively. ELISA assays were performed with the mAb *Onc*-M27 as described in Section 3.3.3 either in the absence (open bars) or presence of 5 μg of the competing peptide, TAP24 (closed bars).

3.5 Summary and Future prospects

In this chapter I have described the successful construction of a simple tripeptide library in the SLT-1 A chain. The library variants were screened exhaustively using an ELISA-based assay to reconstitute a known epitope. I was able to explore the entire diversity of the library by screening 10,000 variants. The screening of this library identified the expected number of TRP peptides (3), suggesting that the constructed library expressed most of the expected mutants of the SLT-1A chain. This strategy was also successful in identifying weak binders of the mAb *Onc*-M27.

When we screened this library on cells (about 1,000 variants) that were resistant to the wt-SLT-1, we did not obtain a toxin mutant that was able to kill the cells. This finding was not surprising, since a tripeptide library provides a very limited diversity for displaying a binding domain recognizing surface receptors. We thus proceeded to construct a SLT-1A library harboring a 7–residue random element this site (residues 245-246) and screened this library on cells using cytotoxicity as our cell-based functional assay (Chapter 4).

CHAPTER 4: CONSTRUCTION OF AN SLT-1 A HEPTAPEPTIDE LIBRARY AND THE SCREENING OF A CHAIN VARIANTS ON HUMAN MELANOMA CELL LINES

4.1 Abstract

A heptapeptide library was inserted into the protease sensitive loop of SLT-1 in order to screen for A chain variants able to kill cancer cells. The library was screened on the human melanoma cell line 518-A2. Only two variants namely SLT-1A^{IYSNKLM} and SLT-1A^{AAFADLI}, showed repeated selectivity for the targeted human 518-A2 melanoma cells. When the two variants were cleaved with furin to see if the single chains of the variants can mediate killing, only SLT-1A^{IYSNKLM} retained its specificity to kill the human melanoma cell line. This variant was able to kill seven other melanoma cell lines indicating that a specific marker may be present on human melanoma cell lines. A detoxified version of SLT-1A^{IYSNKLM} was also tested to see whether the catalytic activity of the toxin was necessary to mediate cellular toxicity. The results indicated that the catalytic activity was necessary for killing suggesting that the toxin had to be internalized into melanoma cells to exert its activity. Finally, when this molecule was injected

into two different strains of mice, the immune responses elicited were minimal, indicating that this protein may not be highly immunogenic.

4.2 Introduction

Combinatorial protein libraries based on SLT-1 allows for the identification of receptors on cell surfaces that are internalized since our readout is cell death due to the routing of a toxin variant to the cytosol near ribosomes. If the site of the library insertion is away from the catalytic site and if the size of the library is such that it does not interfere with the folding and stability of the protein, then the enzymatic activity of the toxin can be used as a search engine. Cytotoxicity implies that the toxin of interest has undergone the multi-step process of binding to cells, internalization into cells, and has reached its target in the cytosol in order to exert its enzymatic activity. The concept of the single chain toxin library is similar in principle to other combinatorial libraries with the main difference that it includes a search engine (cell killing) rather than just a receptor binding function. The idea of mining a SLT-1 A subunit library using its cytotoxic function was tested on cancer cell lines that were insensitive to the wild type SLT-1. Our first goal in this study was to design and build a diverse library in SLT-1 A chain (Figure 4.1). Library diversity represents a key parameter in screening combinatorial libraries for ligands with high affinity and specificity. The sampling repertoire of the tripeptide library described previously was shown experimentally to be too limited. However, it served as a useful library to establish proof-of-concept for single chain libraries. A seven amino acid library (20^7 or 1.3×10^9 variants) represents a more commonly used minimal diversity used in phage display [216] as well as other synthetic peptide libraries.

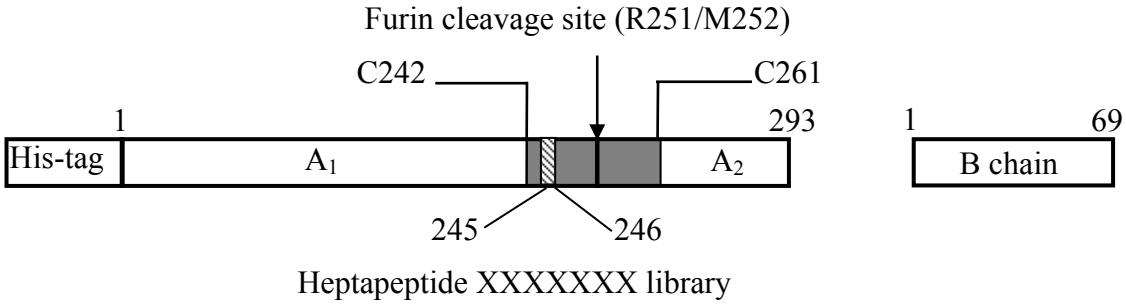

Figure 4.1: Schematic representation of SLT-1 comprising the A and B subunits in tandem.

The construct contains an N-terminal his tag that aids in affinity purification. The protease sensitive loop is shown in grey and it is flanked by two cysteines that form a disulfide bond. The furin cleavage site is marked by the arrow which gives rise to the A_1 and A_2 fragments when cleaved by furin followed by reduction of the disulphide bond. The random heptapeptide was inserted between residues 245 and 246 of SLT-1 A chain.

4.3 Materials and Methods

4.3.1 Cell lines and bacterial strains

The 518-A2 human melanoma cell line was the gift of Burkhard Jansen (Novelix Pharmaceuticals, Pasadena, CA). The 518-A2 cell line was made resistant to the wt-SLT-1 by exposing the cells in flasks to the toxin for a week. After treating the cells with 5 µg to toxin twice, cells were tested in a cytotoxicity assay and found to be resistant to the action of toxin compared to the untreated cells. All other mammalian cell lines as well as VERO cells (African green monkey kidney cells) were purchased from ATCC (Manassas, VA). DNA sequencing and cloning steps were performed using the *E. coli*

strain DH5α (Invitrogen, Carlsbad, CA) while the strain JM101 (Promega, Madison, WI) was employed for recombinant production of wild-type SLT-1 and its variants.

4.3.2 Construction of a heptapeptide library (SLT-1A^{XXXXXXX})

A heptapeptide library, SLT-1A^{XXXXXXX}, was prepared (method is very similar to the tripeptide library construction) by a two stage PCR approach. The first PCR was performed with three-step approach involving the co-annealing and amplification, using primers F and G, of the dsDNA products resulting from parallel PCRs of the SLT-1A^{PDTRPAP} construct with primers F and H (the latter containing seven degenerate NNS codons), and primers G and I. After cutting with Hind III and Pst I, the resulting library cassette was ligated into pECHE10A (Molecular Templates Inc, Toronto), which was then digested with Nsi I to linearize wild-type material. The DNA was transformed into JM101 and expressed as described for the tripeptide library. The construction of the library is illustrated in Figure 4.2. A diagram of the pECHE10A vector is shown in Figure 4.3.

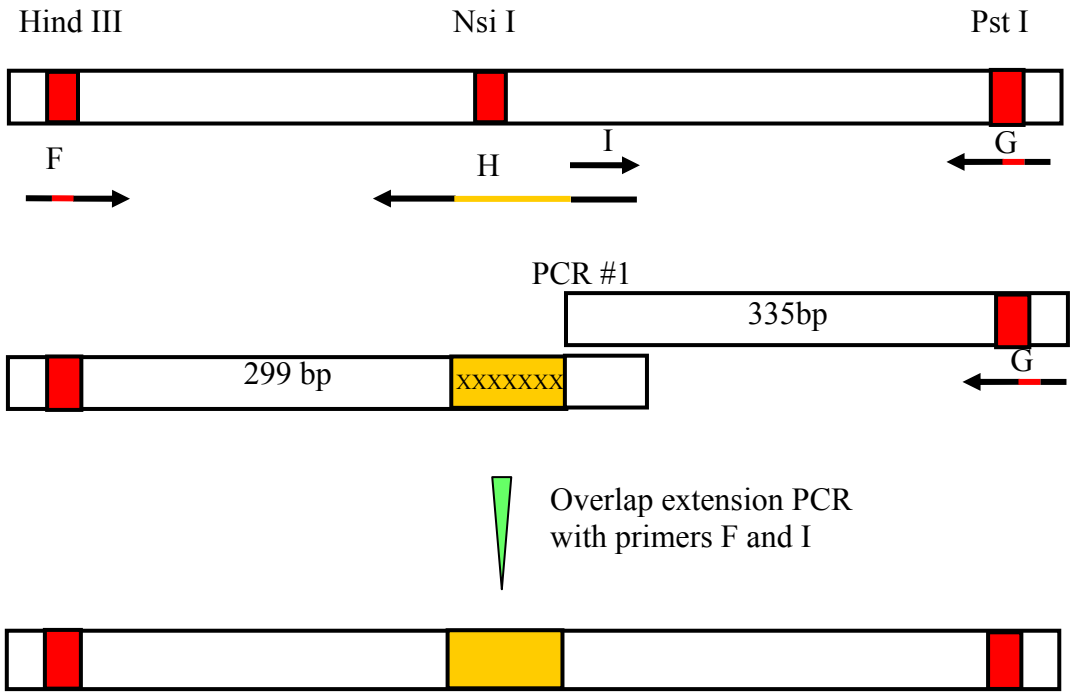

Figure 4.2: Construction of a heptapeptide library in SLT-1 A chain.

pECHE10A plasmid containing the wt-SLT-1 gene was used as the template for a PCR using primers F (flanking primer containing Hind III site) and the mutagenic primer H. Another PCR reaction was performed with primers I and G (flanking primer with the Pst I site). The two PCR products were used in an overlap extension PCR using the flanking primers F and G. The final PCR product was digested with Pst I and Hind III and cloned into pECHE10A. The synthesized primers used in this study have the following sequences:

Primer F: CT GAA GCT TTA CGT TTT CGG C

Primer G: G AGA CTG CAG ATT CCA TCT GTT GG

Primer H: GA TGC CAT TCT GGC AAC TCG CGA TGC SNN SNN SNN SNN SNN SNN SNN ATG ATG ATG ACA ATT CAG TAT TAA TGC

Primer I: GCA TCG CGA GTT GCC AGA ATG GCA TC.

Figure 4.3: A circular map of pECHE10A plasmid used for SLT-1 expression.

The SLT-1 A chain and B chain are shown in pink and green respectively. The His-tag at the N-terminus is shown in red and the signal sequences at the N-termini of both chains are shown in blue. The unique restriction sites used in this study are marked.

4.3.3 Cell viability assays

Human 518-A2 melanoma cells were maintained in Dulbecco's Modified Eagle's Medium supplemented with 5% fetal bovine serum (FBS, Invitrogen) and an antibiotic cocktail of 100 units/ml penicillin and 0.1mg/ml streptomycin. All other cell-lines were cultured according to the supplier's recommendations (ATCC), supplemented with 10-20% FBS and antibiotics. The sensitivity of mammalian cell-lines to wt-SLT-1 and SLT-1 library variants was determined by seeding 2,000 cells/well into 96-well flat-bottom microtitre plates (NUNC Inc., Naperville, IL) and culturing overnight at 37° C to

a semi-confluent monolayer. The cells were then treated with purified toxins diluted in phosphate buffered saline (PBS) for 1 hour at 37° C, followed by removal of excess toxin. Once fresh medium was added to the wells, the plates were returned to 37° C for 48 hours. The plates were then fixed with 10% w/v ice-cold trichloroacetic acid for 30 min at 4° C, washed extensively with water, and stained with a 0.4% w/v solution of sulforhodamine B in 1% v/v acetic acid to assay total cellular protein [194]. After extensive washing with 1% v/v acetic acid, the residual dye was released with 10 mM Tris-HCl (pH 10.0) and the absorbance at 570 nm was recorded using a microtitre plate reader.

4.3.4 Purification and furin cleavage of A subunit toxins

Wild-type SLT-1 and related library variants were extracted from 6-liter bacterial culture pellets and purified by metal affinity chromatography on a Ni-NTA HIS-SELECT column (Sigma-Aldrich) using the method described in chapter 2. Bound A-subunits were selectively recovered by treating the column with 50 mM phosphate buffer, 300 mM NaCl, and 10 mM imidazole, pH8.0 containing 6 M guanidinium-HCl, a condition that removes the B subunit. Proteolytic cleavage under reducing conditions to release the A_1 fragments from toxin was achieved by incubating the purified A subunits with recombinant furin (New England Biolabs, MA) in 100 mM MES buffer (pH 6.0), 5 mM $CaCl_2$ and 1mM β-mercaptoethanol. Typically, 1 mg of SLT-1-A chain was cleaved with 10 units of furin for 48 hours at 30° C and then subjected to washing with PBS containing 100 mM DTT and subsequent buffer exchange into PBS using an Amicon ultra-filtration unit (Millipore; 10,000 kDa cut off). The resulting A_1 fragments were isolated by a second round of affinity purification on Ni-NTA HIS-SELECT resin. The

disulfide-linked pair of A_1 and A_2 chains from SLT-1A^{IYSNKLM} was generated by performing the same purification and furin cleavage steps in the absence of reducing conditions.

4.3.5 Generation of catalytically inactive $A_1^{IYSNKLM}$

Tyrosine 77 within the A chain of wt SLT-1 is critical for its catalytic function [223]. It was mutated to a serine (Y77S) within the scaffold of the SLT-1 $A_1^{IYSNKLM}$ variant using the quick change multi-site directed mutagenesis kit from Stratagene. The ability of the Y77S variant to inhibit protein synthesis with respect to the $A_1^{IYSNKLM}$ was measured using the *in vitro* coupled transcription/translation reticulocyte lysate assay as described in chapter 2 (section 2.3.6) [224]. The catalytic activity of the Y77S mutant of SLT-1 $A_1^{IYSNKLM}$ was also compared to that of SLT-1 $A_1^{IYSNKLM}$ in a cell killing assay on human melanoma 518-A2 cells. The assay was performed with both A_1 fragment and the disulfide-linked A_1 and A_2 chains in the context of catalytically inactive and active forms.

4.3.6 Immunogenicity studies

The immunogenicity of SLT-1 A^{IYSNKLM} was measured in two host mouse strains (namely CD-1 and C57 Black). Briefly, animal test groups (3 animals per group) were subjected to daily intravenous (*i.v.)* tail-vein injections (10 μg per injection) over five consecutive days. Animal control groups received subcutaneously (*s.c.*) 50 μg of the peptide toxin emulsified in Freund's Complete Adjuvant on Day 1 and were subsequently boosted on Days 21 and 35 with 25 μg of the antigen prepared in Freund's Incomplete Adjuvant. Sera were collected from mice over the entire 42-day study and

subsequently analyzed by ELISA using anti-mouse IgM and IgG peroxidase conjugate. IgM and IgG responses were detected using ABTS as the colorimetric substrate.

4.4 Results anddiscussion

Phenotypic cell-based assays provide information including specificity, cytotoxicity and bioavailability. Cell-based assays enhance the success rate of drug discovery since more than 90% of drug candidates derived from cell-free assays fail to show any effect in follow up cell culture assays [225]. In this study, the purpose of constructing a heptapeptide library was to screen the library variants on cancer cells using the cytotoxic function of the A chain in a cell-based assay. The ability to use cytotoxicity for screening indicated that the protein variant not only binds to cell surface target but also leads to toxin internalization, cell routing and eventually cell death. Searches based on cytotoxicity assays also permit high throughput screening strategies and may allow a thorough exploration of SLT-1 libraries. A schematic of the SLT-1 A chain construct along with the position of the library are presented in Figure 4.1.

4.4.1 Construction and screening of the SLT-1A^{XXXXXXX} heptapeptide library

4.4.1.1 Successful construction of the library at the genetic level

Using the same genetic strategy described for the SLT-1A^{PDXXXAP} library, a more diverse SLT-1 A heptapeptide library (20^7 variants) was generated in which all seven positions were randomly mutated within the insert, positioned between residues 245 and 246 of the A_1 sequence of SLT-1A (Figure 4.1). The insertion of any sequence at this specific site at the genetic level removes a unique restriction site (Nsi I) from the gene. This feature was useful in eliminating wt-SLT-1 contaminants during the construction of library by simply cutting the ligated DNA with Nsi I and then cloning it into pECHE10A (Figure 4.2). The efficiency of the cloning step was characterized by digesting DNA isolated from 47 randomly selected bacterial colonies with restriction enzymes Pst I and Hind III (Figure 4.4). The DNA bands corresponding to library clones were running higher than the band corresponding to wt-SLT-1. One of the library clones (#12) had a band similar to the wt-SLT-1 band indicating the absence of the insert in the gene. Clone #42 did not have a PCR band at all implying that the gene was not in the plasmid.

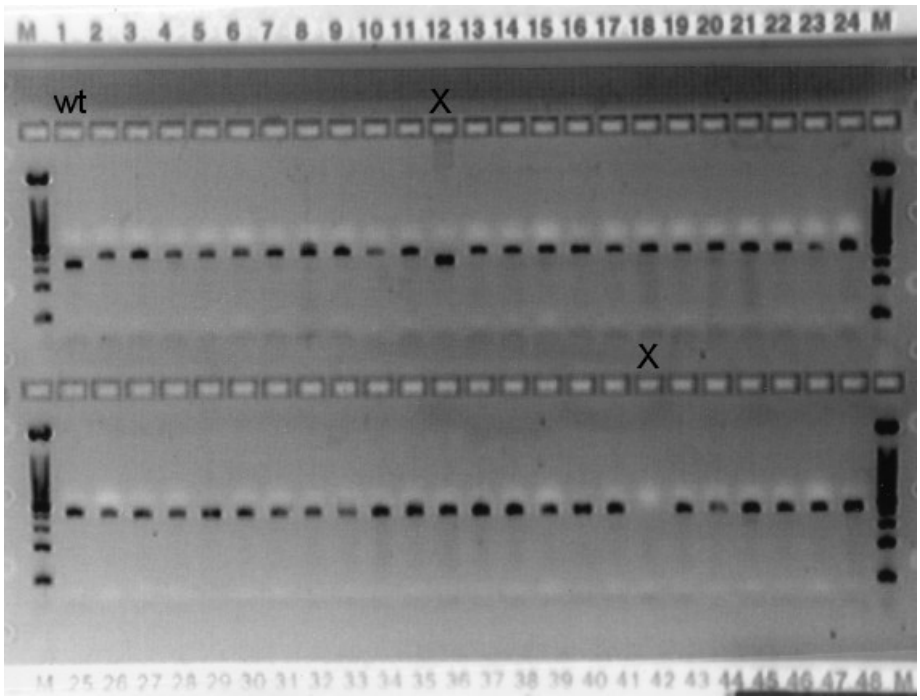

Figure 4.4: Restriction enzyme analysis of library variants.

DNA was isolated from randomly selected library colonies and digested with Hind III and Pst I. DNA from wt-SLT-1 was used as a control. The wt-SLT-1 gives the expected band of 606 bp and the library clones with the random inserts yielded a band at 627 bp. Clone #12 and clone #42 (marked as "X") had no band. Therefore 45 out of the 47 clones tested had the correct size insert.

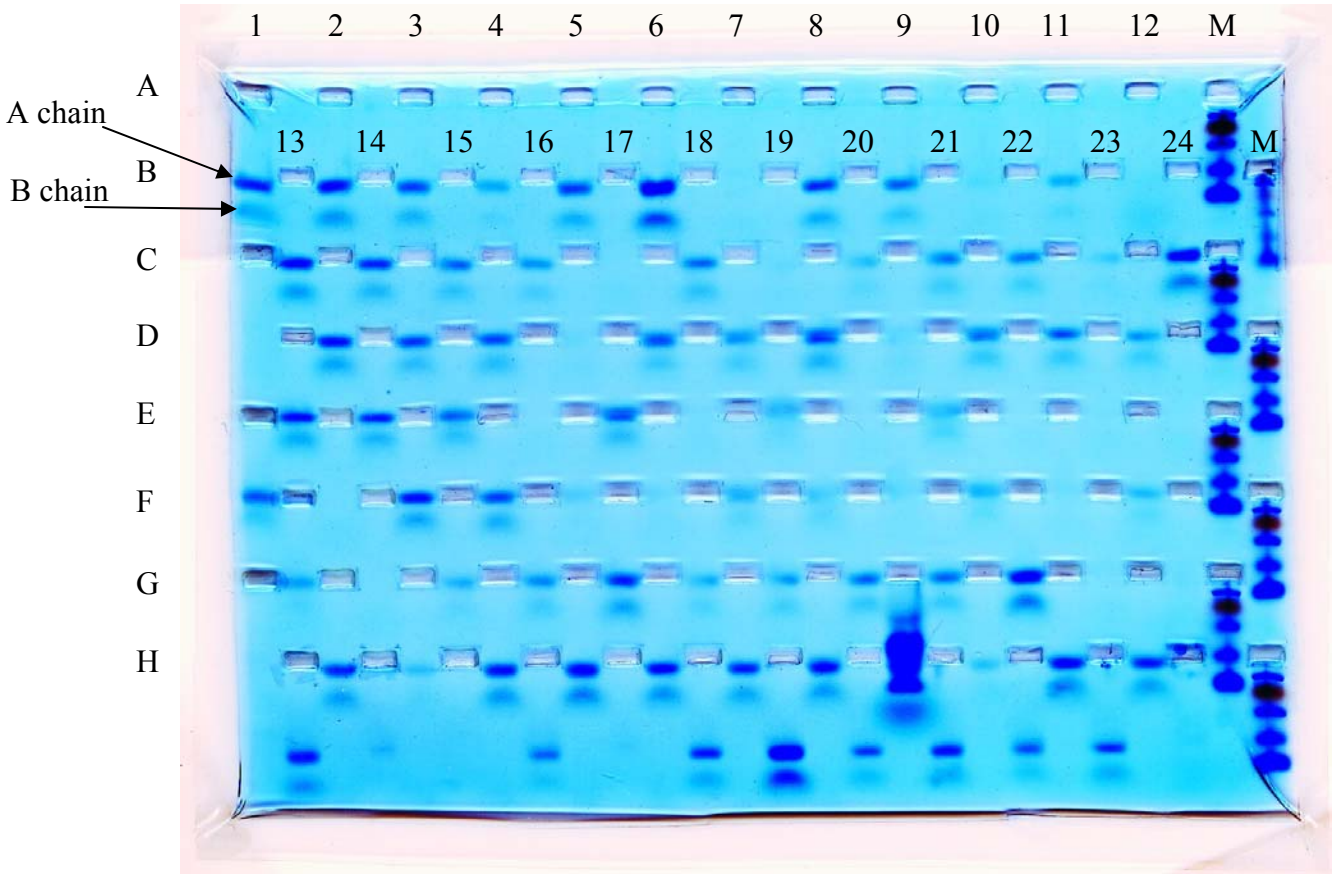

Figure 4.5: An SDS-PAGE gel showing the protein expression of 96 library variants.

There are 8 rows (labeled A to H) of 13 wells (numbered) and only 24 wells and the two marker lanes are marked. The first twenty four (1-24) and the two marker lanes (M) are labeled for clarity. The last well in each row was loaded with protein markers (M). Ni-NTA affinity purified proteins from randomly selected library mutants were loaded in each well and the gel was stained with Coomassie Blue. Sixty nine (69) out of 96 clones expressed the A and B subunits as marked in lane 1.

4.4.1.2 Screening of the heptapeptide library

The expression profile of the heptapeptide library, termed SLT-1A^{XXXXXXX}, was comparable to that of the tripeptide library. An SDS-PAGE gel containing 96 different library variants showed that 69 out of 96 clones expressed A and B chain (Figure 4.5). The library was then screened for holotoxin variants capable of killing wt-SLT-1-resistant

human melanoma 518-A2 cells. A total of 9,400 clones were picked from this library and the cytotoxicity of their purified holotoxin variants towards 518-A2 melanoma cells, human breast cancer CAMA-1 cells and human prostate cancer PC-3 cells were quantified using the sulforhodamine B cell viability assay [194]. The screening approach is illustrated in Figure 4.6. The strategy for screening the A chain library in a cell-based assay was as follows: Adherent cancer cell lines were grown in 96-well plates and used as targets in the primary screen stages. The cell line selected for screening purpose was made resistant to the wt-SLT-1 since we were using the holotoxin template (wt B subunit) for building and screening our A chain libraries. The need for constructing the A chain library in this manner was discussed in Section 2.4.1. Since these library variants had a functional B subunit pentamer, they retained their binding to cells expressing CD77. Cell lines were made resistant to the wt-SLT-1 by growing them in the presence of 2µg/mL of wt-SLT-1 for 3 to 4 passages. Afterwards, we confirmed their resistance by performing cytotoxicity screens using the wt-SLT-1. We also performed flow cytometry using FITC-labeled SLT-B to verify the absence of CD77 expression on 518-A2 cells (Figure 4.7). Consequently, the 518-A2 cell line was insensitive to the wt-SLT-1 toxin and this feature was confirmed by the weak binding of FITC labeled SLT-1 B subunit to these cells. Alternatively one could mutate the binding sites in the wt-SLT-1 B subunits in the future so that the B subunit loses its ability to bind to CD77.

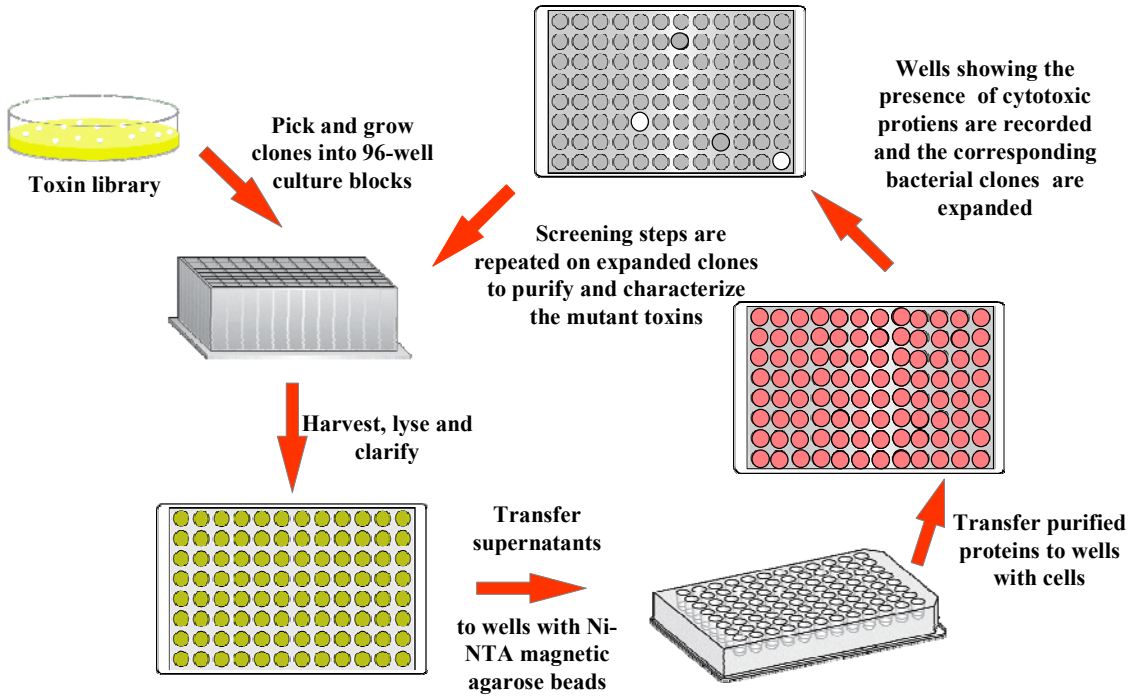

Figure 4.6: A depiction of the cell screening strategy.

Bacterial colonies from our library were picked, grown overnight and glycerol stock of each clone was made. The expressed toxin variants were purified by metal affinity chromatography. The toxin variants were then added to wells (96 well plates) containing target cells and cytotoxicity assay using SRB was performed. Toxins able to kill cells were re-tested and subsequently sequenced if they demonstrated selectivity for cancer cells.

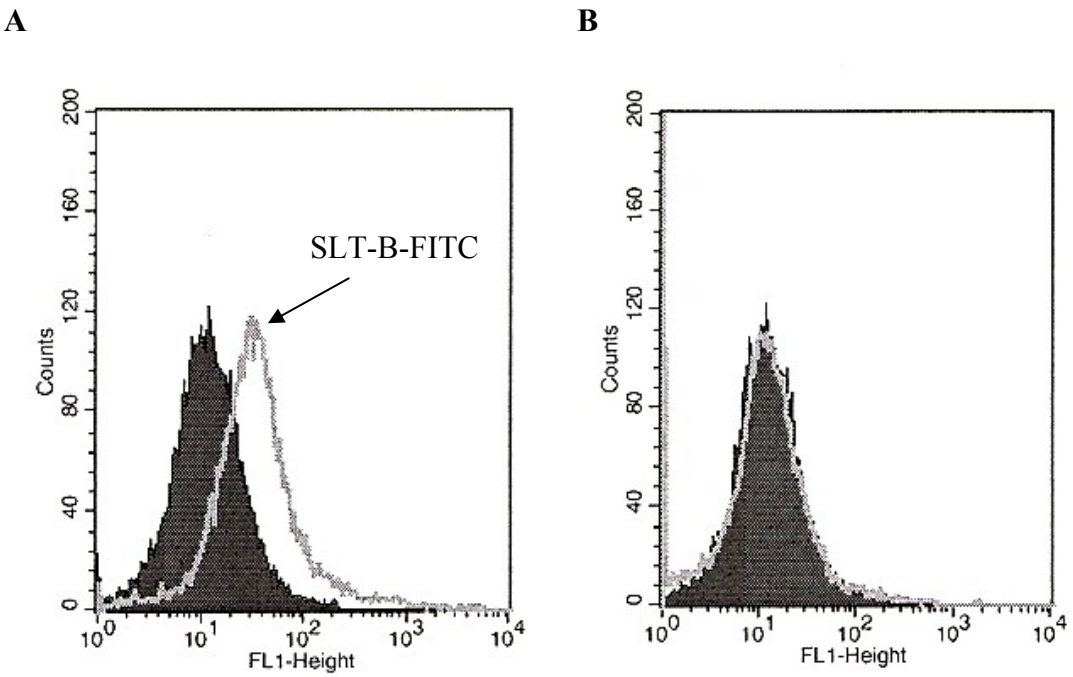

Figure 4.7: Flow cytometry on normal and wt-SLT treated human melanoma cells 518-A2 cells.

Normal 518-A2 cells and 518-A2 cells grown in the presence of wt-SLT-1 toxin were treated with SLT-B labeled with FITC. The results from treated and untreated cells are shown in panels A & B in histogram format. The filled curves on both graphs show the unstained population of cells and the white curve (unfilled) shows the FITC-SLT-B stained population of cells. The cells grown in the presence of wt-SLT-1 show no binding to FITC-labeled SLT-1B.

A representative scatter plot depicting the viability of 518-A2 cells treated with 94 different purified SLT-1A^{XXXXXXX} variants is presented in Figure 4.8. Holotoxin variants that reduced cell viability by more than 3 standard deviations beyond the mean value of all other non-cytotoxic variants were selected as possible hits and retained for further evaluation. A total of 112 different SLT-1A^{XXXXXXX} variants were re-screened against 518-A2 cells, as well as against a panel of 12 other cell lines (human unless otherwise indicated), comprising PC-3 (prostate cancer), SKBR-3 (breast cancer), CAMA-1 (breast cancer), U87 (glioma), OVCar-3 (ovarian carcinoma), SiHa (cervical cancer), PanC (pancreatic cancer), B16-F10 (mouse melanoma), Vero (monkey, normal kidney), HS-216 (normal fibroblast), H-MEC (normal mammary epithelial cells), and H-REC (normal kidney cells). Only two variants, SLT-1A^{IYSNKLM} and SLT-1A^{AAFADLI}, showed repeated selectivity for the targeted human 518-A2 melanoma cells (Figure 4.9). Both variants were then cleaved with furin and their respective A_1 fragments were purified and re-tested to determine in each case whether the observed cell-selectivity were uniquely associated with the cytotoxic A_1 domains alone and not the holotoxin. The A_1 fragment of the A chain of SLT-1A^{IYSNKLM} (termed $A_1^{IYSNKLM}$) retained its selectivity for 518-A2 cells (Figure 4.10). The LD_{50} of this variant was around 400 nM. One possible explanation for SLT-1A^{AAFADLI} to loose ability to bind to 518-A2 cells after furin cleavage could be that the targeting function was provided by not just the peptide but a combination of the peptide as well as other parts of the toxin molecule.

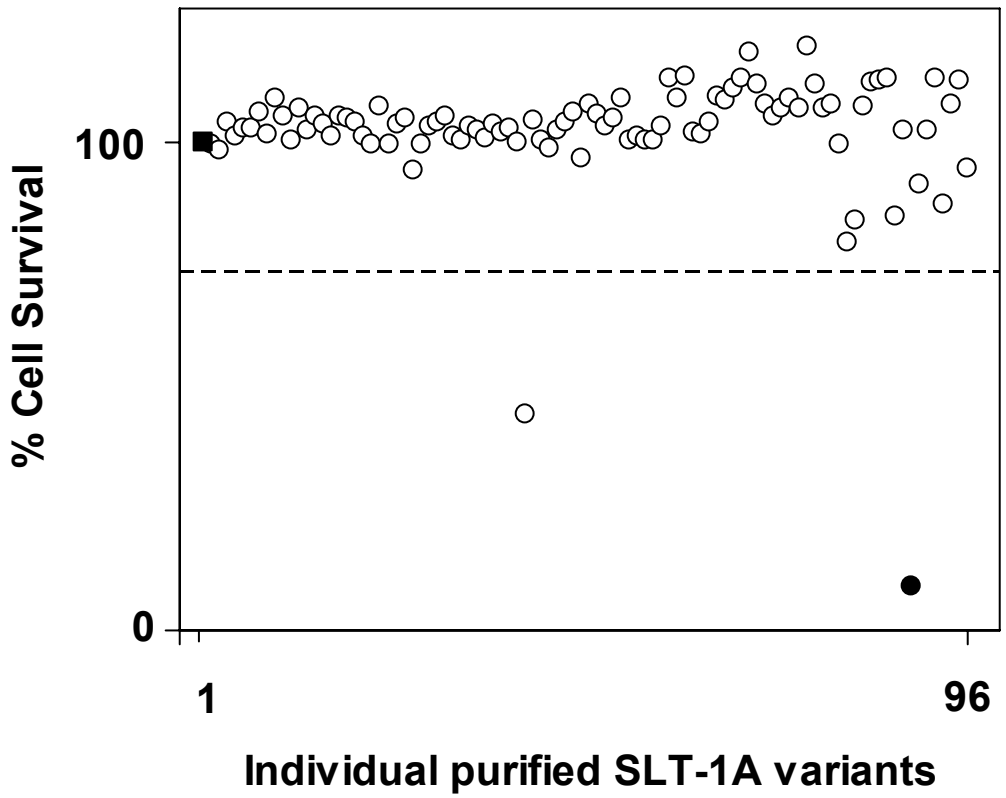

Figure 4.8: A representative scatter-plot of melanoma 518-A2 cells when treated with library mutants.

Wells #1 and #89 were treated with wt-SLT-1 (■), and 8 M urea (●) respectively to serve as negative and positive controls for cell killing. Percent cell survival was calculated using the equation: (sample – positive control)/(negative control – positive control) X 100. The broken line on the graph is the 3 standard deviation line and any value below this line was considered a hit.

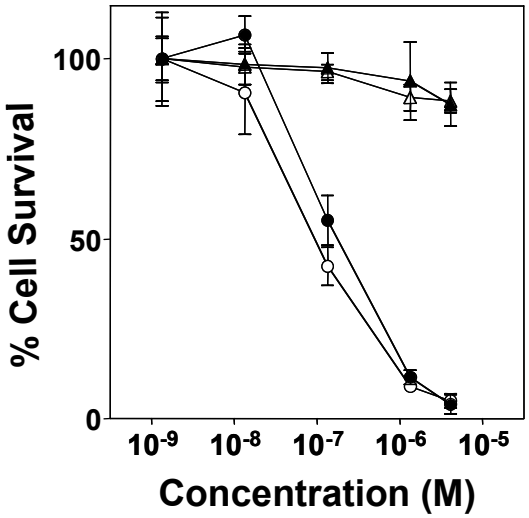

Figure 4.9: Cytototoxicity curves of SLT-1A^{IYSNKLM} and SLT-1A^{AAFADLI} on PC-3 and 518-A2.

Dose-response curves (SRB assay) showing the differential cytotoxic effects of two holotoxin variants, SLT-1A^{IYSNKLM} (▲, ●) and SLT-1A^{AAFADLI} (△, ○), that were hits from the screen on, PC-3 (▲, △; human prostate,) and 518-A2 (●, ○; human melanoma) cell-lines. Each point represents the average of experiments performed in quadruplicate. Error bars represent 95% confidence limits.

4.4.2 Broad specificity of SLT-1 $A^{IYSNKLM}$ for human melanoma cell lines

The SLT-1 $A^{IYSNKLM}$ molecule is able to kill 518-A2 cells. Does SLT-1 $A^{IYSNKLM}$ have similar effects on other melanoma cell lines? We tested the effect of SLT-1 $A^{IYSNKLM}$ on 9 human melanoma cell lines (Figure 4.10). Our results showed that 8 of the human melanoma cell lines (518-A2, A-2058, A-375, C-32, MALME-3M, MeWo, SK-Mel-2, SK-Mel-5, and SK-Mel-28) with the exception of C-32 cell line were sensitive to SLT-1 $A^{IYSNKLM}$ suggesting a broad selectivity for human melanoma cells. This finding was interesting since a ligand directed surface profiling of human cancer cell lines with combinatorial peptide libraries showed that some of the receptors targeted by libraries might be conserved among cell lines derived from a common origin [226].

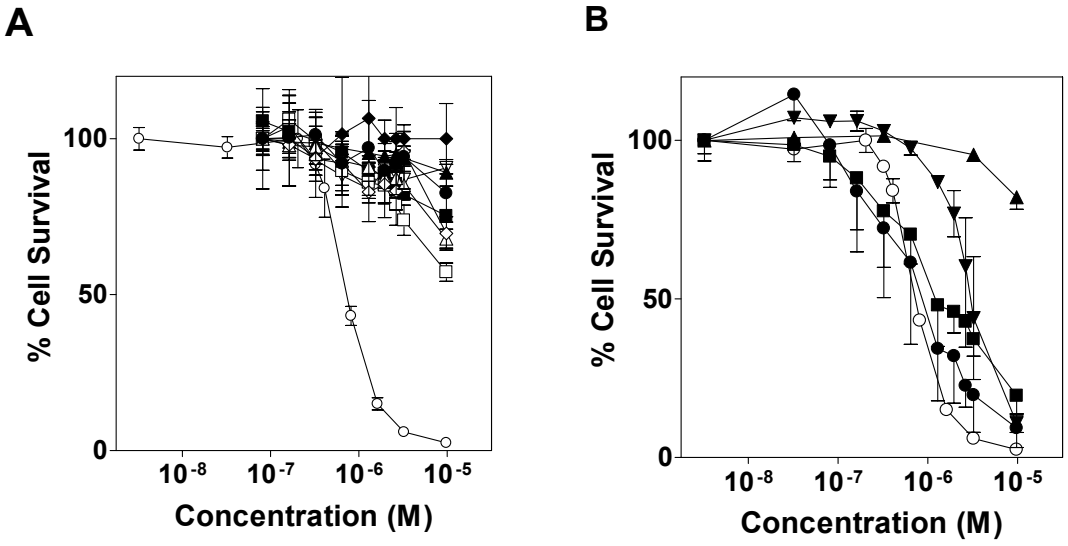

Figure 4.10: Specificity and sensitivity of the A_1 fragment of SLT-1A^{IYSNKLM}.

(A) Dose-response curves illustrating the specific cytotoxicity of the A_1 fragment of SLT-1A^{IYSNKLM} (open symbols) compared to its wt SLT-1 homolog (closed symbols) for the 518-A2 human melanoma cell line. The cell lines depicted are CAMA-1 (◆, ◇; human breast cancer), HepG2 (▲, △; human normal liver), PC-3 (■, □; human prostate cancer), and 518-A2 (●, ○; human melanoma). (B) Dose-response curves illustrating the differential sensitivity of human melanoma cell lines 518-A2 (○), A-375 (▼), SK-Mel-28 (●), MeWo (■), A-2058 (▽), MALME-3M (△), SK-Mel-2 (□), and C-32 (▲) to treatment with SLT-1A^{IYSNKLM}. Each point represents the average % cell survival value (sulforhodamine B assay) from experiments performed in quadruplicate. Error bars represent 95% confidence limits.

4.4.3 The catalytic activity of SLT-1 A^{IYSNKLM} is necessary for cell killing

Mutations of tyrosine 77 within the A chain of SLT-1 are known to dramatically reduce the catalytic activity of wt SLT-1 [223]. A 1,000 fold less active Y77S mutant of SLT-1 A^{IYSNKLM} was subsequently constructed and purified to determine if the catalytic activity of SLT-1 A^{IYSNKLM} was necessary for exhibiting cytotoxicity (Figure 4.11). Our results showed that the catalytic function of SLT-1 A^{IYSNKLM} and indirectly its cellular internalization were required for killing 518-A2 cells (Figure 4.11). These results suggest that

toxin binding to a cell surface receptor was not sufficient for cytotoxicity (as in the case of unmodified mAbs). It was evident that the catalytic activity of SLT-1A^{IYSNKLM} was needed to cause cytotoxicity in 518-A2 melanoma cells indicating that the toxin reached the cytosol of these cells to exert its action on the ribosome (Figure 4.11). The identification of this particular molecule in our cell screen proved that embedding a targeting function in the RIP A chain toxin which has an inherent function (cell killing) was useful in identifying variants that not only bind cells but also enter cells. Interestingly, both the furin-cleaved A chain (A_1 and A_2 chains linked by a disulfide bridge between Cys-242 and Cys-261) and the A_1 fragment of SLT-1 A^{IYSNKLM} displayed similar abilities at killing 518-A2 cells (Figure 4.11). This implies that the presence of the disulfide bond in this case does not have any impact on the binding affinity of the molecule to the cells. It is also possible that the binding event is not the only limiting event but the downstream processing of the molecule inside the cell (examples of downstream events include retrotranslocation from the ER to the cytosol, or escape out of endocytic vessicles).

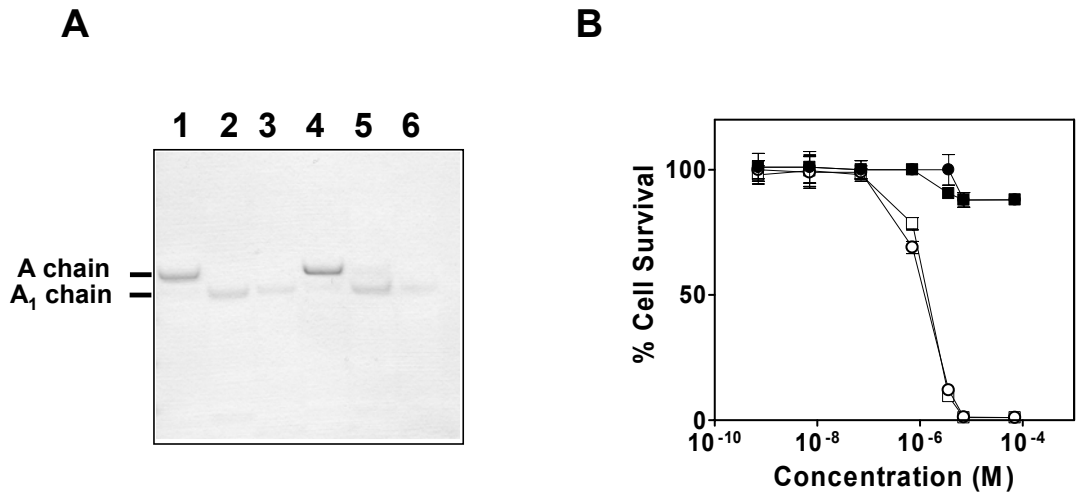

Figure 4.11: Furin cleavage and toxicity of purified, furin-cleaved A chain and A_1 fragment of SLT-1 $A^{IYSNKLM}$ towards 518-A2 cells.

(A) The difference in molecular weight between the A subunit of SLT-1$A^{IYSNKLM}$ (lane 1) and the corresponding A_1 fragment resulting from furin cleavage (lane 2) followed by reduction which yields only the A_1 fragment (lane 3) are shown on a Coomassie-stained SDS PAGE gel. The gel also shows the A and furin-cleaved A_1 chains derived from a catalytically altered (Y77S; 1,000-fold less active) variant of SLT-1$A^{IYSNKLM}$ (lanes 4, 5, 6). (B) Dose-response curves illustrating a comparable cytotoxicity for both the purified, furin-cleaved A chain (A_1 and A_2 chains linked by a disulfide bridge between Cys-242 and Cys-261, □) and A_1 fragment alone of SLT-1 $A^{IYSNKLM}$ (○) towards 518-A2 cells. The detoxified forms (Y77S) of these same molecules (●,■) were not cytotoxic towards 518-A2 human melanoma cells at concentrations of up to 10 μM. Each point represents the average of experiments performed in quadruplicate. Error bars represent 95% confidence limits.

4.4.4 Immunogenicity of single chain SLT-1 $A^{IYSNKLM}$

One eventual challenge of using SLT-1-based, small, single chain ribosome-inactivating proteins as therapeutic agents will be their immunogenicity. It had been established in the past that efficient neutralizing antibodies to SLT-1 are mainly directed at its B subunit [227]. $SLTA_1^{IYSNKLM}$ was not toxic to mice when injected intravenously even at doses reaching 4 mg/kg suggesting that it did not target many cell types or tissues. The

A_1 fragment of SLT-1 $A^{IYSNKLM}$ was thus injected intravenously into CD1 and C57/BL mice as a series of 5 consecutive (daily) tail vein injections to monitor if an immune response could be engendered against this A chain (Figure 4.12). Only weak IgG responses and no IgM responses could be detected in three separate mice as compared with CD1 and C57/BL mice treated with the same molecule prepared in Freund's complete adjuvant. Overall, these results suggest that the repetitive injection of SLT-1 A chain variants such as SLT-1 $A^{IYSNKLM}$ does not yield a strong humoral response in mice.

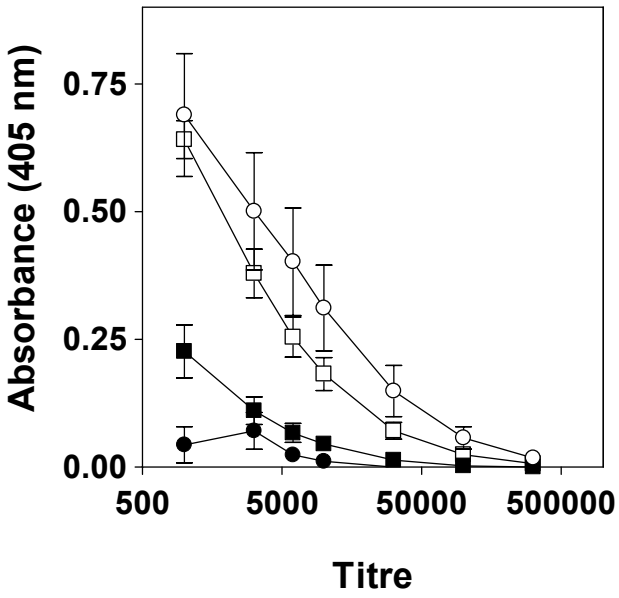

Figure 4.12: Immunogenicity of SLT-1A^{IYSNKLM} in mice.

IgG responses (day 42; anti-mouse IgG-HRP conjugate) determined by ELISA following 5 daily injections (tail vein; day 1 to 5) of the A_1 chain of SLT-1A^{IYSNKLM} in PBS into 2 mice strains (C57/BL, ■; CD1, ●). The A_1 chain in Freund's Complete Adjuvant was also injected subcutaneously into such mice (day 1) and boosted with Freund's Incomplete Adjuvant (days 21 and 35) to generate IgG immune responses as positive controls (C57/BL, □; CD1, ○). Similar responses were observed at day 35 (not shown). Each point represents the average ELISA signal derived from measurements performed on duplicate blood samples drawn from 3 separate mice (6 measurements). Error bars represent 95% confidence limits.

4.4.5 Summary of chapter

In this chapter, a heptapeptide library was designed and constructed with a view to finding new toxin variants able to kill cancer cells. About 70% of the library members expressed protein. More than 9,400 purified A chain variants from the SLT-1A^{XXXXXXX} library were subsequently tested on cancer cell lines with a view to assess if their common ribosome-inactivating function could be used to define mutant A chain able to selectively kill the human melanoma cell line 518-A2. The search identified two library variants, namely SLT-1A^{IYSNKLM} and SLT-1A^{AAFADLI}, selective for 518-A2 cells in relation to a panel of 11 other normal and cancer cell lines. The isolated A chain of SLT-1A^{IYSNKLM} either as a pure A_1 fragment or as a disulfide-linked A_1 and A_2 chains was equally cytotoxic towards 518-A2 cells indicating that its cytotoxicity is not related to the B subunit of SLT-1. The LD_{50} of this molecule is around 400 nM. In addition, this single chain toxin kills most of the other human melanoma cell lines we tested suggesting a broad specificity for melanoma cells. The cytotoxicity of the SLT-1A^{IYSNKLM} A_1 fragment or the disulfide-linked A_1 and A_2 chains towards 518-A2 cells was abolished by mutating a critical residue (tyrosine 77) within the catalytic site implying that protein synthesis inhibition is involved in causing cell death. Furthermore, the immune responses engendered against A chain variants of SLT-1 A^{IYSNKLM} in mice were minimal in terms of affecting a treatment protocol involving the administration of several daily injections of this molecule.

4.4.6 Future prospects

Our preliminary *in vivo* work on mice showed that a combination of the traditional chemotherapy treatment for melanoma, an alkylating agent called dacarbazine (DTIC)

[228], with SLT-1A^{IYSNKLM} improved the survival rates of SCID mice implanted with the 518-A2 tumors (Reveres and Gariepy). A major hurdle with therapeutic proteins is their immunogenicity. If unexpected immune responses were observed in patients, protein PEGylation and T-cell epitope prediction are two strategies that can be utilized to decrease immunogenicity [229-231]. The serum half life of the proteins can also be optimized through PEGylation which is further discussed in Chapter 5. PEGylation offers better stability, decreased proteolysis, enhanced solubility, and longer circulation and body retention of drugs and there are several PEGylated drugs approved by FDA [232-234].

4.4.7 Immediate future work

Identifying the receptor that the SLT-1A^{IYSNKLM} toxin binds will be beneficial in a number of ways. The first benefit involves the successful validation of the combinatorial approach for targeting cancer cells using single chain RIPs. The second benefit would be the discovery of a potentially new target for the treatment of melanoma.

4.4.7.1 Characterization of the Receptor for SLT-1A^{IYSNKLM}

Our initial attempts to characterize the receptor for SLT-1A^{IYSNKLM} involved labeling the toxin with FITC. Even though the labeling reaction was successful (we had green protein) and the toxin retained its ability to cause cytotoxicity in melanoma 518-A2 cells, we did not observe any significant binding of this labeled toxin to the cells in flow cytometry with respect to the labeled wt-SLT-1 A chain (Perampalam and Gariepy). This prompted us to explore radioactive methods to label the protein and perform binding studies to determine the binding constant as well as the number of receptors present on 518-A2 melanoma cells. The octa-histidine tag present at the N-terminus of

SLT-1A^{IYSNKLM} provided an ideal target for radiolabeling with technetium-99m (^{99m}Tc). Waibel et al had shown that the His-tag of recombinant proteins can be labeled with ^{99m}Tc which does not affect the rest of the protein [235]. However, our attempt to use ^{99m}Tc was not successful and it might be because of low labeling yield. Radiolabeling of surface tyrosine residues with ^{125}I is another possibility. However, the presence of a tyrosine residue within the exposed cell-targeting 7-mer peptide (IYSNKLM) could potentially disrupt SLT-1A^{IYSNKLM} binding. There are in total 7 tyrosine residues in this toxin and 2 of them, namely tyrosines 77 and 114 are the most surface exposed tyrosine residues. Even though, these two residues are involved in the catalytic activity of the toxin, it may not influence the binding properties. As future studies, we could explore labeling the wt-SLT-1 A and SLT-1A^{IYSNKLM} with ^{125}I. Saturation binding, kinetic, and competition assays will be useful in determining the number of receptors on the 518-A2 melanoma cells, as well as binding affinity of the toxin to its target [236, 237].

4.4.7.2 Biodistribution studies

If the labeling of SLT-1A^{IYSNKLM} with ^{125}I is successful, then we could perform biodistribution studies with this and wild type labeled toxins. The radiolabeled toxins can be injected into SCID mice with one of two different human xenografts (518-A2 melanoma cells; sensitive to SLT-1A^{IYSNKLM} and PPC-1 prostate cells; insensitive to SLT-1A^{IYSNKLM}). The mice could be imaged using a gamma camera at various time points.

4.4.7.3 Characterization of the receptor

We could also characterize and isolate the receptor for SLT-1A^{IYSNKLM}. This can be done in a number of ways. The first task would be to determine the nature of the receptor to determine whether this ligand interacts with a protein or lipid. One way would be to

treat the 518-A2 melanoma cells with SLT-1A^{IYSNKLM} at 4 ºC and cross-link the complex using bis(sulfosuccinimidyl)suberate (BS^3), a homo-bifunctional, water-soluble, non-cleavable and membrane impermeable crosslinker [238]. The cells can then be lysed in 6M guanidinium HCl and subjected to Ni-NTA column purification (since the SLT-1A^{IYSNKLM} toxin contains an N terminal His tag). The purified proteins could then be analyzed by Western blot using an SLT-1 A chain antibody or they could be subjected to thin layer chromatography.

CHAPTER 5: CONCLUSION AND FUTURE DIRECTIONS

5.1 Summary and highlights of thesis contribution

Combinatorial protein libraries represent a powerful approach to accelerate the evolution of protein scaffolds towards the creation of novel anticancer agents. In this thesis, we have shown that the structural complexities associated with the AB_5 template of SLT-1 could be reduced by just using its A chain. Specifically, we have shown that the SLT-1 A_1 chain can serve as a protein scaffold to display a ligand binding function by inserting a peptide ligand within the protease sensitive loop of the toxin. A 7 amino acid long immunodominant epitope from the tumor-associated mucin MUC-1 was used as the ligand and was inserted between residues 245 and 246 of the SLT-1 A chain as shown in Figure 5.1. The resulting protein, termed SLT-1A^{PDTRPAP}, was shown to express well and displayed a catalytic function that was comparable to that of the wt SLT-1 (Figure 2.6 and 2.7). The mAb *Onc* M27 which recognizes the MUC1 epitope PDTRPAP, was shown to bind to SLT-1A^{PDTRPAP} by ELISA in the context of this peptide sequence being presented as part of the AB_5 holotoxin or within the single A chain (Figure 2.6). From this study we were able to conclude that the SLT-1 A chain can tolerate an insertion

within its protease sensitive loop region and that a ligand inserted within the loop can bind to an antibody while this A chain retains its catalytic function.

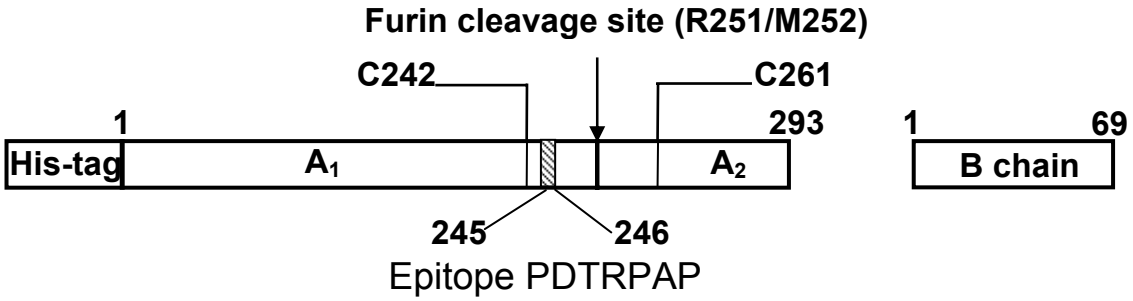

Figure 5.1: A schematic illustration of SLT-1 construct comprising its A and B subunits.

A histidine tag was inserted at the N-terminus of the A chain for affinity purification. Furin cleavage occurs between residues 251 and 252 of the A subunit (arrow) within its protease-sensitive loop (residues 242-261), releasing a cytotoxic A_1 fragment (residues 1-251) and an A_2 fragment (residues 252-293) non-covalently linked to the B subunit pentamer. The peptide epitope PDTRPAP was inserted between residues 245 and 246 of the A_1 domain.

As a proof of principle, we also demonstrated that a combinatorial SLT-$1A^{PDXXXAP}$ library where the key tripeptide epitope TRP recognized by the mAb *Onc*-M27 could be screened to identify the sequence TRP as the mAb epitope. The tripeptide motif within the 7 amino acid ligand in the protease sensitive loop was thus randomized as shown in Figure 3.1. The tripeptide library generated had optimal properties with respect to sequence diversity and protein expression (Table 3.1 and Figure 3.3). By screening 10,000 colonies from the library, we observed that the theoretical or predicted outcomes

of the library were similar to the observed outcome from the tripeptide library (Table 3.2 and 3.3). From this study we were able to conclude that an unbiased library with good sequence diversity and protein expression can be generated when the library was inserted between residues 245 and 246 of the SLT-1 A chain. Moreover, the library generated could be effectively screened with molecules as large as antibodies.

A heptapeptide library was subsequently inserted in the protease sensitive loop of SLT-1 at the same site in order to screen for A chain variants able to kill cancer cells (Figure 4.1). From screening 9,400 bacterial colonies on a human melanoma cell line 518-A2, the variant SLT-1A^{IYSNKLM} and its A_1 chain were identified as able to specifically kill these melanoma cells (Figure 4.9 and 4.10). We also showed that the catalytic activity of this toxin variant was indeed necessary for the cytotoxicity (Figure 4.11). This toxin variant did not elicit a strong immune response in mice (Figure 4.12). In preliminary studies, this molecule was shown to lengthen the survival of SCID mice harboring a 518-A2 tumor xenograft, when used in combination with a standard melanoma treatment (dacarbazine; DTIC). Thus, by screening a heptapeptide library in the A chain of SLT-1, we identified a molecule that was able to bind to a specific cancer cell, be internalized and mediated cell killing. This is the first study which explored the potential of a single chain combinatorial toxin library as a discovery tool to define toxin variants able to target cancer cells. This strategy can be adapted to use any toxin scaffolds and the resulting libraries can be screened on any normal or tumor cell lines.

5.2 General challenges in targeting solid tumors with protein therapeutics

Even though, more than 85% of human cancers are solid tumors, only 3 out of the 8 approved mAbs to date can be used for solid tumors. Out of the 3 mAbs (trastuzumab, cetuximab, and bevacizumab), one of them (bevacizumab) targets a soluble ligand while the other 2 target a surface protein [54]. Achieving effective concentrations of mAbs within solid tumor masses is a major challenge. However, in the case of hematological cancers, the dosage of Abs can be adjusted to reach the desired serum concentration. In general, protein therapeutics have to overcome several barriers in order to exert an effect on solid tumors. These barriers include the vascular endothelium, stromal and epithelial layers and high interstitial pressure as well as the heterogeneous nature of solid tumors [239]. It is advantageous to target solid tumors with smaller recombinant proteins such as single-chain antibodies instead of larger molecules since they can penetrate into tumor more efficiently [127]. However, this benefit is in fact counter balanced by the disadvantage that such smaller molecules are rapidly cleared from the plasma leading to shorter circulating half-lives [240].

5.3 Toxin-based anti-cancer therapeutics

Immunotoxins (ITs) are presently designed in a two-step procedure, where an antibody domain, growth factor or cytokine directed at a validated target is initially identified and subsequently fused or coupled to a catalytic domain of a protein toxin such as Pseudomonas exotoxin A, diphtheria toxin or ricin [241-243].

Small, single chain toxins can address some of the challenges facing immunotoxins. Specifically, immunotoxin constructs are structurally large (over 200 kDa), require the derivation of a monoclonal antibody or selection of an established ligand to a known target and may necessitate that either part or the entire construct be expressed in a eukaryotic host [244, 245]. Specifically, immunotoxins are protein constructs with an overall mass significantly greater than the ~30 kDa of SLT-1A_1 chains described in my thesis, a feature that can adversely limit their ability to diffuse into solid tumors [59]. For example, several ricin based ITs have been tested in phase I and phase II clinical trials and failed due to low tumor penetration [246, 247]. The cytotoxicity of ITs are often not as high as expected because they rely on a number of properties such as antigen-binding affinity, internalization rate, intracellular routing and processing [248]. It has been observed that due to the inefficient uptake of the ITs into intracellular compartments, their toxicities are often not as high as expected. By screening libraries of a single chain toxin molecule that retains their intracellular functions on tumor cells for cytotoxicity, we are selecting molecules that may seek their intracellular targets more efficiently.

5.4 Improving the therapeutic potentials of SLT-1 protein

An ideal protein therapeutic should bind to its target efficiently, be non-immunogenic, easily produced, while displaying an optimal serum half-life, shelf-life and be safe to use. Monoclonal antibodies, antibody fragments, alternate binding proteins (such as those described in Section 1.4.6), immunotoxins and SLT-1 A_1 variants all have their own benefits and issues. Since most of the preclinical and clinical studies have been done with mAbs and their fragments, my analysis will be limited to mAbs. Alternate

binding proteins and antibody fragments have, up-to-now, been used as targeted carriers for drugs, while intact immunoglobulins possess effector functions such as ADCC and complement activation. Additional functions could be introduced by conjugating mAbs, their fragments or alternate binding proteins to functional domains such as toxins, cytotoxic drugs, cytokines, enzymes, and radioisotopes. In this regard, the SLT-1 A_1 scaffold has an intrinsic advantage of being a cytotoxic enzyme.

5.4.1 Pharmacokinetics and biodistribution of protein therapeutics

Pharmacokinetic parameters include clearance rate, serum stability and tissue penetration. It has been confirmed by *in vivo* studies that size is a critical parameter in pharmacokinetics and biodistribution of mAb molecules [57, 58, 190]. For example, intact IgG molecules penetrate tumors slowly, distribute non-uniformally, and reach high serum levels. Since a major parameter affecting the rate of diffusion through tumors is molecular size, single chain antibody fragments diffuse at least 6 times faster than IgG [58, 59, 249]. However, small antibody fragments such as scFv on the other hand are cleared very rapidly and have poor tumor retention because of their monovalent binding [126, 250-252]. Pharmacokinetic analysis of blood clearance levels showed that the half lives of IgG, scFv, sc(Fv)2, and (sc(fv)2)2 is 331 min, 10 min, 80 min and 169 min respectively [253]. Alternate scaffold proteins due to their small sizes (less than 30 kDa) would exhibit rapid clearance from the bloodstream just as antibody fragments of similar sizes. This property (small size) on the other hand would provide these molecules with improved tissue penetration. SLT-1 A_1 chain is about 30 kDa which makes it similar to the size of the scFv molecules and most of the alternate scaffold proteins. Hence, SLT-1 A chain would have better tumor penetration potential but might be cleared rapidly from

the bloodstream. The serum half-life of proteins can be improved by reducing renal clearance. The molecular weight cut off for their elimination through the kidneys is around 60 kDa and most of the scaffold proteins and SLT-1 A chain are below this threshold [254]. Many strategies can be employed to improve the serum half life of proteins including site specific PEGylation [255], or by the fusion of long-lived serum proteins such as albumin binding peptides [256] and serum immunoglobulin [257] or by oligomerization of the proteins.

5.4.2 Protein expression and stability

It is desirable to produce therapeutic proteins using the cheapest and most efficient manner. Most studies have reported the preference for scFv over Fab due to their expression levels in bacteria (over 1g/L from fermentors). Alternate binding proteins can be produced by fermentation in *E.coli* or yeast [102, 109]. Most of these proteins fold properly under reducing conditions which enables cytoplasmic expression in stable, soluble form, a beneficial feature for preclinical and clinical studies. SLT-1 exhibits a good stability profile because it is produced under denaturing conditions and subsequently refolds to become cytotoxic again. Furthermore, the molecule can be treated with furin (to activate its catalytic activities) for over 3 days at 30 °C without any degradation taking place.

The nature of a protein scaffold does not guaranty good expression or protein stability after mutation. In fact protein expression yields can typically be improved by orders of magnitude during process optimization with industrial vectors and strains [258]. A

challenge that needs to be overcome with using SLT-1 A_1 chain as a template, is that it cannot be expressed at very high levels in bacteria compared to non-toxic scaffold proteins such as ankyrin repeat, lipocallin and Z domain of protein A. This is due to the fact that prokaryotic ribosomes are a weak substrate for SLT-1 at high concentrations. Surprisingly, ricin is not toxic to bacterial ribosomes and can be produced in high yields (50-100 mg/L). We had attempted to express the A_1 chain of SLT-1 in two different vectors (namely the pET expression system and the pECHE expression system). Results from expression in pET vector indicate that the A1 chain expresses poorly (results not shown). These results suggest that it may be possible to improve the expression yields of the A_1 chain in bacteria. We have experimentally observed that A chain variants must be expressed as part of an AB_5 holotoxin, in order to obtain A variants in good yield. The B subunit appears to act as a chaperone for it's A chain. Protein expression is also an issue in terms of screening SLT-1 A libraries since we are only picking a small fraction (single bacterial colonies) of the 7-mer library due to the technical nature of the screening process. Screening more colonies from the library would yield more "lead" protein therapeutics.

Over the last five years, there has been great progress towards expressing proteins that are toxic to cells. Bowers and her collegues have engineered a new *E. coli* host/vector system to allow tight and uniform modulation of gene expression and γ origin (ori) plasmid copy number [259]. This host/vector system was used to overproduce a potent toxin knows as colicin. However, one has to bear in mind the dangers (bioterrorism and

new pathogenic strains) of creating and giving growth advantage to bacterial strains with toxic genes.

5.4.3 Screening on wild type tumor cell lines

The wild type B subunits bind to CD77 receptors on normal cells. Thus combinatorial libraries of the AB_5 template may require a modification in the B subunit to knock down its binding to CD77 which would allow us to screen our respective library directly on tumor cells without growing them under the presence of wt-SLT-1 toxin. Up to now, we have used cell lines as targets that are resistant to wt-SLT-1. Growing cells under stress (ie. the presence of toxin) may in theory alter their phenotype by changing the expression of cell surface markers. The effect of different site specific mutations on SLT-1 B subunits in the three sites known to be crucial for binding (shown in Chapter 1, Figure 1.6) are summarized in Table 5.2 [260]. Single mutations (such as D17E, A56Y and W34A) cause modest changes in B subunit binding to CD77 (as indirectly measured using a cytotoxicity assay). Other mutations such as F30A, and G62T have a dramatic impact on toxin binding and have been shown from crystal structures of the B subunit to carbohydrate receptor mimics to be associated with the receptor binding surface of the B subunit. It might be beneficial to try single mutations and combinations to compare protein expression and to choose B subunit variants which lack CD77 binding and are still well expressed in bacteria.

Table 5.1: Site directed SLT-1 mutants and their cytotoxicity

Mutations	Site	CD_{50} (ng/mL)	Fold reduction
Wild type	1	0.0061±0.0018	1
F30A	1	1,100±600	10^5
D17E	1	6.7±3.2	10^3
A56Y	2	1.4±1	10^2
G62T	2	10,000±2,500	10^6
G62A	2	1,900±820	10^5
W34A	3	0.046±0.002	10
F30A/G62T	1, 2	360,000±100,000	10^8
F30A/W34A	1, 3	3,300±510	10^5
D17E/W34A	1,3	3,300±10	10^5
A56Y/W34A	2, 3	3,300±510	10^5
G62T/W34A 2, 3	2, 3	11,000±3,200	10^6
F30A/G62T/W34A 1, 2, 3	1, 2, 3	740,000±55,000	10^8

*** Table adapted from [260]**

5.4.4 Improving the ligand binding and cytotoxicity of our lead compound, SLT-1A^{IYSNKLM}

The CD_{50} for SLT-1A^{IYSNKLM} is around 400 nM and there are ITs with CD_{50} in the picomolar range [261] that did not provide good clinical results. There are a number of reasons for this including low number of receptors on target cells, inefficient internalization of ligand/receptor complex, or inefficient escape from endosomal compartments or ER lumen into the cytosol. Some of these issues will be better addressed once the receptor for SLT-1A^{IYSNKLM} is identified. Thus one major future challenge in exploring SLT-1A libraries will be to develop a generic strategy (a new proteomic approach) to identify receptor(s) targeted by "lead" SLT-1A variants. Clearly, new receptors will represent important new tumor markers and thus valuable intellectual property.

5.4.4.1 Improvement of ligand binding affinity

If the CD_{50} of SLT-1A^{IYSNKLM} is only dependent on the affinity of the molecule to the receptor, then the affinity constant would also be in the sub-micromolar range. For mAbs, the avidity is much higher and even for ITs the CD_{50} is in picomolar range [127]. There are two approaches that are used to improve the affinity of antibodies. The first approach is to create very large libraries of the CDR loops and to select for higher affinity variants [240, 262]. The second approach involves making sublibraries of known CDR loops or hot spots to provide small improvements in affinity [263-267].

In the case of SLT-1A^{IYSNKLM}, if our dissociation constant from the radiolabeling studies is close to our cytotoxic constant, then each of the positions in the 7 amino acid ligand (IYSNKLM) could be randomized using the NNS scheme and better binders/killers

could be selected. This approach would resemble the sublibrary strategy used for evolving antibodies.

5.4.4.2 Addressing routing of the toxin

Our study has shown that SLT-1A^{IYSNKLM} needs to be internalized in order to cause cytotoxicity in human 518-A2 melanoma cells (Figure 4.11). We are currently performing studies to verify the apoptotic pathway that is involved in this toxin mediated cell death. Previous studies have shown that routing of wt-SLT-1 through the Golgi apparatus was crucial for mediating toxicity [268, 269]. Cells that were normally sensitive to the effects of SLT-1 were protected by Brefeldin A which disrupts Golgi cisterns [177]. Brefeldin A mediated protection against intoxication by toxins was shown for cholera, pertussis toxin, *E.coli* heat labile enterotoxin, Pseudomonas exotoxin A and ricin but not for diphtheria toxin (which enters the cytosol through endosome), demonstrating that the routing through the Golgi represents an important step in the pathogenesis of these toxins [171, 173, 176, 270, 271]. We could treat the 518-A2 melanoma cells with Brefeldin A and determine if this drug will protect them from toxicity which might indicate whether routing through Golgi is crucial for SLT-1A^{IYSNKLM}. Toxins such as cholera toxin, PE and *E.coli* heat labile enterotoxin contain a KDEL-like motifs and the C-termini of their A chains that are thought to play a role in their retrograde transport to the ER. Removal of the KDEL sequence from PE had severely attenuated its toxicity while removal from cholera and LT did not alter their toxicity to the same extent [271-273]. It was also observed that addition of the KDEL sequence to the ricin C-terminus greatly enhanced toxicity [274-276]. The addition of the KDEL motif to the SLT-

$1A^{IYSNKLM}$ is another strategy that could be done to see if it enhances toxicity towards 518-A2 cells.

5.4.4.3 Avidity effects

In the context of tumor environment, even high affinity monovalent interactions provide fast dissociation rates and only modest retention times on target antigen. It has been observed that scFvs have better tumor penetration, lower retention times in non-target tissues and rapid blood clearance [277]. Due to the rapid clearance from the blood pool of these 30 kDa proteins, the absolute amount of scFv uptake by a tumor is limited. Valency is an effective way of increasing the affinity of an protein to the antigen. Hence it is beneficial to re-engineer the monovalent Fab or scFv fragments into multivalent molecules which lead to significant increases in avidity for cell surface molecules [278, 279]. The effect of valency has been observed in other systems as well (for example, the affinity of dimeric hemagglutin to its ligand on human A erythrocytes is 10,000 fold higher than that of the monovalent hemagglutin [280]. PEGylation using bifunctional PEG molecules is a simple strategy to make bi-valent SLT-$1A^{IYSNKLM}$. However, an increase in valency also results in increased molecular size, which will affect pharmacokinetics, extravasation, and tumor penetration.

Another strategy that may be utilized for making dimeric or tetrameric form of SLT-$1A^{IYSNKLM}$ is by using self associating peptides. Willuda et al constructed mono-, di-, and tetrameric variants of the anti-tumor p185HER-2 scFv fragment 4D5 by fusion of self-associating peptides to the carboxyl terminus. They generated dimeric miniantibodies with a synthetic helix-turn-helix domain (dhlx) and tetrameric ones with the tetramerization domain of the human p53 protein in the periplasm of *E.coli* [281].

Dimerization and tetramerization of the antibody fragment resulted in increased serum half life, significantly reduced off-rate, due to the avidity effect, both on purified $p185^{HER-2}$ and on SK-OV-3 cells. The sequence for the 2 domains and the possible constructs are presented in Figure 5.2.

A

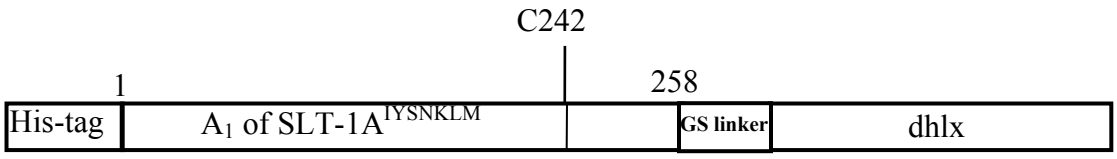

helix turn helix dimeric domain (dhlx):

GELEELLKHLKELLKGPRKGELEELLKHLKELLKG

B

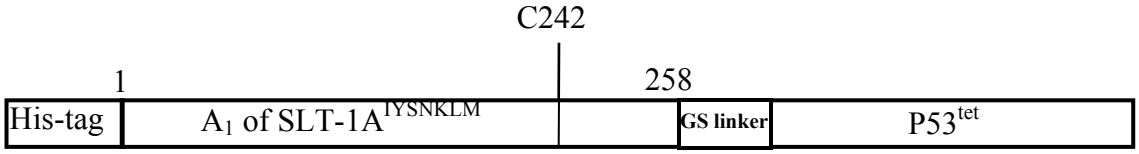

P53 tetramerization domain:

KPLDGEYFTLQIRGPERFEMFRELNEALELKDAQAKEP

Figure 5.2: Possible dimerization and tetramerization constructs of SLT-1A^{IYSNKLM}

At the C-terminus of the A1 chain, a GS linker is fused to which a 35 amino acid helix turn helix domain is attached. Similarly a p53 tetramerization domain is fused at the C-terminus of the A1 chain through a GS linker.

5.4.5 Immunogenicity and protein therapeutics

Immunogenicity elicited by protein therapeutics can limit their potential. Even though, SLT-1A^{IYSNKLM} did not elicit a strong immune response in mice, it is possible that it might produce immune responses in patients when chronically administered just as in the case of ITs. Researchers have tried to reduce immune responses by choosing scaffold proteins of human origin. Therapeutic proteins with a human origin can lead to the production of human anti-human antibodies upon repeated administration [282]. The same immunogenicity problems may arise for alternate binding proteins since many mutations are introduced during library generation.

5.4.5.1 Lessons from immunotoxins to reduce immunogenicity

Immunotoxins have been shown to have high specificity and potency in tissue culture and in immunocompromised mice bearing human tumor xenografts. However, clinical benefits from these molecules have been hampered by the immune responses which reduce their serum half life and their cytotoxicity [128, 283-286]. The question of whether one toxin is more immunogenic than another has been asked and the answer appears to be no [287-289]. All ITs used clinically have induced immune responses in patients to both toxin and mAb regions. A number of strategies have been explored to reduce the immunogenicity problem associated with ITs. The first strategy was the administration of immunosuppressive agents such as cyclosphosphamide and cyclosporine with ITs which did not result in prevention of anti-IT antibodies [290, 291]. Another strategy explored was altering the structure of the ITs by (1) adding polyethylene glycol (PEG) groups or (2) by site directed mutagenesis to remove immunodominant epitopes [292, 293]. ITs modified using these strategies have not been tested in patients

yet. Another approach was to use human RNase (cytotoxins when in the cytosol cause degradation of cellular RNA and lead to cell death) with single chain antibody molecules [294-296]. Fusion proteins consisting of angiogenin (pancreatic RNase A) and a humanized anti-CD22 single chain antibody or human pancreatic RNase and a human anti-ErbB2 single chain antibody were generated and shown to be very specific and to inhibit tumor growth in a murine model [294-296]. The values of IC50 (*i.e.,* the concentration capable of reducing cell viability by 50%) were found to be 12.5, 47, 52, and 60 nM for SKBR3, MDA-MB361, MDA-MB453, and TUBO cells, respectively. However, it is still a concern that the combinations of human toxins with ligand may generate immune responses.

5.4.5.2 PEGylation of SLT-1A^{IYSNKLM}

PEGylation is one of the best known methods for post-translational modification of proteins that impact therapeutic efficacy. PEG or polyethylene glycol is a non-toxic, and a non-immunogenic, and has been used in modifying many therapeutics that have the FDA approval including adenosine deaminase, asparaginase, α-interferon, and a growth hormone antagonist [232, 234, 297, 298]. PEGylated proteins have a number of advantages such as inhibition of protein degradation by metabolic enzymes, and extended protein half-life (ref). PEGylation also decreases immunogenicity by decreasing proteolysis, interfering with protein processing and presentation and by blocking antibody-or HLA-epitope binding [289, 299]. PEGylation can also prolong protein residence time in plasma and increase their solubility [300].

A common way to PEGylate a protein is by modifying free lysine groups on the surface of the protein, however, this method is often associated with protein inactivation [301, 302]. Furthermore, the presence of a lysine residue in the ligand binding site of SLT-1A^{IYSNKLM}, encourages us to look at alternate sites for PEGylation. If we look at the A_1 chain of SLT-1A^{IYSNKLM}, there is a cysteine residue with a thiol group, which could be used in the covalent attachment of a PEG molecule (Figure 5.3). We can evaluate the relative conjugation efficiency of several A_1 chain of SLT-1A^{IYSNKLM} with PEG molecules varying in size, structure, and reactive thiol groups, including mono- and bifunctional PEG molecules in linear and branched formats (Figure 5.4 and Table 5.2). PEGylation also offers the opportunity to form multidentate structures through the use of star or branched PEG polymers which may increase avidity and hence residence time on target sites [303]. PEGylation efficiency can be analyzed by SDS-PAGE where free SLT-1A^{IYSNKLM} and PEGylated SLT-1A^{IYSNKLM} migrate at different positions. The PEGylated proteins can also by tested for their ability to cause cytotoxicity on the human melanoma cell line 518-A2 to verify if any particular PEGylation strategy is superior to others and to make sure that PEGylation at that site does not impose any steric hindrance on ligand binding function.

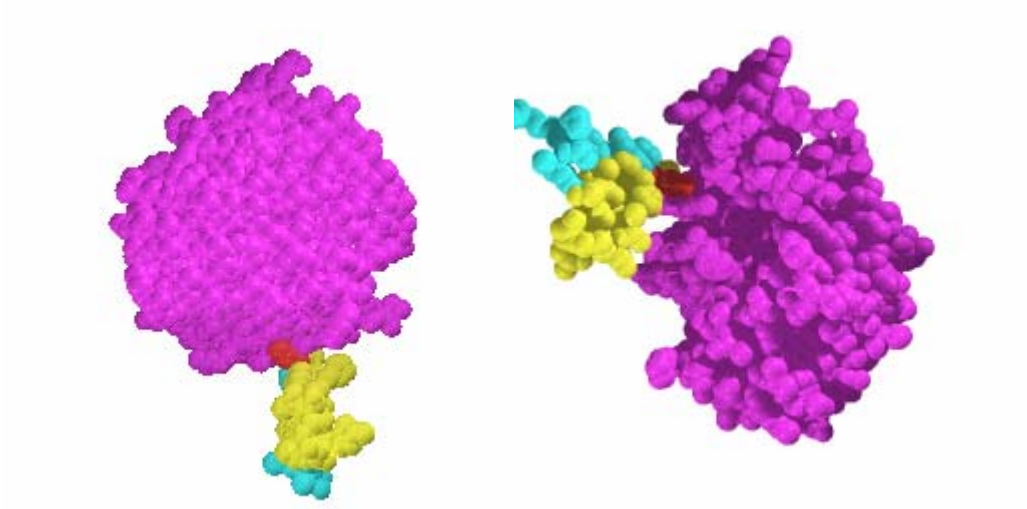

Figure 5.3: Two space filling models of SLT-1A^{IYSNKLM} showing the free cysteine residue at position 242

Residues (1-245) that includes the catalytic domain of the A_1 chain is shown in magneta. The ligand binding domain (7 aa insert) is highlighted in cyan while the rest of the protease sensitive loop is colored in yellow. The free cysteine which lies at the N-terminal of the protease sensitive loop is shown in red.

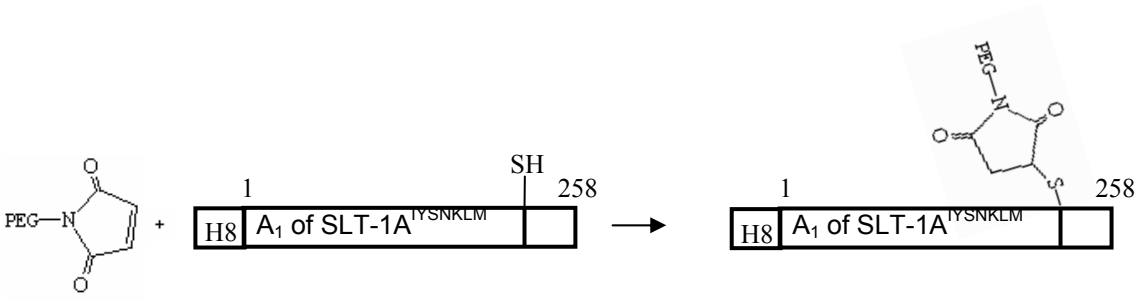

Figure 5.4: Modification of Cys 242 of SLT-1A^{IYSNKLM} with PEG maleimide

The coupling of PEG to the A_1 chain of SLT-1AIYSNKLM is achieved by using PEG-maleimide which reacts with the free cysteine residue at position 242 on the A_1 chain.

Table 5.2: List of reactive PEG derivatives used for site-specific PEGylation of proteins

Functionalized PEGs	Molecular weight (kDa)
PEG-$(Mal)_2$	2, 3, 4
NHS-PEG-Mal	3, 4
PEG-Mal	5
PEG-Mal	10
PEG-Mal	20
$(PEG)_2$-Mal	40

5.4.5.3 Other strategies to de-immunize protein therapeutics

Protein sequence modification resulting in the removal of T cell epitopes from recombinant proteins could reduce the immune response to the protein. Many mAbs have been de-immunized and successful deimmunization of therapeutic proteins has been demonstrated by Genencor Inc., and EpiVax Inc [304].

5.4.5.4 Immunotoxins and vascular leak syndrome

A major side effect of ITs is vascular leak syndrome which is characterized by increased vascular permeability causing extravasation of fluids and proteins leading to interstitial edema and organ failure [305]. It has been observed that VLS causing toxins such as ricin and PE, and IL-2 share a 3 amino acid disintegrin-like consensus motif (xDy) where x = L, I, G, or V and y = V, L, or S and it has been shown that those proteins can bind and damage human endothelial cells *in vitro* [306]. These studies have revealed

that mutations in this site or in residues flanking these sites in the three-dimensional structure might prevent VLS [306]. It is also believed that larger ITs (over 200 kDa) due to their longer circulating lifetimes display higher incidence of VLS in patients when compared to smaller ITs [307, 308].

In the A_1 chain of SLT-1, there are 5 putative motifs that may contribute to VLS although this information is speculative. One way to address this issue would be to make point mutations in these sites and assess their ability to induce VLS symptoms in endothelial cells. These putative VLS causing endothelial cell binding sites are highlighted in Figure 5.5.

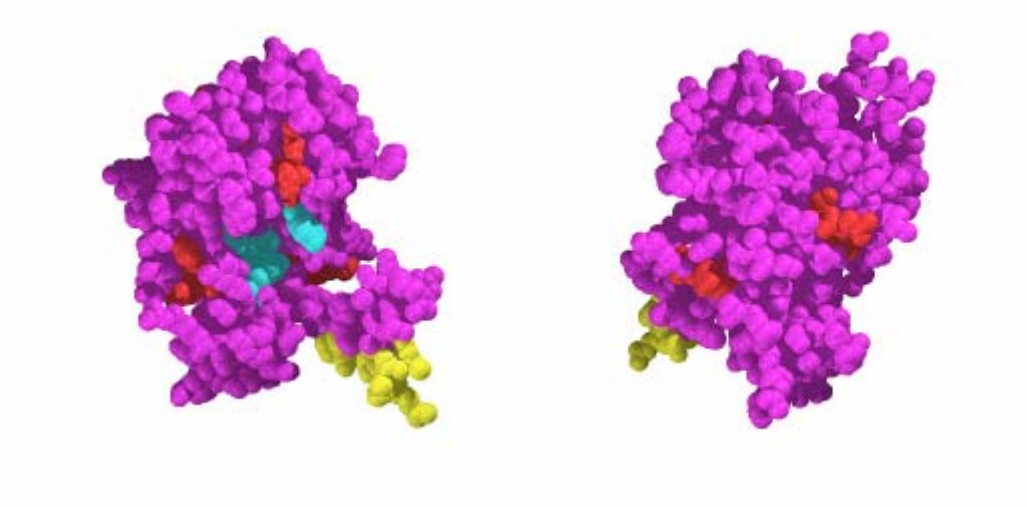

Figure 5.5: Two space filling models of SLT-1A^{IYSNKLM} showing the VLS causing motifs

The 5 VLS causing motifs are shown in red. The catalytic cleft containing residues Y77, E167, R170 and W203 are shown in cyan while the ligand binding peptide (7 aa insert) is shown in yellow.

5.5 Future studies

An ideal platform for developing protein therapeutics should offer potent specific activity against a target, be non-immunogenic and meet practical standards related to manufacture, serum half-life, delivery and safety as discussed in Section 5.4. These traits must either be inherent to the protein scaffold or easily added. In this thesis, I have shown that the A_1 chain of SLT-1 has potential as a therapeutic agent against a human melanoma cell line, 518-A2 and I have also proposed a number of strategies to optimize the therapeutic potential of SLT-1A^{IYSNKLM} further.

In our study, the library element had been inserted into the protease sensitive loop which is a structurally unconstrained region of the A_1 fragment (residues 245-246), meaning that the conformational space associated with each peptide bond within the ligand is large. Indeed, in the crystal structure of SLT-1, this region is not defined [149]. Embedding the random peptide library into a stable structural scaffold would limit the flexibility of the resulting peptide ligands, potentially yielding ligands with better affinity constants and selectivity for a targeted receptor. In the future, the C-terminal of SLT-1 A_1 chain could be fused to small stable protein scaffolds which can express well with fusions at the N-termini (Figure 5.6).

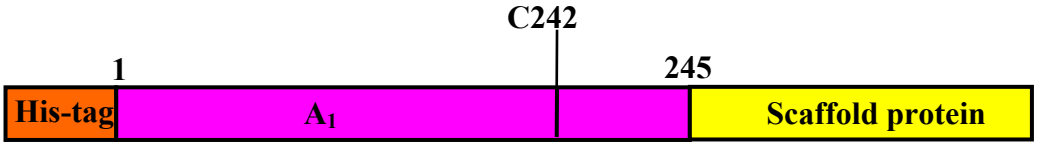

Figure 5.6: A schematic illustration of C-terminal fusion of a scaffold protein to the cytotoxic domain of SLT-1

The construct includes a His-tag for purification (red) and the cytotoxic domain of SLT-1 A chain (1-245 in purple). A putative scaffold protein to create a library can be fused at the C-terminal end of the A_1 chain (shown in yellow).

Although, numerous protein scaffolds are described (Table 1.3) as suitable for generating binding reagents, only some would better the potential of SLT-1 A_1 chain as a therapeutic when used as a fusion to the A_1 chain. Some of the protein scaffolds that may be useful for this purpose are shown in Figure 5.7. My selection is mainly based on size and a rigid framework for selecting high affinity binders. The reason for using smaller scaffolds is to incorporate multiple domains of the scaffold in order to increase the avidity of binding. I believe that the human LDL receptor A-domains (Figure 5.7) provide most of the criteria for developing a therapeutic protein platform along with the A_1 chain of SLT-1. These proteins offer simple, thermodynamically stable folds that occur as strings of multiple domains on several cell surface receptors mediating binding to over 100 different targets [309]. Each of the A domains are about 35 aa long (4 kDa), stabilized by 3 disulfide bonds and are separated by linkers that average 5 aa in length.

In each A domain, 28 residues are non-conserved and hence large diversity libraries can be generated. Silverman and colleagues had generated a phage display library of about 10^{10} clones to provide a pool of A-domains capable of binding immobilized targets [110]. They have shown that rather than mutagenising the protein between cycles, they can add a new pool of domains (random or previously selected) adjacent to the domains selected in previous rounds. The end product was a single chain protein containing multiple domains with independent function and they called these proteins avimers. They selected binders with subnanomolar affinities against many targets including IL-6, cMet, CD28 and CD40L. They also demonstrated that the serum half life of these avimers can be increased by adding IgG binding domains. We thus plan to fuse an A domain to the C terminal of A chain of SLT-1 with the idea of creating a randomized library in the A domain. The A1 chain – A domain libraries could either be screened using phage display or designed to be used in cell-based assays.

Another choice of a protein framework for fusion to the A_1 chain of SLT-1 would be the Z domain of protein A which is a variant of the IgG-binding Protein A from *Staphylo-coccus aureus*. The Z domain is a 58 amino acid, three-helix bundle [101, 310]. In this domain, up to 13 solvent exposed residues in the α–helical structure were randomized and nanomolar affinity ligands were generated against HER2/neu [311, 312].

A third choice would be the single immunoglobulin-binding domain (GB1; HTB1) of protein G which binds to the Fc region of IgG. The GB1 domain comprises of 56 resi-dues with no disulfide bridges and is composed of a four-stranded β-sheet, supporting a

long α-helix [313]. Although the core region of the GB1 scaffold is affected by mutations, its exposed α-helical domain which is involved in binding to the Fc domain of IgG can be altered [314].

Ankyrin repeat proteins present a modular architecture where each of the 33 amino acid modules possess a β-turn and two anti-parallel α–helices [102, 109, 315]. This protein has predominantly been used in ribosome display strategies and high-affinity binders (KDs in the nanomolar range) against different protein targets including the maltose binding protein were selected [79]. Since this scaffold protein has not been successful with phage display strategies and ribosome display is not a suitable approach for displaying SLT-1 A chain, only the cell-based assay is feasible.

Members of the knottin family are very stable proteins of around 30 aa and typically contain a small triple-stranded anti-parallel β–sheet and a cysteine knot motif [316]. Since they are used to present an inserted peptide loop of high variability in terms of both length and sequence, they may not be ideal to provide rigid framework in our molecule.

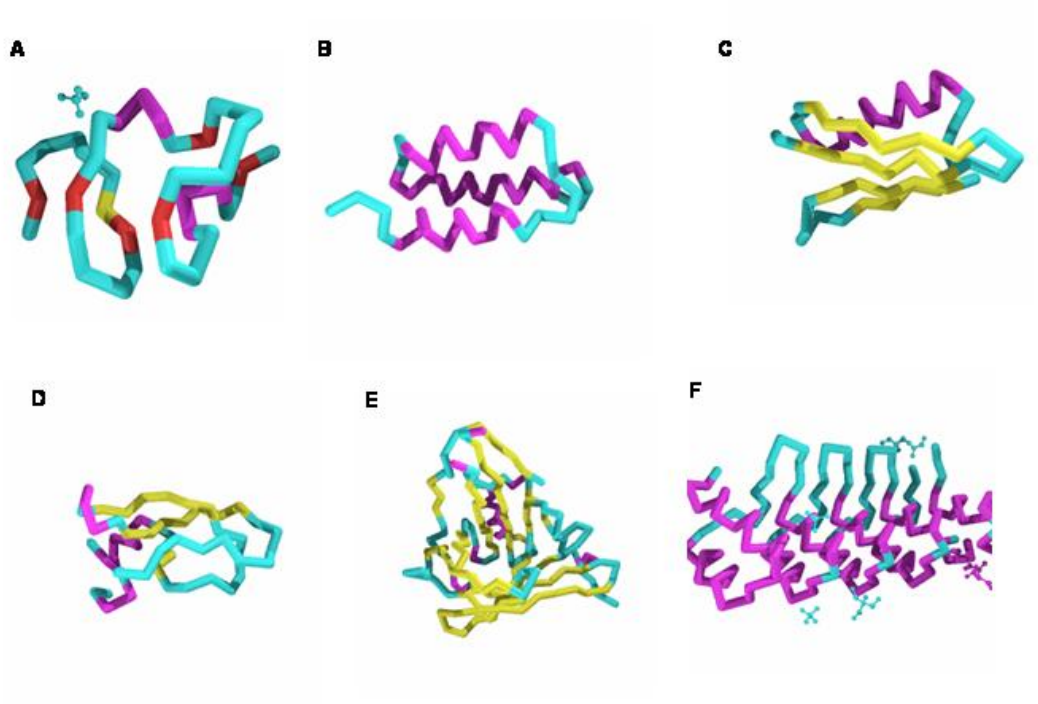

Figure 5.7: Proteins in use as scaffolds for generating binding reagents.

A) A-domain of LDL receptor, B) Z domain of protein A provides secondary structure elements for randomization, C) Single immunoglobulin-binding domain (GB1; HTB1) of protein G from group G Streptococcus which binds to the Fc region of IgG, D) Kunitz domain (chain A from 1AAP) provides a rigid protein framework for the insertion or randomization of single loop peptides, E) lipocallin (chain A from 1BBP) provides a framework similar to the CDR loops of antibodies, and F) Ankyrin repeat protein (1MJ0) is shown as an example of a modular repeat protein.

REFERENCES

1. Leyland-Jones, B. and I. Smith, *Role of Herceptin in primary breast cancer: views from North America and Europe.* Oncology, 2001. **61 Suppl 2**: p. 83-91.
2. Witzig, T.E., et al., *Treatment with ibritumomab tiuxetan radioimmunotherapy in patients with rituximab-refractory follicular non-Hodgkin's lymphoma.* J Clin Oncol, 2002. **20**(15): p. 3262-9.
3. Maloney, D.G., et al., *IDEC-C2B8: results of a phase I multiple-dose trial in patients with relapsed non-Hodgkin's lymphoma.* J Clin Oncol, 1997. **15**(10): p. 3266-74.
4. McLaughlin, P., et al., *Rituximab chimeric anti-CD20 monoclonal antibody therapy for relapsed indolent lymphoma: half of patients respond to a four-dose treatment program.* J Clin Oncol, 1998. **16**(8): p. 2825-33.
5. Bray, M.R., et al., *Probing the surface of eukaryotic cells using combinatorial toxin libraries.* Curr Biol, 2001. **11**(9): p. 697-701.
6. Ehrlich, P., *[The partial function of cells. (Nobel Prize address given on 11 December 1908 at Stockholm).].* Int Arch Allergy Appl Immunol, 1954. **5**(2): p. 67-86.
7. Kohler, G. and C. Milstein, *Continuous cultures of fused cells secreting antibody of predefined specificity.* Nature, 1975. **256**(5517): p. 495-7.
8. Baselga, J., *The EGFR as a target for anticancer therapy--focus on cetuximab.* Eur J Cancer, 2001. **37 Suppl 4**: p. S16-22.
9. Chen, H.X., R.E. Gore-Langton, and B.D. Cheson, *Clinical trials referral resource: Current clinical trials of the anti-VEGF monoclonal antibody bevacizumab.* Oncology (Williston Park), 2001. **15**(8): p. 1017, 1020, 1023-6.
10. Press, O.W., et al., *A phase 2 trial of CHOP chemotherapy followed by tositumomab/iodine I 131 tositumomab for previously untreated follicular non-Hodgkin lymphoma: Southwest Oncology Group Protocol S9911.* Blood, 2003. **102**(5): p. 1606-12.
11. Pawson, R., et al., *Treatment of T-cell prolymphocytic leukemia with human CD52 antibody.* J Clin Oncol, 1997. **15**(7): p. 2667-72.

12. Capdeville, R., S. Silberman, and S. Dimitrijevic, *Imatinib: the first 3 years.* Eur J Cancer, 2002. **38 Suppl 5**: p. S77-82.
13. Capdeville, R., et al., *Glivec (STI571, imatinib), a rationally developed, targeted anticancer drug.* Nat Rev Drug Discov, 2002. **1**(7): p. 493-502.
14. Birnbaum, A. and N. Ready, *Gefitinib therapy for non-small cell lung cancer.* Curr Treat Options Oncol, 2005. **6**(1): p. 75-81.
15. Smith, J., *Erlotinib: small-molecule targeted therapy in the treatment of non-small-cell lung cancer.* Clin Ther, 2005. **27**(10): p. 1513-34.
16. Motzer, R.J. and R.M. Bukowski, *Targeted therapy for metastatic renal cell carcinoma.* J Clin Oncol, 2006. **24**(35): p. 5601-8.
17. Strumberg, D., *Preclinical and clinical development of the oral multikinase inhibitor sorafenib in cancer treatment.* Drugs Today (Barc), 2005. **41**(12): p. 773-84.
18. Kelly, W.K., et al., *Phase I study of an oral histone deacetylase inhibitor, suberoylanilide hydroxamic acid, in patients with advanced cancer.* J Clin Oncol, 2005. **23**(17): p. 3923-31.
19. Mitchell, B.S., *The proteasome--an emerging therapeutic target in cancer.* N Engl J Med, 2003. **348**(26): p. 2597-8.
20. Richardson, P.G., et al., *A phase 2 study of bortezomib in relapsed, refractory myeloma.* N Engl J Med, 2003. **348**(26): p. 2609-17.
21. Collins, I. and P. Workman, *New approaches to molecular cancer therapeutics.* Nat Chem Biol, 2006. **2**(12): p. 689-700.
22. Kim, S.J., Y. Park, and H.J. Hong, *Antibody engineering for the development of therapeutic antibodies.* Mol Cells, 2005. **20**(1): p. 17-29.
23. Baselga, J. and J. Mendelsohn, *The epidermal growth factor receptor as a target for therapy in breast carcinoma.* Breast Cancer Res Treat, 1994. **29**(1): p. 127-38.
24. Slamon, D.J., et al., *Human breast cancer: correlation of relapse and survival with amplification of the HER-2/neu oncogene.* Science, 1987. **235**(4785): p. 177-82.
25. Osta, W.A., et al., *EpCAM is overexpressed in breast cancer and is a potential target for breast cancer gene therapy.* Cancer Res, 2004. **64**(16): p. 5818-24.
26. Kolonin, M., R. Pasqualini, and W. Arap, *Molecular addresses in blood vessels as targets for therapy.* Curr Opin Chem Biol, 2001. **5**(3): p. 308-13.
27. Arap, W., R. Pasqualini, and E. Ruoslahti, *Cancer treatment by targeted drug delivery to tumor vasculature in a mouse model.* Science, 1998. **279**(5349): p. 377-80.
28. Ruoslahti, E., *Drug targeting to specific vascular sites.* Drug Discov Today, 2002. **7**(22): p. 1138-43.
29. Ellerby, H.M., et al., *An artificially designed pore-forming protein with anti-tumor effects.* J Biol Chem, 2003. **278**(37): p. 35311-6.
30. Ellerby, H.M., et al., *Anti-cancer activity of targeted pro-apoptotic peptides.* Nat Med, 1999. **5**(9): p. 1032-8.
31. Koivunen, E., et al., *Tumor targeting with a selective gelatinase inhibitor.* Nat Biotechnol, 1999. **17**(8): p. 768-74.

32. Curnis, F., et al., *Enhancement of tumor necrosis factor alpha antitumor immunotherapeutic properties by targeted delivery to aminopeptidase N (CD13).* Nat Biotechnol, 2000. **18**(11): p. 1185-90.
33. Hong, F.D. and G.L. Clayman, *Isolation of a peptide for targeted drug delivery into human head and neck solid tumors.* Cancer Res, 2000. **60**(23): p. 6551-6.
34. Cargill, J.F. and M. Lebl, *New methods in combinatorial chemistry-robotics and parallel synthesis.* Curr Opin Chem Biol, 1997. **1**(1): p. 67-71.
35. Baldino, C.M., *Perspective Articles on the utility and application of solution-phase combinatorial chemistry.* J Comb Chem, 2000. **2**(2): p. 89-103.
36. Wennemers, H., *Combinatorial chemistry: a tool for the discovery of new catalysts.* Comb Chem High Throughput Screen, 2001. **4**(3): p. 273-85.
37. Huang, S., et al., *Dual-agent molecular targeting of the epidermal growth factor receptor (EGFR): combining anti-EGFR antibody with tyrosine kinase inhibitor.* Cancer Res, 2004. **64**(15): p. 5355-62.
38. Famulok, M., G. Mayer, and M. Blind, *Nucleic acid aptamers-from selection in vitro to applications in vivo.* Acc Chem Res, 2000. **33**(9): p. 591-9.
39. Reichert, J.M., et al., *Monoclonal antibody successes in the clinic.* Nat Biotechnol, 2005. **23**(9): p. 1073-8.
40. Kola, I. and J. Landis, *Can the pharmaceutical industry reduce attrition rates?* Nat Rev Drug Discov, 2004. **3**(8): p. 711-5.
41. Neuberger, M.S., et al., *Monitoring and interpreting the intrinsic features of somatic hypermutation.* Immunol Rev, 1998. **162**: p. 107-16.
42. Wabl, M., M. Cascalho, and C. Steinberg, *Hypermutation in antibody affinity maturation.* Curr Opin Immunol, 1999. **11**(2): p. 186-9.
43. Cawley, D.B., et al., *Epidermal growth factor-toxin A chain conjugates: EGF-ricin A is a potent toxin while EGF-diphtheria fragment A is nontoxic.* Cell, 1980. **22**(2 Pt 2): p. 563-70.
44. Akhtar, S. and I. Maghfoor, *Rituximab plus CHOP for diffuse large-B-cell lymphoma.* N Engl J Med, 2002. **346**(23): p. 1830-1; author reply 1830-1.
45. Gelderman, K.A., et al., *Complement function in mAb-mediated cancer immunotherapy.* Trends Immunol, 2004. **25**(3): p. 158-64.
46. Golay, J., et al., *Biologic response of B lymphoma cells to anti-CD20 monoclonal antibody rituximab in vitro: CD55 and CD59 regulate complement-mediated cell lysis.* Blood, 2000. **95**(12): p. 3900-8.
47. Treon, S.P., et al., *Tumor Cell Expression of CD59 Is Associated With Resistance to CD20 Serotherapy in Patients With B-Cell Malignancies.* J Immunother, 2001. **24**(3): p. 263-271.
48. Cartron, G., et al., *Therapeutic activity of humanized anti-CD20 monoclonal antibody and polymorphism in IgG Fc receptor FcgammaRIIIa gene.* Blood, 2002. **99**(3): p. 754-8.
49. Ferguson, K.M., *Active and inactive conformations of the epidermal growth factor receptor.* Biochem Soc Trans, 2004. **32**(Pt 5): p. 742-5.
50. Shan, D., J.A. Ledbetter, and O.W. Press, *Signaling events involved in anti-CD20-induced apoptosis of malignant human B cells.* Cancer Immunol Immunother, 2000. **48**(12): p. 673-83.

51. Smallshaw, J.E., et al., *Genetic engineering of an immunotoxin to eliminate pulmonary vascular leak in mice.* Nat Biotechnol, 2003. **21**(4): p. 387-91.
52. Griffin, J.D., et al., *A monoclonal antibody reactive with normal and leukemic human myeloid progenitor cells.* Leuk Res, 1984. **8**(4): p. 521-34.
53. Medzihradszky, K.F., et al., *Glycoforms obtained by expression in Pichia pastoris improve cancer targeting potential of a recombinant antibody-enzyme fusion protein.* Glycobiology, 2004. **14**(1): p. 27-37.
54. Adams, G.P. and L.M. Weiner, *Monoclonal antibody therapy of cancer.* Nat Biotechnol, 2005. **23**(9): p. 1147-57.
55. Dvorak, H.F., J.A. Nagy, and A.M. Dvorak, *Structure of solid tumors and their vasculature: implications for therapy with monoclonal antibodies.* Cancer Cells, 1991. **3**(3): p. 77-85.
56. Shockley, T.R., et al., *Penetration of tumor tissue by antibodies and other immunoproteins.* Ann N Y Acad Sci, 1991. **618**: p. 367-82.
57. Pluen, A., et al., *Role of tumor-host interactions in interstitial diffusion of macromolecules: cranial vs. subcutaneous tumors.* Proc Natl Acad Sci U S A, 2001. **98**(8): p. 4628-33.
58. Nugent, L.J. and R.K. Jain, *Extravascular diffusion in normal and neoplastic tissues.* Cancer Res, 1984. **44**(1): p. 238-44.
59. Graff, C.P. and K.D. Wittrup, *Theoretical analysis of antibody targeting of tumor spheroids: importance of dosage for penetration, and affinity for retention.* Cancer Res, 2003. **63**(6): p. 1288-96.
60. Nellis, D.F., et al., *Preclinical manufacture of anti-HER2 liposome-inserting, scFv-PEG-lipid conjugate. 2. Conjugate micelle identity, purity, stability, and potency analysis.* Biotechnol Prog, 2005. **21**(1): p. 221-32.
61. Adams, G.P., et al., *A single treatment of yttrium-90-labeled CHX-A"-C6.5 diabody inhibits the growth of established human tumor xenografts in immunodeficient mice.* Cancer Res, 2004. **64**(17): p. 6200-6.
62. Kenanova, V., et al., *Tailoring the pharmacokinetics and positron emission tomography imaging properties of anti-carcinoembryonic antigen single-chain Fv-Fc antibody fragments.* Cancer Res, 2005. **65**(2): p. 622-31.
63. Grosse-Hovest, L., et al., *Supraagonistic, bispecific single-chain antibody purified from the serum of cloned, transgenic cows induces T-cell-mediated killing of glioblastoma cells in vitro and in vivo.* Int J Cancer, 2005. **117**(6): p. 1060-4.
64. Holliger, P. and P.J. Hudson, *Engineered antibody fragments and the rise of single domains.* Nat Biotechnol, 2005. **23**(9): p. 1126-36.
65. Hudson, P.J. and C. Souriau, *Engineered antibodies.* Nat Med, 2003. **9**(1): p. 129-34.
66. Duda, T.F., Jr. and S.R. Palumbi, *Molecular genetics of ecological diversification: duplication and rapid evolution of toxin genes of the venomous gastropod Conus.* Proc Natl Acad Sci U S A, 1999. **96**(12): p. 6820-3.
67. Bradbury, A.R. and J.D. Marks, *Antibodies from phage antibody libraries.* J Immunol Methods, 2004. **290**(1-2): p. 29-49.

68. Vaughan, T.J., et al., *Human antibodies with sub-nanomolar affinities isolated from a large non-immunized phage display library.* Nat Biotechnol, 1996. **14**(3): p. 309-14.
69. Marks, J.D., et al., *By-passing immunization. Human antibodies from V-gene libraries displayed on phage.* J Mol Biol, 1991. **222**(3): p. 581-97.
70. Smith, G.P., *Filamentous fusion phage: novel expression vectors that display cloned antigens on the virion surface.* Science, 1985. **228**(4705): p. 1315-7.
71. Westerlund-Wikstrom, B., *Peptide display on bacterial flagella: principles and applications.* Int J Med Microbiol, 2000. **290**(3): p. 223-30.
72. Boder, E.T. and K.D. Wittrup, *Yeast surface display for screening combinatorial polypeptide libraries.* Nat Biotechnol, 1997. **15**(6): p. 553-7.
73. Smith, G.H., *Dural fibrillation.* Basal Facts, 1985. **7**(2): p. 173-5.
74. Cwirla, S.E., et al., *Peptides on phage: a vast library of peptides for identifying ligands.* Proc Natl Acad Sci U S A, 1990. **87**(16): p. 6378-82.
75. McCafferty, J., et al., *Phage antibodies: filamentous phage displaying antibody variable domains.* Nature, 1990. **348**(6301): p. 552-4.
76. Lowman, H.B., et al., *Selecting high-affinity binding proteins by monovalent phage display.* Biochemistry, 1991. **30**(45): p. 10832-8.
77. Clackson, T., et al., *Making antibody fragments using phage display libraries.* Nature, 1991. **352**(6336): p. 624-8.
78. Hoogenboom, H.R. and P. Chames, *Natural and designer binding sites made by phage display technology.* Immunol Today, 2000. **21**(8): p. 371-8.
79. Hanes, J. and A. Pluckthun, *In vitro selection and evolution of functional proteins by using ribosome display.* Proc Natl Acad Sci U S A, 1997. **94**(10): p. 4937-42.
80. Mattheakis, L.C., R.R. Bhatt, and W.J. Dower, *An in vitro polysome display system for identifying ligands from very large peptide libraries.* Proc Natl Acad Sci U S A, 1994. **91**(19): p. 9022-6.
81. Roberts, R.W. and J.W. Szostak, *RNA-peptide fusions for the in vitro selection of peptides and proteins.* Proc Natl Acad Sci U S A, 1997. **94**(23): p. 12297-302.
82. Hanes, J., et al., *Ribosome display efficiently selects and evolves high-affinity antibodies in vitro from immune libraries.* Proc Natl Acad Sci U S A, 1998. **95**(24): p. 14130-5.
83. Zahnd, C., et al., *Directed in vitro evolution and crystallographic analysis of a peptide-binding single chain antibody fragment (scFv) with low picomolar affinity.* J Biol Chem, 2004. **279**(18): p. 18870-7.
84. Hanes, J., L. Jermutus, and A. Pluckthun, *Selecting and evolving functional proteins in vitro by ribosome display.* Methods Enzymol, 2000. **328**: p. 404-30.
85. Sidhu, S.S., W.J. Fairbrother, and K. Deshayes, *Exploring protein-protein interactions with phage display.* Chembiochem, 2003. **4**(1): p. 14-25.
86. Barlow, D.J., M.S. Edwards, and J.M. Thornton, *Continuous and discontinuous protein antigenic determinants.* Nature, 1986. **322**(6081): p. 747-8.
87. Jones, S. and J.M. Thornton, *Principles of protein-protein interactions.* Proc Natl Acad Sci U S A, 1996. **93**(1): p. 13-20.
88. Berkower, I., *The promise and pitfalls of monoclonal antibody therapeutics.* Curr Opin Biotechnol, 1996. **7**(6): p. 622-8.

89. Ruoslahti, E. and D. Rajotte, *An address system in the vasculature of normal tissues and tumors.* Annu Rev Immunol, 2000. **18**: p. 813-27.
90. Scott, J.K. and L. Craig, *Random peptide libraries.* Curr Opin Biotechnol, 1994. **5**(1): p. 40-8.
91. Zwick, M.B., J. Shen, and J.K. Scott, *Phage-displayed peptide libraries.* Curr Opin Biotechnol, 1998. **9**(4): p. 427-36.
92. An, P., et al., *Suppression of tumor growth and metastasis by a VEGFR-1 antagonizing peptide identified from a phage display library.* Int J Cancer, 2004. **111**(2): p. 165-73.
93. Pero, S.C., et al., *Identification of a small peptide that inhibits the phosphorylation of ErbB2 and proliferation of ErbB2 overexpressing breast cancer cells.* Int J Cancer, 2004. **111**(6): p. 951-60.
94. Koivunen, E., B. Wang, and E. Ruoslahti, *Phage libraries displaying cyclic peptides with different ring sizes: ligand specificities of the RGD-directed integrins.* Biotechnology (N Y), 1995. **13**(3): p. 265-70.
95. Wrighton, N.C., et al., *Small peptides as potent mimetics of the protein hormone erythropoietin.* Science, 1996. **273**(5274): p. 458-64.
96. Bongartz, T., et al., *Anti-TNF antibody therapy in rheumatoid arthritis and the risk of serious infections and malignancies: systematic review and meta-analysis of rare harmful effects in randomized controlled trials.* Jama, 2006. **295**(19): p. 2275-85.
97. Begent, R.H., et al., *Clinical evidence of efficient tumor targeting based on single-chain Fv antibody selected from a combinatorial library.* Nat Med, 1996. **2**(9): p. 979-84.
98. Lamberts, S.W., et al., *Somatostatin-receptor imaging in the localization of endocrine tumors.* N Engl J Med, 1990. **323**(18): p. 1246-9.
99. Meredith, R.F., et al., *Treatment of metastatic prostate carcinoma with radiolabeled antibody CC49.* J Nucl Med, 1994. **35**(6): p. 1017-22.
100. Padlan, E.A., *X-ray crystallography of antibodies.* Adv Protein Chem, 1996. **49**: p. 57-133.
101. Nord, K., et al., *Binding proteins selected from combinatorial libraries of an alpha-helical bacterial receptor domain.* Nat Biotechnol, 1997. **15**(8): p. 772-7.
102. Binz, H.K., et al., *Designing repeat proteins: well-expressed, soluble and stable proteins from combinatorial libraries of consensus ankyrin repeat proteins.* J Mol Biol, 2003. **332**(2): p. 489-503.
103. Li, R., et al., *Use of phage display to probe the evolution of binding specificity and affinity in integrins.* Protein Eng, 2003. **16**(1): p. 65-72.
104. Dennis, M.S., A. Herzka, and R.A. Lazarus, *Potent and selective Kunitz domain inhibitors of plasma kallikrein designed by phage display.* J Biol Chem, 1995. **270**(43): p. 25411-7.
105. Fuh, G., et al., *Analysis of PDZ domain-ligand interactions using carboxyl-terminal phage display.* J Biol Chem, 2000. **275**(28): p. 21486-91.
106. Xu, L., et al., *Directed evolution of high-affinity antibody mimics using mRNA display.* Chem Biol, 2002. **9**(8): p. 933-42.
107. Karatan, E., et al., *Molecular recognition properties of FN3 monobodies that bind the Src SH3 domain.* Chem Biol, 2004. **11**(6): p. 835-44.

108. Hitoshi, Y., et al., *Cellular localization and antiproliferative effect of peptides discovered from a functional screen of a retrovirally delivered random peptide library.* Chem Biol, 2003. **10**(10): p. 975-87.
109. Binz, H.K., et al., *High-affinity binders selected from designed ankyrin repeat protein libraries.* Nat Biotechnol, 2004. **22**(5): p. 575-82.
110. Silverman, J., et al., *Multivalent avimer proteins evolved by exon shuffling of a family of human receptor domains.* Nat Biotechnol, 2005. **23**(12): p. 1556-61.
111. Lipovsek, D., et al., *Evolution of an interloop disulfide bond in high-affinity antibody mimics based on fibronectin type III domain and selected by yeast surface display: molecular convergence with single-domain camelid and shark antibodies.* J Mol Biol, 2007. **368**(4): p. 1024-41.
112. Roberts, B.L., et al., *Directed evolution of a protein: selection of potent neutrophil elastase inhibitors displayed on M13 fusion phage.* Proc Natl Acad Sci U S A, 1992. **89**(6): p. 2429-33.
113. Schneider, S., et al., *Mutagenesis and selection of PDZ domains that bind new protein targets.* Nat Biotechnol, 1999. **17**(2): p. 170-5.
114. Ferrer, M., et al., *Directed evolution of PDZ variants to generate high-affinity detection reagents.* Protein Eng Des Sel, 2005. **18**(4): p. 165-73.
115. Vita, C., et al., *Scorpion toxins as natural scaffolds for protein engineering.* Proc Natl Acad Sci U S A, 1995. **92**(14): p. 6404-8.
116. Schlehuber, S. and A. Skerra, *Lipocalins in drug discovery: from natural ligand-binding proteins to "anticalins".* Drug Discov Today, 2005. **10**(1): p. 23-33.
117. Skerra, A., *Alternative non-antibody scaffolds for molecular recognition.* Curr Opin Biotechnol, 2007. **18**(4): p. 295-304.
118. Smith, G.P., et al., *Small binding proteins selected from a combinatorial repertoire of knottins displayed on phage.* J Mol Biol, 1998. **277**(2): p. 317-32.
119. McConnell, S.J. and R.H. Hoess, *Tendamistat as a scaffold for conformationally constrained phage peptide libraries.* J Mol Biol, 1995. **250**(4): p. 460-70.
120. Binz, H.K., P. Amstutz, and A. Pluckthun, *Engineering novel binding proteins from nonimmunoglobulin domains.* Nat Biotechnol, 2005. **23**(10): p. 1257-68.
121. Sandvig, K. and B. van Deurs, *Endocytosis, intracellular transport, and cytotoxic action of Shiga toxin and ricin.* Physiol Rev, 1996. **76**(4): p. 949-66.
122. Sandvig, K. and B. van Deurs, *Endocytosis and intracellular transport of ricin: recent discoveries.* FEBS Lett, 1999. **452**(1-2): p. 67-70.
123. Rodal, S.K., et al., *Extraction of cholesterol with methyl-beta-cyclodextrin perturbs formation of clathrin-coated endocytic vesicles.* Mol Biol Cell, 1999. **10**(4): p. 961-74.
124. Hall, W.A. and O. Fodstad, *Immunotoxins and central nervous system neoplasia.* J Neurosurg, 1992. **76**(1): p. 1-12.
125. MacDonald, G.C. and N. Glover, *Effective tumor targeting: strategies for the delivery of Armed Antibodies.* Curr Opin Drug Discov Devel, 2005. **8**(2): p. 177-83.
126. Yokota, T., et al., *Microautoradiographic analysis of the normal organ distribution of radioiodinated single-chain Fv and other immunoglobulin forms.* Cancer Res, 1993. **53**(16): p. 3776-83.

127. Yokota, T., et al., *Rapid tumor penetration of a single-chain Fv and comparison with other immunoglobulin forms.* Cancer Res, 1992. **52**(12): p. 3402-8.
128. Olsen, E., et al., *Pivotal phase III trial of two dose levels of denileukin diftitox for the treatment of cutaneous T-cell lymphoma.* J Clin Oncol, 2001. **19**(2): p. 376-88.
129. Pai, L.H., et al., *Treatment of advanced solid tumors with immunotoxin LMB-1: an antibody linked to Pseudomonas exotoxin.* Nat Med, 1996. **2**(3): p. 350-3.
130. Kreitman, R.J., et al., *Efficacy of the anti-CD22 recombinant immunotoxin BL22 in chemotherapy-resistant hairy-cell leukemia.* N Engl J Med, 2001. **345**(4): p. 241-7.
131. Laske, D.W., et al., *Efficacy of direct intratumoral therapy with targeted protein toxins for solid human gliomas in nude mice.* J Neurosurg, 1994. **80**(3): p. 520-6.
132. Rand, R.W., et al., *Intratumoral administration of recombinant circularly permuted interleukin-4-Pseudomonas exotoxin in patients with high-grade glioma.* Clin Cancer Res, 2000. **6**(6): p. 2157-65.
133. Driscoll, P.C., et al., *Structure of domain 1 of rat T lymphocyte CD2 antigen.* Nature, 1991. **353**(6346): p. 762-5.
134. Jones, E.Y., et al., *Crystal structure at 2.8 A resolution of a soluble form of the cell adhesion molecule CD2.* Nature, 1992. **360**(6401): p. 232-9.
135. Ryu, S.E., et al., *Crystal structure of an HIV-binding recombinant fragment of human CD4.* Nature, 1990. **348**(6300): p. 419-26.
136. Klein, C. and G.E. Schulz, *Structure of cyclodextrin glycosyltransferase refined at 2.0 A resolution.* J Mol Biol, 1991. **217**(4): p. 737-50.
137. Williams, A.F. and A.N. Barclay, *The immunoglobulin superfamily--domains for cell surface recognition.* Annu Rev Immunol, 1988. **6**: p. 381-405.
138. Russell, D.W., et al., *Domain map of the LDL receptor: sequence homology with the epidermal growth factor precursor.* Cell, 1984. **37**(2): p. 577-85.
139. Tam, P.J. and C.A. Lingwood, *Membrane cytosolic translocation of verotoxin A1 subunit in target cells.* Microbiology, 2007. **153**(Pt 8): p. 2700-10.
140. Chung, D.W. and R.J. Collier, *Enzymatically active peptide from the adenosine diphosphate-ribosylating toxin of Pseudomonas aeruginosa.* Infect Immun, 1977. **16**(3): p. 832-41.
141. Passador, L. and W. Iglewski, *ADP-ribosylating toxins.* Methods Enzymol, 1994. **235**: p. 617-31.
142. Chang, P.P., et al., *Type II heat-labile enterotoxin of Escherichia coli activates adenylate cyclase in human fibroblasts by ADP ribosylation.* Infect Immun, 1987. **55**(8): p. 1854-8.
143. Klinz, F.J. and T. Costa, *Cholera toxin ADP-ribosylates the receptor-coupled form of pertussis toxin-sensitive G-proteins.* Biochem Biophys Res Commun, 1989. **165**(2): p. 554-60.
144. West, R.E., Jr., et al., *Pertussis toxin-catalyzed ADP-ribosylation of transducin. Cysteine 347 is the ADP-ribose acceptor site.* J Biol Chem, 1985. **260**(27): p. 14428-30.
145. Skinner, L.M. and M.P. Jackson, *Inhibition of prokaryotic translation by the Shiga toxin enzymatic subunit.* Microb Pathog, 1998. **24**(2): p. 117-22.

146. Riley, L.W., *The epidemiologic, clinical, and microbiologic features of hemorrhagic colitis.* Annu Rev Microbiol, 1987. **41**: p. 383-407.
147. Karmali, M.A., *Infection by verocytotoxin-producing Escherichia coli.* Clin Microbiol Rev, 1989. **2**(1): p. 15-38.
148. Rutenber, E., et al., *Crystallographic refinement of ricin to 2.5 A.* Proteins, 1991. **10**(3): p. 240-50.
149. Fraser, M.E., et al., *Crystal structure of the holotoxin from Shigella dysenteriae at 2.5 A resolution.* Nat Struct Biol, 1994. **1**(1): p. 59-64.
150. Montfort, W., et al., *The three-dimensional structure of ricin at 2.8 A.* J Biol Chem, 1987. **262**(11): p. 5398-403.
151. Choe, S., et al., *The crystal structure of diphtheria toxin.* Nature, 1992. **357**(6375): p. 216-22.
152. Wedekind, J.E., et al., *Refined crystallographic structure of Pseudomonas aeruginosa exotoxin A and its implications for the molecular mechanism of toxicity.* J Mol Biol, 2001. **314**(4): p. 823-37.
153. Sixma, T.K., et al., *Refined structure of Escherichia coli heat-labile enterotoxin, a close relative of cholera toxin.* J Mol Biol, 1993. **230**(3): p. 890-918.
154. Stein, P.E., et al., *The crystal structure of pertussis toxin.* Structure, 1994. **2**(1): p. 45-57.
155. Zhang, R.G., et al., *The three-dimensional crystal structure of cholera toxin.* J Mol Biol, 1995. **251**(4): p. 563-73.
156. Endo, Y., et al., *Site of action of a Vero toxin (VT2) from Escherichia coli O157:H7 and of Shiga toxin on eukaryotic ribosomes. RNA N-glycosidase activity of the toxins.* Eur J Biochem, 1988. **171**(1-2): p. 45-50.
157. Saxena, S.K., A.D. O'Brien, and E.J. Ackerman, *Shiga toxin, Shiga-like toxin II variant, and ricin are all single-site RNA N-glycosidases of 28 S RNA when microinjected into Xenopus oocytes.* J Biol Chem, 1989. **264**(1): p. 596-601.
158. Furutani, M., et al., *Comparison of the modes of action of a Vero toxin (a Shiga-like toxin) from Escherichia coli, of ricin, and of alpha-sarcin.* Arch Biochem Biophys, 1992. **293**(1): p. 140-6.
159. Gluck, A., Y. Endo, and I.G. Wool, *Ribosomal RNA identity elements for ricin A-chain recognition and catalysis. Analysis with tetraloop mutants.* J Mol Biol, 1992. **226**(2): p. 411-24.
160. Hovde, C.J., et al., *Evidence that glutamic acid 167 is an active-site residue of Shiga-like toxin I.* Proc Natl Acad Sci U S A, 1988. **85**(8): p. 2568-72.
161. Jackson, M.P., R.L. Deresiewicz, and S.B. Calderwood, *Mutational analysis of the Shiga toxin and Shiga-like toxin II enzymatic subunits.* J Bacteriol, 1990. **172**(6): p. 3346-50.
162. Yamasaki, S., et al., *Importance of arginine at position 170 of the A subunit of Vero toxin 1 produced by enterohemorrhagic Escherichia coli for toxin activity.* Microb Pathog, 1991. **11**(1): p. 1-9.
163. Lindberg, A.A., et al., *Identification of the carbohydrate receptor for Shiga toxin produced by Shigella dysenteriae type 1.* J Biol Chem, 1987. **262**(4): p. 1779-85.
164. Lingwood, C.A., et al., *Glycolipid binding of purified and recombinant Escherichia coli produced verotoxin in vitro.* J Biol Chem, 1987. **262**(18): p. 8834-9.

165. Boyd, B. and C. Lingwood, *Verotoxin receptor glycolipid in human renal tissue.* Nephron, 1989. **51**(2): p. 207-10.
166. Mangeney, M., et al., *CD77: an antigen of germinal center B cells entering apoptosis.* Eur J Immunol, 1991. **21**(5): p. 1131-40.
167. Jacewicz, M.S., et al., *Maturational regulation of globotriaosylceramide, the Shiga-like toxin 1 receptor, in cultured human gut epithelial cells.* J Clin Invest, 1995. **96**(3): p. 1328-35.
168. Cooling, L.L., et al., *Shiga toxin binds human platelets via globotriaosylceramide (Pk antigen) and a novel platelet glycosphingolipid.* Infect Immun, 1998. **66**(9): p. 4355-66.
169. Kitov, P.I., et al., *Shiga-like toxins are neutralized by tailored multivalent carbohydrate ligands.* Nature, 2000. **403**(6770): p. 669-72.
170. Thompson, G.S., et al., *Localization of the binding site for the oligosaccharide moiety of Gb3 on verotoxin 1 using NMR residual dipolar coupling measurements.* Biochemistry, 2000. **39**(43): p. 13153-6.
171. Sandvig, K., et al., *Retrograde transport of endocytosed Shiga toxin to the endoplasmic reticulum.* Nature, 1992. **358**(6386): p. 510-2.
172. Okimoto, T., et al., *Brefeldin A protects ricin-induced cytotoxicity in human cancer KB cell line, but not in its resistant counterpart with altered Golgi structures.* Cell Struct Funct, 1993. **18**(4): p. 241-51.
173. Yoshida, T., et al., *Disruption of the Golgi apparatus by brefeldin A inhibits the cytotoxicity of ricin, modeccin, and Pseudomonas toxin.* Exp Cell Res, 1991. **192**(2): p. 389-95.
174. Ktistakis, N.T., M.E. Linder, and M.G. Roth, *Action of brefeldin A blocked by activation of a pertussis-toxin-sensitive G protein.* Nature, 1992. **356**(6367): p. 344-6.
175. Orlandi, P.A., P.K. Curran, and P.H. Fishman, *Brefeldin A blocks the response of cultured cells to cholera toxin. Implications for intracellular trafficking in toxin action.* J Biol Chem, 1993. **268**(16): p. 12010-6.
176. Donta, S.T., S. Beristain, and T.K. Tomicic, *Inhibition of heat-labile cholera and Escherichia coli enterotoxins by brefeldin A.* Infect Immun, 1993. **61**(8): p. 3282-6.
177. Donta, S.T., T.K. Tomicic, and A. Donohue-Rolfe, *Inhibition of Shiga-like toxins by brefeldin A.* J Infect Dis, 1995. **171**(3): p. 721-4.
178. London, E. and C.L. Luongo, *Domain-specific bias in arginine/lysine usage by protein toxins.* Biochem Biophys Res Commun, 1989. **160**(1): p. 333-9.
179. Hazes, B. and R.J. Read, *Accumulating evidence suggests that several AB-toxins subvert the endoplasmic reticulum-associated protein degradation pathway to enter target cells.* Biochemistry, 1997. **36**(37): p. 11051-4.
180. Saleh, M.T., et al., *Insertion and orientation of a synthetic peptide representing the C-terminus of the A1 domain of Shiga toxin into phospholipid membranes.* Biochemistry, 1996. **35**(29): p. 9325-34.
181. LaCasse, E.C., et al., *Shiga-like toxin-1 receptor on human breast cancer, lymphoma, and myeloma and absence from CD34(+) hematopoietic stem cells: implications for ex vivo tumor purging and autologous stem cell transplantation.* Blood, 1999. **94**(8): p. 2901-10.

182. LaCasse, E.C., et al., *Shiga-like toxin purges human lymphoma from bone marrow of severe combined immunodeficient mice.* Blood, 1996. **88**(5): p. 1561-7.
183. Gariepy, J., *The use of Shiga-like toxin 1 in cancer therapy.* Crit Rev Oncol Hematol, 2001. **39**(1-2): p. 99-106.
184. Olsnes, S., et al., *Immunotoxins--entry into cells and mechanisms of action.* Immunol Today, 1989. **10**(9): p. 291-5.
185. Zhang, J., et al., *Pentamerization of single-domain antibodies from phage libraries: a novel strategy for the rapid generation of high-avidity antibody reagents.* J Mol Biol, 2004. **335**(1): p. 49-56.
186. Haicheur, N., et al., *The B subunit of Shiga toxin fused to a tumor antigen elicits CTL and targets dendritic cells to allow MHC class I-restricted presentation of peptides derived from exogenous antigens.* J Immunol, 2000. **165**(6): p. 3301-8.
187. LaPointe, P., X. Wei, and J. Gariepy, *A role for the protease-sensitive loop region of Shiga-like toxin 1 in the retrotranslocation of its A1 domain from the endoplasmic reticulum lumen.* J Biol Chem, 2005. **280**(24): p. 23310-8.
188. Garred, O., B. van Deurs, and K. Sandvig, *Furin-induced cleavage and activation of Shiga toxin.* J Biol Chem, 1995. **270**(18): p. 10817-21.
189. Olsnes, S., R. Reisbig, and K. Eiklid, *Subunit structure of Shigella cytotoxin.* J Biol Chem, 1981. **256**(16): p. 8732-8.
190. Clauss, M.A. and R.K. Jain, *Interstitial transport of rabbit and sheep antibodies in normal and neoplastic tissues.* Cancer Res, 1990. **50**(12): p. 3487-92.
191. Linsley, P.S., et al., *Monoclonal antibodies reactive with mucin glycoproteins found in sera from breast cancer patients.* Cancer Res, 1988. **48**(8): p. 2138-48.
192. Geysen, H.M., R.H. Meloen, and S.J. Barteling, *Use of peptide synthesis to probe viral antigens for epitopes to a resolution of a single amino acid.* Proc Natl Acad Sci U S A, 1984. **81**(13): p. 3998-4002.
193. Georges, E., et al., *Detection of P-glycoprotein isoforms by gene-specific monoclonal antibodies.* Proc Natl Acad Sci U S A, 1990. **87**(1): p. 152-6.
194. Skehan, P., et al., *New colorimetric cytotoxicity assay for anticancer-drug screening.* J Natl Cancer Inst, 1990. **82**(13): p. 1107-12.
195. Madersbacher, S. and P. Berger, *Double wavelength measurement of 3,3',5,5'-tetramethylbenzidine (TMB) provides a three-fold enhancement of the ELISA measuring range.* J Immunol Methods, 1991. **138**(1): p. 121-4.
196. Nagi, A.D. and L. Regan, *An inverse correlation between loop length and stability in a four-helix-bundle protein.* Fold Des, 1997. **2**(1): p. 67-75.
197. Predki, P.F., et al., *Amino-acid substitutions in a surface turn modulate protein stability.* Nat Struct Biol, 1996. **3**(1): p. 54-8.
198. Suh, J.K., C.J. Hovde, and J.D. Robertus, *Shiga toxin attacks bacterial ribosomes as effectively as eucaryotic ribosomes.* Biochemistry, 1998. **37**(26): p. 9394-8.
199. Ready, M.P., Y. Kim, and J.D. Robertus, *Site-directed mutagenesis of ricin A-chain and implications for the mechanism of action.* Proteins, 1991. **10**(3): p. 270-8.
200. Day, P.J., et al., *Structure and activity of an active site substitution of ricin A chain.* Biochemistry, 1996. **35**(34): p. 11098-103.

201. De Grandis, S., et al., *Nucleotide sequence and promoter mapping of the Escherichia coli Shiga-like toxin operon of bacteriophage H-19B.* J Bacteriol, 1987. **169**(9): p. 4313-9.
202. Shine, J. and L. Dalgarno, *Determinant of cistron specificity in bacterial ribosomes.* Nature, 1975. **254**(5495): p. 34-8.
203. Lea, N., J.M. Lord, and L.M. Roberts, *Proteolytic cleavage of the A subunit is essential for maximal cytotoxicity of Escherichia coli O157:H7 Shiga-like toxin-1.* Microbiology, 1999. **145 (Pt 5)**: p. 999-1004.
204. Rye, P.D.a.P., M.R., *ISOBM TD-4 International Workshop on Monoclonal Antibodies against MUC1*, in *Tumour Biol*. 1998. p. 1-151.
205. Schwede, T., et al., *SWISS-MODEL: An automated protein homology-modeling server.* Nucleic Acids Res, 2003. **31**(13): p. 3381-5.
206. Guex, N. and M.C. Peitsch, *SWISS-MODEL and the Swiss-PdbViewer: an environment for comparative protein modeling.* Electrophoresis, 1997. **18**(15): p. 2714-23.
207. Essler, M. and E. Ruoslahti, *Molecular specialization of breast vasculature: a breast-homing phage-displayed peptide binds to aminopeptidase P in breast vasculature.* Proc Natl Acad Sci U S A, 2002. **99**(4): p. 2252-7.
208. McGuire, M.J., et al., *In vitro selection of a peptide with high selectivity for cardiomyocytes in vivo.* J Mol Biol, 2004. **342**(1): p. 171-82.
209. Gui, J., T. Moyana, and J. Xiang, *Selection of a peptide with affinity for the tumor-associated TAG72 antigen from a phage-displayed library.* Biochem Biophys Res Commun, 1996. **218**(1): p. 414-9.
210. Peletskaya, E.N., et al., *Identification of peptide sequences that bind the Thomsen-Friedenreich cancer-associated glycoantigen from bacteriophage peptide display libraries.* Mol Divers, 1996. **2**(1-2): p. 13-8.
211. Oyama, T., et al., *Isolation of lung tumor specific peptides from a random peptide library: generation of diagnostic and cell-targeting reagents.* Cancer Lett, 2003. **202**(2): p. 219-30.
212. al-Jaufy, A.Y., et al., *Cytotoxicity of a shiga toxin A subunit-CD4 fusion protein to human immunodeficiency virus-infected cells.* Infect Immun, 1994. **62**(3): p. 956-60.
213. al-Jaufy, A.Y., S.R. King, and M.P. Jackson, *Purification and characterization of a Shiga toxin A subunit-CD4 fusion protein cytotoxic to human immunodeficiency virus-infected cells.* Infect Immun, 1995. **63**(8): p. 3073-8.
214. Roudkenar, M.H., et al., *Selective cytotoxicity of recombinant STXA1-GM-CSF protein in hematopoetic cancer cells.* Cell Biol Toxicol, 2006. **22**(3): p. 213-9.
215. Arora, N. and S.H. Leppla, *Fusions of anthrax toxin lethal factor with shiga toxin and diphtheria toxin enzymatic domains are toxic to mammalian cells.* Infect Immun, 1994. **62**(11): p. 4955-61.
216. Shadidi, M. and M. Sioud, *Identification of novel carrier peptides for the specific delivery of therapeutics into cancer cells.* FASEB J, 2003. **17**(2): p. 256-8.
217. Scott, J.K. and G.P. Smith, *Searching for peptide ligands with an epitope library.* Science, 1990. **249**(4967): p. 386-90.

218. Ivanenkov, V.V., F. Felici, and A.G. Menon, *Targeted delivery of multivalent phage display vectors into mammalian cells.* Biochim Biophys Acta, 1999. **1448**(3): p. 463-72.
219. Griffiths, A.D., et al., *Isolation of high affinity human antibodies directly from large synthetic repertoires.* Embo J, 1994. **13**(14): p. 3245-60.
220. Noren, K.A. and C.J. Noren, *Construction of high-complexity combinatorial phage display peptide libraries.* Methods, 2001. **23**(2): p. 169-78.
221. Reidhaar-Olson, J.F., et al., *Random mutagenesis of protein sequences using oligonucleotide cassettes.* Methods Enzymol, 1991. **208**: p. 564-86.
222. Rodi, D.J., A.S. Soares, and L. Makowski, *Quantitative assessment of peptide sequence diversity in M13 combinatorial peptide phage display libraries.* J Mol Biol, 2002. **322**(5): p. 1039-52.
223. Deresiewicz, R.L., et al., *Mutations affecting the activity of the Shiga-like toxin I A-chain.* Biochemistry, 1992. **31**(12): p. 3272-80.
224. Brown, J.E., et al., *Shiga toxin from Shigella dysenteriae 1 inhibits protein synthesis in reticulocyte lysates by inactivation of aminoacyl-tRNA binding.* Microb Pathog, 1986. **1**(4): p. 325-34.
225. Corbett, T.H., et al., *Discovery of cryptophycin-1 and BCN-183577: examples of strategies and problems in the detection of antitumor activity in mice.* Invest New Drugs, 1997. **15**(3): p. 207-18.
226. Kolonin, M.G., et al., *Ligand-directed surface profiling of human cancer cells with combinatorial peptide libraries.* Cancer Res, 2006. **66**(1): p. 34-40.
227. Donohue-Rolfe, A., et al., *Pathogenesis of Shigella diarrhea. IX. Simplified high yield purification of Shigella toxin and characterization of subunit composition and function by the use of subunit-specific monoclonal and polyclonal antibodies.* J Exp Med, 1984. **160**(6): p. 1767-81.
228. Luce, J.K., et al., *Clinical trials with the antitumor agent 5-(3,3-dimethyl-1-triazeno)imidazole-4-carboxamide(NSC-45388).* Cancer Chemother Rep, 1970. **54**(2): p. 119-24.
229. Chapman, A.P., *PEGylated antibodies and antibody fragments for improved therapy: a review.* Adv Drug Deliv Rev, 2002. **54**(4): p. 531-45.
230. Flower, D.R., *Towards in silico prediction of immunogenic epitopes.* Trends Immunol, 2003. **24**(12): p. 667-74.
231. Koren, E., L.A. Zuckerman, and A.R. Mire-Sluis, *Immune responses to therapeutic proteins in humans--clinical significance, assessment and prediction.* Curr Pharm Biotechnol, 2002. **3**(4): p. 349-60.
232. Wang, Y.S., et al., *Identification of the major positional isomer of pegylated interferon alpha-2b.* Biochemistry, 2000. **39**(35): p. 10634-40.
233. Holle, L.M., *Pegaspargase: an alternative?* Ann Pharmacother, 1997. **31**(5): p. 616-24.
234. Aguayo, A., et al., *Combination therapy with methotrexate, vincristine, polyethylene-glycol conjugated-asparaginase, and prednisone in the treatment of patients with refractory or recurrent acute lymphoblastic leukemia.* Cancer, 1999. **86**(7): p. 1203-9.

235. Waibel, R., et al., *Stable one-step technetium-99m labeling of His-tagged recombinant proteins with a novel Tc(I)-carbonyl complex.* Nat Biotechnol, 1999. **17**(9): p. 897-901.
236. Kleene, R., et al., *SH3 binding sites of ZG29p mediate an interaction with amylase and are involved in condensation-sorting in the exocrine rat pancreas.* Biochemistry, 2000. **39**(32): p. 9893-900.
237. Salacinski, P.R., et al., *Iodination of proteins, glycoproteins, and peptides using a solid-phase oxidizing agent, 1,3,4,6-tetrachloro-3 alpha,6 alpha-diphenyl glycoluril (Iodogen).* Anal Biochem, 1981. **117**(1): p. 136-46.
238. Mattson, G., et al., *A practical approach to crosslinking.* Mol Biol Rep, 1993. **17**(3): p. 167-83.
239. Stohrer, M., et al., *Oncotic pressure in solid tumors is elevated.* Cancer Res, 2000. **60**(15): p. 4251-5.
240. Adams, G.P., et al., *Increased affinity leads to improved selective tumor delivery of single-chain Fv antibodies.* Cancer Res, 1998. **58**(3): p. 485-90.
241. Jean, L.F. and J.R. Murphy, *Diphtheria toxin receptor-binding domain substitution with interleukin 6: genetic construction and interleukin 6 receptor-specific action of a diphtheria toxin-related interleukin 6 fusion protein.* Protein Eng, 1991. **4**(8): p. 989-94.
242. Vitetta, E.S., *The development of immunotoxins for the therapy of cancer, AIDS, and immune dysfunctions.* Princess Takamatsu Symp, 1988. **19**: p. 333-40.
243. FitzGerald, D.J., *Construction of immunotoxins using Pseudomonas exotoxin A.* Methods Enzymol, 1987. **151**: p. 139-45.
244. Woo, J.H., et al., *Gene optimization is necessary to express a bivalent anti-human anti-T cell immunotoxin in Pichia pastoris.* Protein Expr Purif, 2002. **25**(2): p. 270-82.
245. Friedrich, K., et al., *A two-step selection approach for the identification of ligand-binding determinants in cytokine receptors.* Anal Biochem, 1999. **268**(2): p. 179-86.
246. Schnell, R., et al., *Treatment of refractory Hodgkin's lymphoma patients with an iodine-131-labeled murine anti-CD30 monoclonal antibody.* J Clin Oncol, 2005. **23**(21): p. 4669-78.
247. Schnell, R., et al., *Clinical evaluation of ricin A-chain immunotoxins in patients with Hodgkin's lymphoma.* Ann Oncol, 2003. **14**(5): p. 729-36.
248. Hexham, J.M., et al., *Influence of relative binding affinity on efficacy in a panel of anti-CD3 scFv immunotoxins.* Mol Immunol, 2001. **38**(5): p. 397-408.
249. Gerlowski, L.E. and R.K. Jain, *Microvascular permeability of normal and neoplastic tissues.* Microvasc Res, 1986. **31**(3): p. 288-305.
250. Adams, G.P., et al., *Highly specific in vivo tumor targeting by monovalent and divalent forms of 741F8 anti-c-erbB-2 single-chain Fv.* Cancer Res, 1993. **53**(17): p. 4026-34.
251. Colcher, D., et al., *In vivo fate of monoclonal antibody B72.3 in patients with colorectal cancer.* J Nucl Med, 1990. **31**(7): p. 1133-42.
252. Milenic, D.E., et al., *Construction, binding properties, metabolism, and tumor targeting of a single-chain Fv derived from the pancarcinoma monoclonal antibody CC49.* Cancer Res, 1991. **51**(23 Pt 1): p. 6363-71.

253. Goel, A., et al., *99mTc-labeled divalent and tetravalent CC49 single-chain Fv's: novel imaging agents for rapid in vivo localization of human colon carcinoma.* J Nucl Med, 2001. **42**(10): p. 1519-27.
254. Reff, M.E., K. Hariharan, and G. Braslawsky, *Future of monoclonal antibodies in the treatment of hematologic malignancies.* Cancer Control, 2002. **9**(2): p. 152-66.
255. Knight, D.M., et al., *Pharmacodynamic enhancement of the anti-platelet antibody fab abciximab by site-specific pegylation.* Platelets, 2004. **15**(7): p. 409-18.
256. Huhalov, A. and K.A. Chester, *Engineered single chain antibody fragments for radioimmunotherapy.* Q J Nucl Med Mol Imaging, 2004. **48**(4): p. 279-88.
257. Holliger, P., et al., *Retargeting serum immunoglobulin with bispecific diabodies.* Nat Biotechnol, 1997. **15**(7): p. 632-6.
258. Werner, R.G., *Economic aspects of commercial manufacture of biopharmaceuticals.* J Biotechnol, 2004. **113**(1-3): p. 171-82.
259. Bowers, L.M., et al., *Bacterial expression system with tightly regulated gene expression and plasmid copy number.* Gene, 2004. **340**(1): p. 11-8.
260. Soltyk, A.M., et al., *A mutational analysis of the globotriaosylceramide-binding sites of verotoxin VT1.* J Biol Chem, 2002. **277**(7): p. 5351-9.
261. Mazor, Y., et al., *chFRP5-ZZ-PE38, a large IgG-toxin immunoconjugate outperforms the corresponding smaller FRP5(Fv)-ETA immunotoxin in eradicating ErbB2-expressing tumor xenografts.* Cancer Lett, 2007. **257**(1): p. 124-35.
262. Maynard, J.A., et al., *Protection against anthrax toxin by recombinant antibody fragments correlates with antigen affinity.* Nat Biotechnol, 2002. **20**(6): p. 597-601.
263. Chowdhury, P.S., *Engineering hot spots for affinity enhancement of antibodies.* Methods Mol Biol, 2003. **207**: p. 179-96.
264. Chowdhury, P.S. and I. Pastan, *Improving antibody affinity by mimicking somatic hypermutation in vitro.* Nat Biotechnol, 1999. **17**(6): p. 568-72.
265. Hassan, R., et al., *Antitumor activity of SS(dsFv)PE38 and SS1(dsFv)PE38, recombinant antimesothelin immunotoxins against human gynecologic cancers grown in organotypic culture in vitro.* Clin Cancer Res, 2002. **8**(11): p. 3520-6.
266. Ho, M., et al., *In vitro antibody evolution targeting germline hot spots to increase activity of an anti-CD22 immunotoxin.* J Biol Chem, 2005. **280**(1): p. 607-17.
267. Salvatore, G., et al., *Improved cytotoxic activity toward cell lines and fresh leukemia cells of a mutant anti-CD22 immunotoxin obtained by antibody phage display.* Clin Cancer Res, 2002. **8**(4): p. 995-1002.
268. Girod, A., et al., *Evidence for a COP-I-independent transport route from the Golgi complex to the endoplasmic reticulum.* Nat Cell Biol, 1999. **1**(7): p. 423-30.
269. White, J., et al., *Rab6 coordinates a novel Golgi to ER retrograde transport pathway in live cells.* J Cell Biol, 1999. **147**(4): p. 743-60.
270. Xu, Y. and J.T. Barbieri, *Pertussis toxin-mediated ADP-ribosylation of target proteins in Chinese hamster ovary cells involves a vesicle trafficking mechanism.* Infect Immun, 1995. **63**(3): p. 825-32.

271. Lencer, W.I., et al., *Targeting of cholera toxin and Escherichia coli heat labile toxin in polarized epithelia: role of COOH-terminal KDEL.* J Cell Biol, 1995. **131**(4): p. 951-62.
272. Chaudhary, V.K., et al., *Pseudomonas exotoxin contains a specific sequence at the carboxyl terminus that is required for cytotoxicity.* Proc Natl Acad Sci U S A, 1990. **87**(1): p. 308-12.
273. Majoul, I.V., P.I. Bastiaens, and H.D. Soling, *Transport of an external Lys-Asp-Glu-Leu (KDEL) protein from the plasma membrane to the endoplasmic reticulum: studies with cholera toxin in Vero cells.* J Cell Biol, 1996. **133**(4): p. 777-89.
274. Wales, R., et al., *Addition of an ER retention signal to the ricin A chain increases the cytotoxicity of the holotoxin.* Exp Cell Res, 1992. **203**(1): p. 1-4.
275. Wales, R., L.M. Roberts, and J.M. Lord, *Addition of an endoplasmic reticulum retrieval sequence to ricin A chain significantly increases its cytotoxicity to mammalian cells.* J Biol Chem, 1993. **268**(32): p. 23986-90.
276. Zhan, J., P. Stayton, and O.W. Press, *Modification of ricin A chain, by addition of endoplasmic reticulum (KDEL) or Golgi (YQRL) retention sequences, enhances its cytotoxicity and translocation.* Cancer Immunol Immunother, 1998. **46**(1): p. 55-60.
277. Brinkmann, U., *Recombinant antibody fragments and immunotoxin fusions for cancer therapy.* In Vivo, 2000. **14**(1): p. 21-7.
278. Beresford, G.W., et al., *Binding characteristics and tumor targeting of a covalently linked divalent CC49 single-chain antibody.* Int J Cancer, 1999. **81**(6): p. 911-7.
279. Pack, P., et al., *Tetravalent miniantibodies with high avidity assembling in Escherichia coli.* J Mol Biol, 1995. **246**(1): p. 28-34.
280. Hammarstrom, S., *Binding of Helix pomatia A hemagglutinin to human erythrocytes and their cells. Influence of multivalent interaction on affinity.* Scand J Immunol, 1973. **2**(1): p. 53-66.
281. Willuda, J., et al., *Tumor targeting of mono-, di-, and tetravalent anti-p185(HER-2) miniantibodies multimerized by self-associating peptides.* J Biol Chem, 2001. **276**(17): p. 14385-92.
282. Mirick, G.R., et al., *A review of human anti-globulin antibody (HAGA, HAMA, HACA, HAHA) responses to monoclonal antibodies. Not four letter words.* Q J Nucl Med Mol Imaging, 2004. **48**(4): p. 251-7.
283. Hall, P.D., et al., *Antibody response to DT-GM, a novel fusion toxin consisting of a truncated diphtheria toxin (DT) linked to human granulocyte-macrophage colony stimulating factor (GM), during a phase I trial of patients with relapsed or refractory acute myeloid leukemia.* Clin Immunol, 2001. **100**(2): p. 191-7.
284. Hertler, A.A., L.E. Spitler, and A.E. Frankel, *Humoral immune response to a ricin A chain immunotoxin in patients with metastatic melanoma.* Cancer Drug Deliv, 1987. **4**(4): p. 245-53.
285. FitzGerald, D.J., et al., *Antitumor activity of an immunotoxin in a nude mouse model of human ovarian cancer.* Cancer Res, 1987. **47**(5): p. 1407-10.

286. Posey, J.A., et al., *A phase I trial of the single-chain immunotoxin SGN-10 (BR96 sFv-PE40) in patients with advanced solid tumors.* Clin Cancer Res, 2002. **8**(10): p. 3092-9.
287. Kreitman, R.J., et al., *Phase I trial of recombinant immunotoxin RFB4(dsFv)-PE38 (BL22) in patients with B-cell malignancies.* J Clin Oncol, 2005. **23**(27): p. 6719-29.
288. Damle, B., et al., *Influence of immunogenicity on the pharmacokinetics of BMS-191352, a Pseudomonas exotoxin immunoconjugate, in rats and dogs.* J Pharm Pharmacol, 2000. **52**(6): p. 671-8.
289. Hu, R.G., et al., *Bioactivities of ricin retained and its immunoreactivity to anti-ricin polyclonal antibodies alleviated through pegylation.* Int J Biochem Cell Biol, 2002. **34**(4): p. 396-402.
290. Oratz, R., et al., *Antimelanoma monoclonal antibody-ricin A chain immunoconjugate (XMMME-001-RTA) plus cyclophosphamide in the treatment of metastatic malignant melanoma: results of a phase II trial.* J Biol Response Mod, 1990. **9**(4): p. 345-54.
291. Selvaggi, K., et al., *Phase I/II study of murine monoclonal antibody-ricin A chain (XOMAZYME-Mel) immunoconjugate plus cyclosporine A in patients with metastatic melanoma.* J Immunother Emphasis Tumor Immunol, 1993. **13**(3): p. 201-7.
292. Tsutsumi, Y., et al., *Site-specific chemical modification with polyethylene glycol of recombinant immunotoxin anti-Tac(Fv)-PE38 (LMB-2) improves antitumor activity and reduces animal toxicity and immunogenicity.* Proc Natl Acad Sci U S A, 2000. **97**(15): p. 8548-53.
293. Roscoe, D.M., et al., *Primate antibody response to immunotoxin: serological and computer-aided analysis of epitopes on a truncated form of Pseudomonas exotoxin.* Infect Immun, 1994. **62**(11): p. 5055-65.
294. Arndt, M.A., et al., *A dimeric angiogenin immunofusion protein mediates selective toxicity toward CD22+ tumor cells.* J Immunother (1997), 2005. **28**(3): p. 245-51.
295. Krauss, J., et al., *Targeting malignant B-cell lymphoma with a humanized anti-CD22 scFv-angiogenin immunoenzyme.* Br J Haematol, 2005. **128**(5): p. 602-9.
296. De Lorenzo, C., et al., *A fully human antitumor immunoRNase selective for ErbB-2-positive carcinomas.* Cancer Res, 2004. **64**(14): p. 4870-4.
297. Hershfield, M.S., *PEG-ADA replacement therapy for adenosine deaminase deficiency: an update after 8.5 years.* Clin Immunol Immunopathol, 1995. **76**(3 Pt 2): p. S228-32.
298. Cortes, J.E., et al., *A pilot study of interleukin-2 for adult patients with acute myelogenous leukemia in first complete remission.* Cancer, 1999. **85**(7): p. 1506-13.
299. Wang, M., et al., *Engineering an arginine catabolizing bioconjugate: Biochemical and pharmacological characterization of PEGylated derivatives of arginine deiminase from Mycoplasma arthritidis.* Bioconjug Chem, 2006. **17**(6): p. 1447-59.
300. Maack, T., et al., *Renal filtration, transport, and metabolism of low-molecular-weight proteins: a review.* Kidney Int, 1979. **16**(3): p. 251-70.

301. Veronese, F.M., *Peptide and protein PEGylation: a review of problems and solutions.* Biomaterials, 2001. **22**(5): p. 405-17.
302. Yamamoto, Y., et al., *Site-specific PEGylation of a lysine-deficient TNF-alpha with full bioactivity.* Nat Biotechnol, 2003. **21**(5): p. 546-52.
303. Lee, L.S., et al., *Prolonged circulating lives of single-chain Fv proteins conjugated with polyethylene glycol: a comparison of conjugation chemistries and compounds.* Bioconjug Chem, 1999. **10**(6): p. 973-81.
304. Mire-Sluis, A.R., *Challenges with current technology for the detection, measurement and characterization of antibodies against biological therapeutics.* Dev Biol (Basel), 2002. **109**: p. 59-69.
305. Baluna, R., et al., *Decreases in levels of serum fibronectin predict the severity of vascular leak syndrome in patients treated with ricin A chain-containing immunotoxins.* Clin Cancer Res, 1996. **2**(10): p. 1705-12.
306. Baluna, R., et al., *Evidence for a structural motif in toxins and interleukin-2 that may be responsible for binding to endothelial cells and initiating vascular leak syndrome.* Proc Natl Acad Sci U S A, 1999. **96**(7): p. 3957-62.
307. Kreitman, R.J., *Recombinant toxins for the treatment of cancer.* Curr Opin Mol Ther, 2003. **5**(1): p. 44-51.
308. Kreitman, R.J., *Taming ricin toxin.* Nat Biotechnol, 2003. **21**(4): p. 372-4.
309. North, C.L. and S.C. Blacklow, *Structural independence of ligand-binding modules five and six of the LDL receptor.* Biochemistry, 1999. **38**(13): p. 3926-35.
310. Nord, K., et al., *A combinatorial library of an alpha-helical bacterial receptor domain.* Protein Eng, 1995. **8**(6): p. 601-8.
311. Wahlberg, E., et al., *An affibody in complex with a target protein: structure and coupled folding.* Proc Natl Acad Sci U S A, 2003. **100**(6): p. 3185-90.
312. Wikman, M., et al., *Selection and characterization of HER2/neu-binding affibody ligands.* Protein Eng Des Sel, 2004. **17**(5): p. 455-62.
313. Gronenborn, A.M., et al., *A novel, highly stable fold of the immunoglobulin binding domain of streptococcal protein G.* Science, 1991. **253**(5020): p. 657-61.
314. Du, H.N., et al., *Effects of segment substitution on the structure and stability of immunoglobulin G binding domain of streptococcal protein G.* Biopolymers, 2005. **79**(1): p. 9-17.
315. Sedgwick, S.G. and S.J. Smerdon, *The ankyrin repeat: a diversity of interactions on a common structural framework.* Trends Biochem Sci, 1999. **24**(8): p. 311-6.
316. Krause, S., et al., *Grafting of thrombopoietin-mimetic peptides into cystine knot miniproteins yields high-affinity thrombopoietin antagonists and agonists.* Febs J, 2007. **274**(1): p. 86-95.